

**University of Alberta**

**Identification and Characterization of Interactions Between Rubella Virus Capsid and  
Host Cell Proteins**

by

**Martin Denis Beatch**



**A thesis submitted to the Faculty of Graduate Studies and Research in partial fulfillment  
of the requirements for the degree of Doctor of Philosophy**

**Department of Cell Biology**

**Edmonton, Alberta  
Fall 2004**



Library and  
Archives Canada

Bibliothèque et  
Archives Canada

Published Heritage  
Branch

Direction du  
Patrimoine de l'édition

395 Wellington Street  
Ottawa ON K1A 0N4  
Canada

395, rue Wellington  
Ottawa ON K1A 0N4  
Canada

*Your file* *Votre référence*

*ISBN: 0-612-95905-8*

*Our file* *Notre référence*

*ISBN: 0-612-95905-8*

The author has granted a non-exclusive license allowing the Library and Archives Canada to reproduce, loan, distribute or sell copies of this thesis in microform, paper or electronic formats.

L'auteur a accordé une licence non exclusive permettant à la Bibliothèque et Archives Canada de reproduire, prêter, distribuer ou vendre des copies de cette thèse sous la forme de microfiche/film, de reproduction sur papier ou sur format électronique.

The author retains ownership of the copyright in this thesis. Neither the thesis nor substantial extracts from it may be printed or otherwise reproduced without the author's permission.

L'auteur conserve la propriété du droit d'auteur qui protège cette thèse. Ni la thèse ni des extraits substantiels de celle-ci ne doivent être imprimés ou autrement reproduits sans son autorisation.

---

In compliance with the Canadian Privacy Act some supporting forms may have been removed from this thesis.

Conformément à la loi canadienne sur la protection de la vie privée, quelques formulaires secondaires ont été enlevés de cette thèse.

While these forms may be included in the document page count, their removal does not represent any loss of content from the thesis.

Bien que ces formulaires aient inclus dans la pagination, il n'y aura aucun contenu manquant.

# Canada

## ABSTRACT

Rubella virus (RV) is a positive strand RNA virus belonging to the family *Togaviridae*. It is the etiological agent of German measles, a normally benign human disease. However, when contracted during the first trimester of pregnancy RV is highly teratogenic and causes a series of birth defects known as congenital rubella syndrome. In the developing world, RV remains a major cause of congenital abnormalities. Despite the importance of RV as a human pathogen, the molecular basis of virus disease remains poorly understood. In order to understand the role of individual proteins during RV infection, we have focused our studies on the capsid protein. While the primary function of this protein is to package genomic RNA into nucleocapsids, recent studies have identified several additional roles for capsid. In an attempt to elucidate the mechanisms by which capsid conducts its various functions, we identified a number of host cell proteins that bind to capsid. In addition, we found that capsid expression, in the absence of other viral proteins, affects mitochondrial distribution and morphology. Furthermore, the interaction between capsid and the mitochondrial matrix protein p32 was shown to be important for capsid-induced aggregation of mitochondria. In addition, recombinant viruses encoding capsids with mutations in the p32 binding site displayed altered plaque morphology and replicated poorly suggesting that capsid-p32 interactions are important for virus replication. From this work, it appears that the RV capsid protein plays an even more dynamic role in RV biology than previously suspected.

## ACKNOWLEDGEMENTS

Completion of this thesis would not have been possible if it wasn't for the help of many very wonderful people. First of all, I must thank my supervisor Tom Hobman for providing an excellent environment from which to learn. Tom has been an excellent mentor and has taught me much scientifically. In addition, he has given me many great opportunities and has shown great patience at times.

The members of my supervisory committee, Paul Melançon, Jim Smiley, and Bruce Stevenson, have also been instrumental in directing this work and teaching me many very important lessons. I must also give Bruce Stevenson, who gave me my first chance to work in a lab environment, extra thanks. Without this opportunity it is unlikely that I would have been the one to do this work. I would also like to thank Carolyn Machamer and Luis Schang for sitting on my thesis defense committee.

All members of the Hobman Lab, past and present, deserve much thanks for providing a working environment like non other. I leave here with a lifetime of memories. Extra special thanks go out to Mike Garbutt and Darren Cikaluk who taught me many skills and techniques when I was starting out and to John Law who has been a great friend and labmate (he even did some experiments for me). I can't imagine how much more difficult this project would have been without the excellent technical help of Margaret Hughes and Eileen Reklow. But of course, all other members have been extremely knowledgeable and helpful. Thank you: Kevin Bainey, Jon Carmichael, Anh Dang, Jason Everitt, Tracey Hunt, Kasia Jaronczyk, Colin Nash, Henry Parker, Kail Ross, Cezar Stoica, and Nasser Tahbaz.

My family has been extremely supportive and has helped me out beyond what could reasonably be expected. Their help during my university years is greatly appreciated.

Additional thanks are also due to all of my friends who have supported me in numerous ways throughout my time in graduate school. I am extremely lucky to have such wonderful friends. I won't mention names for fear of forgetting someone. I rest assured that you know who you are. This has been a wonderful period of time for me and you have all contributed greatly.

## TABLE OF CONTENTS

**ABSTRACT**

**ACKNOWLEDGEMENTS**

**TABLE OF CONTENTS**

**LIST OF TABLES**

**LIST OF FIGURES**

**LIST OF ABBREVIATIONS**

<b>CHAPTER 1. INTRODUCTION .....</b>	<b>1</b>
1.1. Clinical features of rubella virus infection.....	2
1.2. Historical and current medical significance of rubella virus .....	3
1.3. The Family <i>Togaviridae</i> .....	4
1.4. The study of rubella virus .....	5
1.5. Genomic organization and replication .....	6
1.5.1. Genomic organization .....	6
1.5.2. Rubella virus replication .....	6
1.5.3. Macromolecular synthesis .....	8
1.6. Rubella virus proteins .....	8
1.6.1. Nonstructural proteins.....	8
1.6.2. Structural proteins.....	9
1.6.2.1. Capsid.....	10
1.6.2.2. Envelope proteins.....	14
1.7. Rubella virus life cycle .....	15
1.7.1. Attachment and internalization.....	15
1.7.2. Replication.....	17
1.7.3. Targeting of structural proteins to the budding site.....	18
1.7.4. Virus assembly and secretion .....	20
1.8. Rubella virus cytopathic effects .....	21
1.8.1. Effects of RV replication on cellular morphology.....	21
1.8.2. Cytopathic effect.....	23
1.9. Multifunctional capsid proteins.....	25
1.10. Project rationale.....	27
<b>CHAPTER 2. MATERIALS AND METHODS.....</b>	<b>28</b>
2.1. Reagents and Materials .....	29
2.1.1. Reagents .....	29
2.1.2. Multicomponent systems.....	32
2.1.3. Modifying enzymes.....	33
2.1.4. Radiochemicals.....	33
2.1.5. Detection systems .....	33
2.1.6. Molecular size standards .....	33
2.2. Commonly used buffers .....	34
2.3. Antibodies .....	35
2.3.1. Primary antibodies .....	35
2.3.2. Secondary antibodies .....	35

2.4. Cell lines and viruses .....	35
2.4.1. Cell lines.....	35
2.4.2. Viruses.....	35
2.5. DNA analysis and modification .....	36
2.5.1. Isolation of plasmid DNA from <i>E. coli</i> .....	36
2.5.2. Restriction endonuclease digestion.....	36
2.5.3. Polymerase chain reaction.....	36
2.5.4. Agarose gel electrophoresis.....	36
2.5.5. Purification of DNA.....	37
2.5.6. Dephosphorylation of 5' ends.....	37
2.5.7. Filling in of 5' overhangs .....	37
2.5.8. Ligation of DNA fragments.....	37
2.5.9. Chemical transformation of DH5 $\alpha$ .....	38
2.5.10. Electroporation of DH5 $\alpha$ .....	38
2.5.11. Automated DNA sequencing.....	39
2.6. Recombinant plasmids.....	39
2.6.1. Constructs used in yeast two-hybrid analysis.....	39
2.6.2. Constructs for <i>in vitro</i> transcription/translation.....	41
2.6.3. Constructs for bacterial expression.....	41
2.6.4. Constructs for mammalian expression.....	42
2.6.5. Introduction of RA mutations into the infectious clone.....	43
2.7. Protein gel electrophoresis and protein detection.....	43
2.7.1. SDS-PAGE.....	43
2.7.2. Fluorography .....	44
2.7.3. Silver staining .....	44
2.7.4. Western blotting.....	44
2.8. Culture and transfection of mammalian cell lines.....	45
2.8.1. Mammalian cell culture.....	45
2.8.2. Transient transfection of cell cultures.....	45
2.8.3. Generation of HEK 293T-REx cells inducibly expressing capsid .....	45
2.9. Immunoprecipitation and radioimmunoprecipitation .....	46
2.9.1 Immunoprecipitation.....	46
2.9.2. Metabolic labeling and radioimmunoprecipitation.....	46
2.10. Identification of capsid interacting proteins by yeast two-hybrid screening .....	47
2.11. Identification of capsid interacting proteins by GST pulldown .....	47
2.12. <i>In vitro</i> binding interactions .....	48
2.12.1. Purification of GST fusion proteins from bacteria .....	48
2.12.2. Conjugation of glucose oxidase to CNBr activated beads .....	48
2.12.3. <i>In vitro</i> binding assay .....	49
2.13. Microscopy.....	49
2.13.1. Immunofluorescence microscopy .....	49
2.13.2. Electron microscopy.....	50
2.14. Virus infection, propagation and titering techniques.....	50
2.14.1. Infection of Vero cells with rubella virus.....	50
2.14.2. One step growth curves .....	51
2.14.3. Synthesis of infectious viral RNA and production of mutant virus.....	51

2.14.4. Plaque assay.....	51
2.15. Generation of polyclonal antibodies.....	52
2.15.1. Generation of polyclonal antibodies to capsid.....	52
2.15.2. Generation of polyclonal antibodies to p32.....	52
2.16. Analysis of the effects of capsid on mitochondrial membrane potential and cell growth.....	53
2.16.1. MTT assay.....	53
2.16.2. Flow cytometry.....	53
2.17. Analysis of capsid arginine to alanine mutants.....	54
2.17.1. Virion assembly (RLP) assay.....	54
2.17.2. <sup>33</sup> P labeling of capsid.....	54
2.17.3. <i>In vitro</i> RNA binding assay.....	54
2.18. Luciferase assay.....	55

**CHAPTER 3. IDENTIFICATION AND CHARACTERIZATION OF CAPSID-INTERACTING HOST CELL PROTEINS .....57**

3.1. Overview.....	58
3.2. Identification of capsid-binding proteins.....	58
3.2.1. Yeast two-hybrid screen.....	58
3.2.2. GST pulldown experiments.....	64
3.3. Confirmation and characterization of the capsid-p32 interaction.....	68
3.3.1. Capsid and p32 interact <i>in vitro</i> .....	68
3.3.2. Capsid and p32 interact <i>in vivo</i> .....	68
3.3.3. The amino-terminus of capsid binds the carboxy-terminus of p32.....	73
3.4. Confirmation and characterization of the capsid -Par-4 interaction.....	76
3.4.1. Capsid and Par-4 interact <i>in vitro</i> .....	76
3.4.2. Capsid and Par-4 interact <i>in vivo</i> .....	78
3.4.3. Capsid and Par-4 co-localize at intracellular membranes.....	80
3.4.4. Identification of the Par-4 binding region of capsid.....	80
3.5. Summary.....	81

**CHAPTER 4. INTERACTIONS BETWEEN CAPSID AND p32 ARE IMPORTANT FOR VIRAL REPLICATION .....84**

4.1. Overview.....	85
4.2. Analysis of the capsid-p32 interacting domain.....	85
4.3. Effects of the capsid-p32 interaction on mitochondrial aggregation.....	92
4.3.1. The arginine rich regions of capsid are necessary for clustering of mitochondria.....	92
4.3.2. Capsid recruits p32 lacking the amino terminus to mitochondria.....	95
4.4. Capsid expression induces the formation of mitochondrial plaques.....	102
4.5. Effects of capsid expression on mitochondrial membrane potential.....	102
4.6. Effects of the capsid-p32 interaction on virus replication.....	104
4.7. Capsid arginine to alanine mutants do not display altered cytopathic effect.....	112
4.8. Summary.....	112

<b>CHAPTER 5. DISCUSSION.....</b>	<b>115</b>
5.1. Overview .....	116
5.2. The amino terminus of the RV capsid is multifunctional and interacts with host cell proteins p32 and Par-4 .....	117
5.3. Localization of capsid to mitochondria.....	118
5.4. Effects of capsid on mitochondrial distribution .....	121
5.5. The capsid-p32 interaction.....	122
5.5.1. Model of the capsid-p32 interaction .....	122
5.5.2. Function of the capsid-p32 interaction.....	126
5.6. Interaction of capsid with other host cell proteins.....	131
5.6.1. Par-4 .....	131
5.6.2. PKC $\zeta$ .....	133
5.6.3. The Poly(A) binding protein .....	134
5.7. Concluding remarks.....	135
<b>REFERENCES.....</b>	<b>137</b>
<b>APPENDIX I. Effect of capsid expression on host cell signaling pathways .....</b>	<b>153</b>
<b>CURRICULUM VITAE .....</b>	<b>158</b>

## LIST OF TABLES

Table 2-1. Reagents.....	29
Table 2-2. Buffered Solutions.....	34
Table 2-3. Oligonucleotide Primers .....	40
Table 3-1. P32 Interacting Proteins.....	62
Table 4-1. Percentage of Electroporated Cells Expressing E1 .....	110

## LIST OF FIGURES

Figure 1.1. Replication of rubella virus.....	7
Figure 1.2. Rubella virus structural proteins are translated from the subgenomic RNA ..	11
Figure 1.3. Schematic diagram of the rubella virus capsid .....	12
Figure 1.4. The rubella virus life cycle.....	16
Figure 3.1. The structure and sequence of p32 .....	61
Figure 3.2. The structure and sequence of Par-4.....	65
Figure 3.3. Identification of capsid-binding proteins by GST pulldown .....	67
Figure 3.4. Capsid binds to p32 <i>in vitro</i> .....	69
Figure 3.5. Coimmunoprecipitation of capsid and p32.....	70
Figure 3.6. Capsid colocalizes with p32 at the mitochondria.....	72
Figure 3.7. Capsid is associated with the cytoplasmic surface of mitochondria .....	74
Figure 3.8. Characterization of the capsid-p32 binding regions using the yeast two-hybrid system .....	75
Figure 3.9. Capsid binds to Par-4 <i>in vitro</i> .....	77
Figure 3.10. Coimmunoprecipitation of capsid and Par-4.....	79
Figure 3.11. Capsid colocalizes with Par-4 at intracellular membranes .....	82
Figure 3.12. Identification of the Par-4 binding region of capsid using the yeast two-hybrid system .....	83
Figure 4.1. The p32 binding region of capsid.....	86
Figure 4.2. Two clusters of arginines in capsid are required for binding to p32 but not for phosphorylation of capsid, assembly of virus-like particles, or RNA binding.....	89
Figure 4.3. Capsid expression results in clustering of mitochondria .....	94
Figure 4.4. Capsid recruits GFPp32m to a juxtannuclear region.....	97
Figure 4.5. Co-localization of capsid and GFPp32m occurs at mitochondria.....	98
Figure 4.6. Capsid arginine to alanine mutants are unable to efficiently target GFPp32m to the juxtannuclear region .....	101

Figure 4.7. Expression of capsid induces the formation of electron dense zones between mitochondria .....	103
Figure 4.8. Effects of capsid on mitochondrial membrane potential .....	105
Figure 4.9. Viruses encoding arginine to alanine mutations in capsid exhibit replication defects.....	108
Figure 4.10. Rubella virus mutant genomic RNAs support synthesis of RV structural proteins. ....	109
Figure 4.11. Capsid arginine to alanine mutations do not alter cell viability.....	114
Figure 5.1. Model of the interaction between rubella virus capsid and p32.....	124
Figure A.1. Mechanism by which capsid may alter cell signaling pathways via its interaction with cellular proteins.....	156
Figure A.2. Effects of capsid expression on NF- $\kappa$ B and AP-1 activity .....	157

## LIST OF ABBREVIATIONS

AP-1	activator protein-1
ATP	adenosine triphosphate
BHK	baby hamster kidney
°C	degrees Celsius
cDNA	complementary DNA
Ci	Curie
CIP	calf intestinal alkaline phosphatase
CTP	cytosine triphosphate
cm	centimeter
CRS	congenital rubella syndrome
DNA	deoxyribonucleic acid
g	gram
<i>g</i>	gravitational force
GFP	green fluorescent protein
GST	glutathione S-transferase
h	hour
HCV	hepatitis C virus
HEK 293T	human embryonic kidney 293T
HRP	horseradish peroxidase
IgG	immunoglobulin G
kDa	kilo Dalton
M	moles per litre
mA	milli Ampere
MALDI-TOF	matrix assisted laser desorption ionization-time of flight
µg	microgram
µl	microlitre
mg	milligram
min	minute
ml	milliliter

MMR	measles mumps rubella
mRNA	messenger RNA
MOI	multiplicity of infection
NF- $\kappa$ B	nuclear factor – kappaB
ng	nanogram
NP-40	nonidet P-40
ORF	open reading frame
PBS	phosphate buffered saline
PCR	polymerase chain reaction
PFU	plaque forming units
pH	$-\log[H^+]$
PKC	protein kinase C
PMSF	phenylmethylsulfonyl fluoride
PVDF	polyvinylidenefluoride
RK-13	rabbit kidney-13
RLP	rubella-like particle
RNA	ribonucleic acid
RV	rubella virus
S	Svedberg unit
SDS	sodium dodecyl sulfate
SDS-PAGE	sodium dodecyl sulfate-polyacrylamide gel electrophoresis
SFV	Semliki Forest virus
TMRE	tetra-methyl rhodamine ester
TNF- $\alpha$	tumor necrosis factor- $\alpha$
U	units of enzyme activity
UV	ultraviolet
v	volume
V	Volts
VSV	Vesicular Stomatitis virus
w	weight

## **CHAPTER 1. INTRODUCTION**

## **1.1. Clinical features of rubella virus infection**

Rubella virus (RV) is the infectious agent responsible for the disease known as rubella, German measles or three day measles in humans. Postnatal infection may result in a series of symptoms such as a maculopapular rash, malaise, lymphadenopathy and a low-grade fever. Symptoms are generally short lived and mild and it is estimated that approximately half of all cases are subclinical (Frey, 1994). Complications from viral infection can be considerably more serious. The most common complications are the occurrence of arthralgia and arthritis which tend to occur more often in females than in males with up to 70% of infected women reporting such complications (Smith et al., 1987). Typically, these symptoms are short lived (2 to 4 weeks) but chronic arthritis can develop. Other, more rare, complications include thrombocytopenic purpura (approximately 1 in 3000 cases) and encephalopathy (approximately 1 in 8000 cases) (Frey, 1994). The encephalitis is usually short lived but can be fatal in rare cases.

The major health significance of RV infection relates to the teratogenic effects of the virus. The virus is capable of crossing the placenta during pregnancy resulting in infection of the fetus. During the first trimester of pregnancy this has devastating effects on the fetus resulting in spontaneous abortion, stillbirth or a condition known as congenital rubella syndrome (CRS). Symptoms of CRS include low birth weight, deafness, cataracts, mental retardation and heart disease (Cooper et al., 1969). CRS babies also have an increased risk of developing endocrine or neurological diseases such as insulin-dependent diabetes mellitus or schizophrenia later in life (Brown et al., 2001; Ginsberg-Fellner et al., 1985). Approximately 80% of neonates born to mothers infected during the first trimester of pregnancy develop CRS (Frey, 1994). Although the virus is able to cross the placenta throughout gestation, the risk to the fetus is limited if infection occurs after the 16<sup>th</sup> week of pregnancy.

Another serious complication of RV infection is a condition known as progressive rubella panencephalitis (Frey, 1997). This condition results in a slow neurodegeneration which ultimately is fatal. Progressive rubella panencephalitis can develop in both pre and postnatally infected individuals but is extremely rare.

RV is spread, from person to person, by respiratory aerosols. Initially, virus infects and replicates in cells of the upper respiratory tract and nasopharyngeal lymphoid tissue. Shortly afterwards, virus spreads to regional lymph nodes and viremia occurs 5 to 7 days post-infection allowing the virus to establish a systemic infection. The characteristic rash occurs 16 to 20 days following exposure. Typically, virus is shed from 1 week post-infection up to 1 to 2 weeks following the rash (Chantler et al., 2001).

## **1.2. Historical and current medical significance of rubella virus**

RV was identified as an infectious agent by German scientists in the 19<sup>th</sup> century. The teratogenic effects of the virus, however, went unnoticed until 1941 when the ophthalmologist Norman Gregg noticed the correlation between an outbreak of rubella and the appearance of children born with birth defects such as cataracts (Gregg, 1941). The seriousness of the risk RV posed to public health became apparent during a major outbreak of rubella in 1964-65 when over 20,000 cases of CRS were reported in the United States (Orenstein et al., 1984). In response to this epidemic, several live attenuated vaccines were developed and a routine vaccination program was introduced in the United States in 1969 resulting in a rapid decrease in the number of cases of rubella and CRS (Herrmann, 1991). A similar reduction of CRS cases in Canada and other developed countries has occurred as a result of widespread vaccination programs. Currently, the rubella vaccine is given as a trivalent mixture, known as MMR, in conjunction with vaccines against mumps and measles to all preschool aged children.

CRS remains a major problem in many parts of the world due to a lack of extensive vaccination programs. As of 2001, only 58% of countries worldwide had vaccination plans against RV in place. Typically, it is developing countries which lack such programs. It is estimated that over 100,000 infants are born with CRS every year worldwide (Robertson et al., 2003).

Despite the success of vaccination programs, rubella remains a risk to public health in North America and Western Europe since a portion of the population remains unvaccinated due to issues such as vaccine failure, incomplete vaccine coverage and immigration from areas of low vaccine coverage (Reef et al., 2002; Sheridan et al., 2002).

Furthermore, there is decreasing vaccination coverage in parts of the developed world due to fears regarding vaccine safety. These fears are largely due to A) a perceived causal link between MMR vaccination and the onset of autism and B) a single study which reported inflammatory bowel disease and autism in children who had received the MMR vaccine (Wakefield et al., 1998). Several co-authors of the paper by Wakefield *et al.*, have since retracted the interpretation that a causal link between the MMR vaccine and autism may exist due to insufficient data (Murch et al., 2004). Furthermore, several large-scale studies have disputed the connection between MMR vaccination and autism and have determined that the vaccine is safe (Dales et al., 2001; Kaye et al., 2001; Madsen et al., 2002; Taylor et al., 2002). Nonetheless, vaccine coverage has become dangerously low in parts of the UK and public health officials are predicting outbreaks of measles and an increase in the number of congenital defects due to RV in the near future if vaccination levels do not increase (Jansen et al., 2003). Thus, despite the existence of a safe and effective vaccine, RV remains an important human pathogen worldwide.

### 1.3. The Family *Togaviridae*

The family *Togaviridae* is comprised of a number of small, enveloped animal viruses. The togavirus genome consists of a single stranded, positive sense RNA molecule of approximately 10,000 to 12,000 nucleotides. The genome contains two large, non-overlapping open reading frames (ORFs): a 5' proximal ORF which encodes the nonstructural proteins and a 3' proximal ORF encoding the structural proteins. The structural proteins are translated from a subgenomic RNA that is generated from a negative polarity, genome length RNA (van Regenmortel et al., 2000).

Virions are composed of an icosahedral nucleocapsid surrounded by a host cell derived lipid envelope containing the viral spike proteins. The nucleocapsid contains a single copy of the genomic RNA and multiple copies of the capsid protein. When viewed by electron microscopy, virions have a characteristic morphology (Schlesinger and Schlesinger, 2001). The virions are spherical, 50 to 70 nm in diameter and have an electron dense core of 30 to 40 nm in diameter. Between the core and the envelope is an electron lucent region giving the virions the appearance of having a ring or "toga"

surrounding the nucleocapsid. Togaviruses are named for this characteristic appearance.

The family *Togaviridae* is divided into two genera: the genus *Rubivirus* and the genus *Alphavirus*. There is limited sequence similarity between the two genera but they share a similar genomic organization and have similar replication strategies. RV is the sole member of the genus *Rubivirus*. The only known natural host for RV is humans. The genus *Alphavirus* includes 26 viruses of which Sindbis (SIN) and Semliki Forest virus (SFV) are the best studied. Alphaviruses utilize both arthropods and vertebrates as hosts.

#### **1.4. The study of rubella virus**

Despite the importance of RV as a human pathogen, the biology of the virus is poorly understood in comparison to alphaviruses. One reason for this is that there are currently no animal models for RV. Although RV is able to replicate in several laboratory animals including mice, rats, rabbits and ferrets, symptoms are generally subclinical in these organisms (Avila et al., 1972; Kono et al., 1969; Patterson et al., 1973; Rorke et al., 1968; Sato et al., 1976). Therefore, the study of RV is largely conducted using established tissue culture cell lines. The most commonly used cell lines are Vero, BHK-21 or RK-13 cells. These cell types are highly permissive for RV replication possibly because they lack a functioning interferon system. However, RV replicates poorly in most cultured cell lines reaching peak titers which are 10 to 100 times lower than that of alphaviruses (Kaariainen and Soderlund, 1978; Strauss and Strauss, 1994). The reasons for the low replicative ability of RV are unknown, but possible explanations include the high GC content of the genome and/or the unusual codon usage by the virus (Frey, 1994).

Another complicating factor for the study of RV is that infection of cells is asynchronous. Regardless of the multiplicity of infection (MOI) used, not all cells in a culture can be infected 12 to 24 hours post-infection (Hemphill et al., 1988; Sedwick and Sokol, 1970). However, within 48 hours all cells become infected when high MOIs are employed. The reasons for this are not known but it has been suggested that host factors expressed at certain stages of the cell cycle might be important for virus replication.

For the reasons mentioned above, RV has proven more difficult to study than its alphavirus cousins. As a result, it has previously been assumed that RV biology is

largely similar to that of alphaviruses. Only recently, has work shown that there are several important differences between RV and alphaviruses.

## **1.5. Genomic organization and replication**

### **1.5.1. Genomic organization**

The complete nucleotide sequence has been determined for several wild type and vaccine strains of RV (Clarke et al., 1987; Dominguez et al., 1990; Frey and Marr, 1988; Nakhasi et al., 1989; Takkinen et al., 1988; Zheng et al., 1989). The GC content of the RV genome is 69.5%, the highest of any RNA virus sequenced to date. The genomic RNA contains a 7-methyl guanosine cap at the 5' terminus and is polyadenylated at the 3' terminus (Oker-Blom et al., 1984; Wang et al., 1994). Excluding the poly(A) tail, the genomic RNA is 9,762 nucleotides in length and, like other togaviruses, contains two, non-overlapping polycistronic ORFs (**Figure 1.1**). The 5' proximal ORF encoding the nonstructural proteins is 6385 nucleotides and the 3' proximal ORF encoding the structural proteins is 3189 nucleotides. The structural proteins are translated from a subgenomic RNA containing the 3' one third of the genome. The subgenomic RNA is also capped and polyadenylated (Oker-Blom et al., 1984).

### **1.5.2. Rubella virus replication**

Three species of viral RNA are detected in RV infected cells: a genome length, positive sense RNA with a sedimentation coefficient of 40S; a negative sense copy of the genomic RNA; and a subgenomic RNA with a sedimentation coefficient of 24S (Hemphill et al., 1988; Hovi and Vaheri, 1970; Sedwick and Sokol, 1970) (**Figure 1.1**). The plus sense genomic RNA is infectious when introduced into cells (Hovi and Vaheri, 1970; Sedwick and Sokol, 1970). Initially, it serves as the mRNA for translation of the nonstructural proteins. The nonstructural proteins, in turn, function as the viral replicase and transcribe the full length negative sense RNA using genomic RNA as a template. The genomic RNA contains a 29 nucleotide region in the 5' ORF which binds capsid resulting in the selective packaging of the genomic RNA into virions late in infection (Liu et al.,

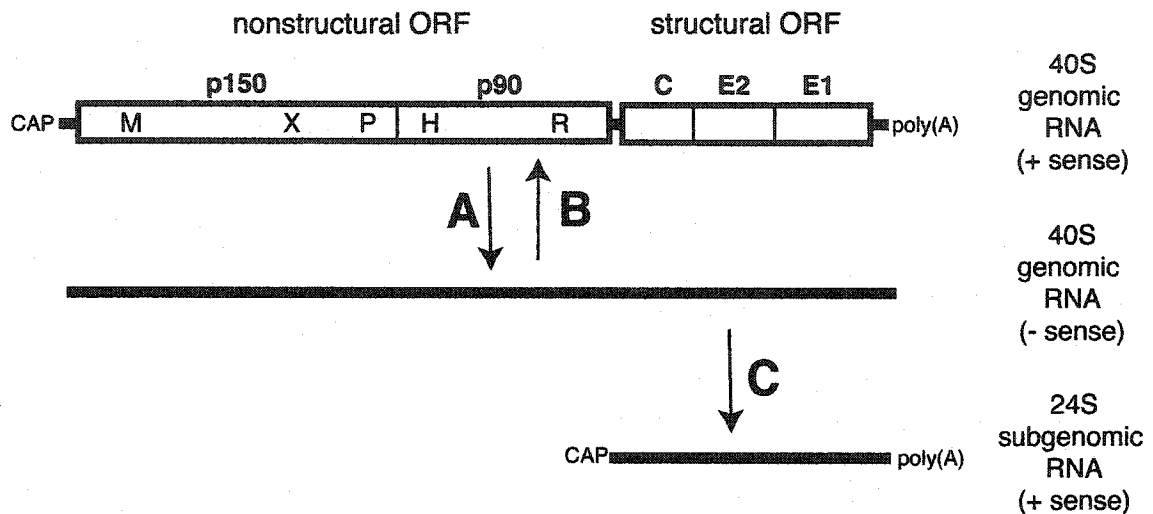


**Figure 1.1. Replication of rubella virus.** The virus genomic RNA (40S) is 9,762 nucleotides in length and contains a 7-methyl guanosine cap at its 5' end and a poly(A) tail at its 3' end. The genomic RNA contains two non-overlapping reading frames (ORFs). The 5' proximal ORF encodes the nonstructural proteins necessary for virus replication. The 5' proximal ORF is translated from genomic RNA as a polyprotein which is subsequently cleaved into two proteins: p150 and p90. These proteins contain methyltransferase (M), X domain (X), protease (P), helicase (H), and replicase (R) domains as indicated. Replication of the virus occurs as follows: (A) The nonstructural proteins mediate the production of a negative strand copy of the genome length RNA using the genomic positive sense RNA as a template; (B) Genomic RNA is synthesized using the negative sense RNA as a template; (C) The negative strand RNA also serves as the template for the generation of a 24S subgenomic RNA. This RNA contains the 3' proximal ORF encoding the structural proteins. These proteins are translated from the subgenomic RNA as a polyprotein in the order NH<sub>2</sub>-capsid-E2-E1-COOH.

1996). The genome length negative strand RNA serves as template for both the genomic positive strand and for the subgenomic RNA (Hemphill et al., 1988). The subgenomic RNA serves as the template for translation of the structural proteins. It is generally not packaged into virions (Oker-Blom et al., 1984).

### **1.5.3. Macromolecular synthesis**

Viral genomic and subgenomic RNA can be first detected in RV infected Vero cells approximately 12 hours post-infection with peak production of both RNAs occurring at 26 to 30 hours (Hemphill et al., 1988). Similar rates of viral RNA synthesis occur in RV infected BHK-21 cells (Sedwick and Sokol, 1970). The virus structural proteins are detected shortly after the appearance of viral RNA at 12 to 16 hours post-infection (Hemphill et al., 1988). Secretion of peak virus levels into the medium occurs at 24 to 36 hours post-infection and is maintained until at least 72 hours (Hemphill et al., 1988). In contrast, alphaviruses have a much shorter latent period with viral macromolecules being detected within 2 hours of infection and maximum virus production occurs at 4 to 8 hours post-infection (Kaariainen and Soderlund, 1978; Strauss and Strauss, 1994).

## **1.6. Rubella virus proteins**

### **1.6.1. Nonstructural proteins**

The 5' ORF of the RV genome encodes two nonstructural proteins that are involved in replication of the viral RNA. The nonstructural ORF is translated as a polyprotein precursor of approximately 200 kDa and subsequently cleaved by a virally encoded protease into two proteins of 150 kDa (1,301 amino acids) and 90 kDa (815 amino acids) (Marr et al., 1994). The order of the 5' ORF is NH<sub>2</sub>-p150-p90-COOH.

P150 contains several domains which are conserved amongst a number of RNA viruses. A papain-like cysteine protease domain located in the carboxy portion of p150 is responsible for the cleavage of the nonstructural precursor protein (Chen et al., 1996; Marr et al., 1994; Yao et al., 1998). A putative methyltransferase domain in the amino

terminus is believed to have a role in capping the viral RNA (Roazanov et al., 1992). P150 also contains an X domain which has homology to the nonstructural proteins of alphaviruses, coronaviruses and hepatitis E virus (Gorbalenya et al., 1991). The function of the X domain is not known but it has been shown to be important for trans cleavage by the RV protease and it appears to be important for replication of alphaviruses (Hahn et al., 1989; Liang et al., 2000). Interestingly, the X domain is the region that is the most highly conserved between RV and alphaviruses at the level of predicted amino acids (Dominguez et al., 1990). P150 also contains a Y domain and a proline hinge domain, both of unknown function. The order of these domains in p150 is NH<sub>2</sub>-methyltransferase-Y domain-proline hinge domain-X domain-protease-COOH. P90 contains domains which share similarity with RNA-dependent RNA polymerases and helicases of other RNA viruses (Gros and Wengler, 1996; Kamer and Argos, 1984).

Together, p150 and p90 form the viral replicase which is necessary for replication of the virus genome. Not surprisingly, deletion mutations of various regions of the nonstructural proteins resulted in the inability of RV replicons to replicate (Tzeng et al., 2001). Proteolytic processing of the p200 polyprotein marks the switch from synthesis of negative strand genomic RNA to synthesis of plus strand RNA (Liang and Gillam, 2000).

In Vero cells infected with RV, p150 localizes to long tubular structures late in infection (48 hours post-infection) (Kujala et al., 1999). Detailed study of these structures, using confocal microscopy, revealed that they colocalized with both anti-tubulin and anti-bromodeoxyuridine antibodies in cells in which newly synthesized RNA was labeled with bromouridine. Furthermore, transmission electron microscopy showed that p150 localizes to RV replication complexes (the RV replication complex is discussed in greater detail in section 1.7.2.) indicating that the tubular structures observed in RV infected cells are the sites of viral RNA synthesis and confirm that p150 localizes to sites of virus replication. The subcellular localization of p90 has not been reported.

### **1.6.2. Structural proteins**

The RV genome encodes three structural proteins: a capsid protein and two envelope proteins, E2 and E1 (Oker-Blom et al., 1983). The structural proteins are

translated as a polyprotein precursor from the subgenomic RNA in the order NH<sub>2</sub>-C-E2-E1-COOH (Oker-Blom, 1984) (Figure 1.2). *In vitro* transcription/translation of the cDNA encoding the RV structural proteins results in a polyprotein of 110 kDa. In the presence of microsomes, the polyprotein is cleaved into the three structural components indicating that cleavage is carried out by host cell signal peptidase in the lumen of the ER (Clarke et al., 1987; Marr et al., 1991; Suomalainen et al., 1990).

Coordinated expression of the RV structural proteins in mammalian cells, in the absence of genomic RNA, results in the assembly and secretion of virus-like particles (RLPs) which resemble native virions in terms of morphology and antigenicity (Hobman et al., 1994; Qiu et al., 1994). RLPs have served as a very useful tool for studying virus assembly and as a consequence, the role of RV structural proteins and their domains in assembly is relatively well understood.

#### **1.6.2.1. Capsid**

Capsid is a phosphoprotein with an apparent molecular mass of 35 kDa (Figure 1.3) (Clarke et al., 1987; Marr et al., 1991). The protein contains 300 amino acid residues, is rich in arginine and proline residues, particularly in its amino terminus, and has a net positive charge (pI=8.8) (Frey, 1994). Capsid often migrates as a doublet on SDS-PAGE gels. The reason for this remains unknown but it is not due to the use of an alternate translation start site or phosphorylation (Clarke et al., 1988; Marr et al., 1991). In virions, capsid exists as disulphide linked dimers but disulphide bonding of capsid is not necessary for formation of RLPs (Baron and Forsell, 1991; Lee et al., 1996b).

Cleavage of the RV capsid from the polyprotein precursor is distinct from that of alphaviruses. Alphavirus capsids contain an autoprotease that separates capsid from the polyprotein (Melancon and Garoff, 1987). As a consequence, alphavirus capsids are free in the cytoplasm of infected cells. RV capsid, in contrast, lacks autoprotease activity and separation of capsid from E2 is carried out by host cell signal peptidase (Clarke et al., 1987). As a result, the E2 signal peptide, which resides in the carboxy terminus of capsid, is retained as part of capsid (Hobman and Gillam, 1989; Suomalainen et al., 1990). Retention of this 23 amino acid hydrophobic sequence facilitates the membrane

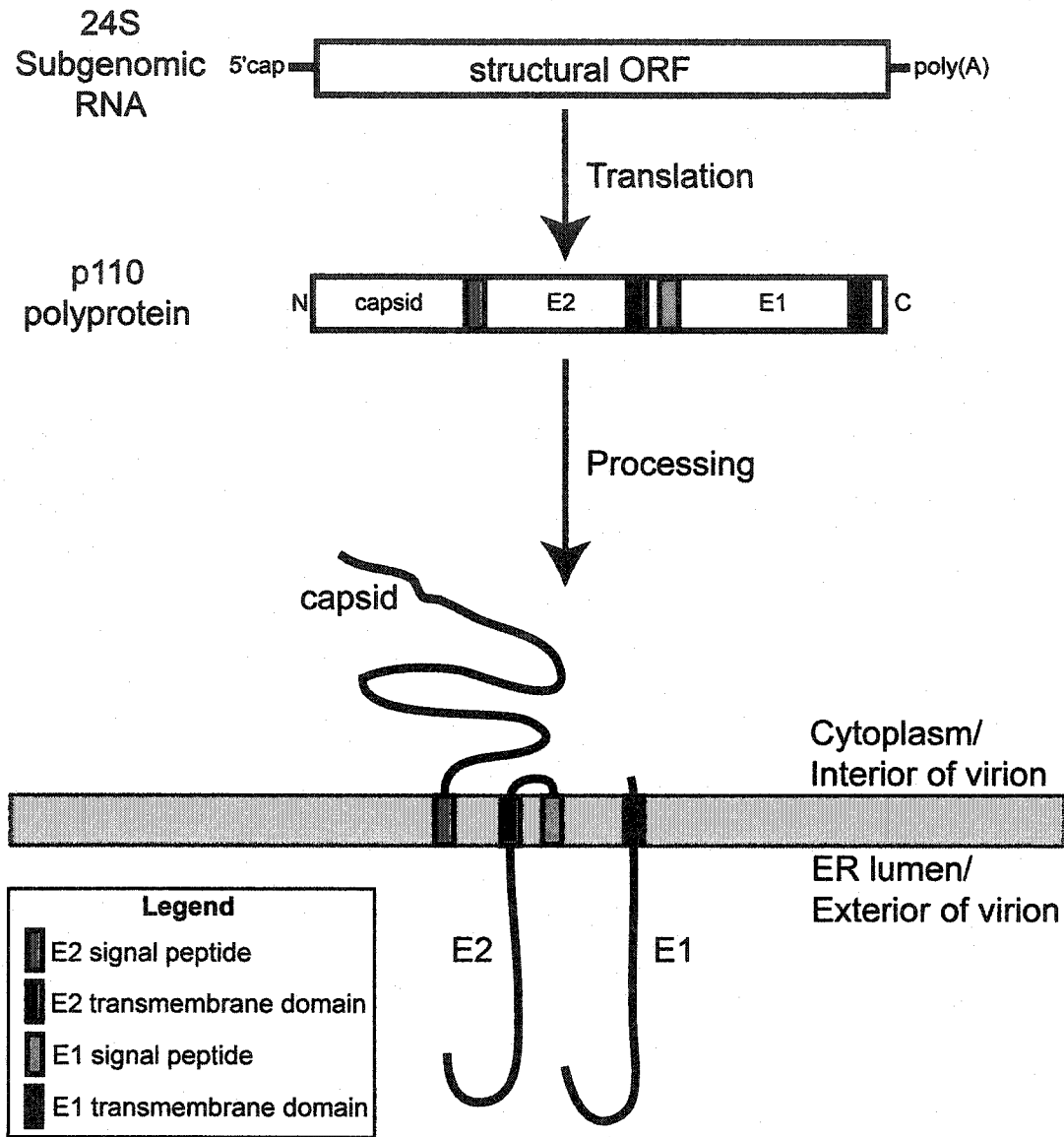


**Figure 1.2. Rubella virus structural proteins are translated from the subgenomic RNA.** The RV subgenomic RNA contains the 3' proximal open reading frame (ORF) encoding the structural proteins. The RV structural proteins are translated from the subgenomic RNA as a 110 kDa polyprotein precursor which is cotranslationally translocated into the ER. Two cleavages by host-cell signal peptidase result in the separation of the three structural proteins; the capsid phosphoprotein and the two envelope glycoproteins E2 and E1. E2 and E1 remain membrane associated via transmembrane domains in the carboxy terminus of each protein. Capsid retains the E2 signal peptide and, as a result, is also membrane associated.



**Figure 1.3. Schematic diagram of the rubella virus capsid.** Capsid is 300 amino acids in length and retains the E2 signal peptide (E2SP) as its carboxy terminus. The RNA binding region (RNA) of capsid resides between amino acids 28 to 56 and specifically interacts with the RV genomic RNA. Phosphorylation of serine 46 (Ser 46) within the RNA binding domain negatively regulates RNA binding. Capsid possesses an overall positive charge and contains a number of basic residues clustered in the amino portion of the protein (solid vertical lines).

association of a pool of capsid (Marr et al., 1991; Suomalainen et al., 1990). The membrane association of capsid has been proposed to have several important implications for assembly of RV virions (discussed below) (Baron and Forsell, 1991; Suomalainen et al., 1990). Indeed, retention of the E2 signal peptide on capsid was found to be necessary for assembly of RLPs (Law et al., 2001).

The primary function of capsid is to oligomerize with itself and bind viral genomic RNA to form the nucleocapsid during virus assembly. The RNA-binding domain of capsid resides within a 28 amino acid region between amino acid residues 28 to 56 which specifically binds to a packaging signal in the genomic RNA (Liu et al., 1996). Post-translational modification of capsid may play an important role in regulating the formation of nucleocapsids since phosphorylation of serine 46 within the RNA-binding domain has been shown to negatively regulate RNA binding (Law et al., 2003). This is thought to prevent nonspecific binding of cellular RNAs to capsid and to delay binding of genomic RNA until the virion components are targeted to the budding site. In addition, capsid may also regulate the events that drive budding of the virus through interactions with the envelope glycoproteins in a manner analogous to alphaviruses (Strauss et al., 1995). However, direct interactions between RV capsid and E2 and/or E1 have not yet been detected.

In addition to nucleocapsid assembly, capsid may also have functions in regulating virus replication. It has recently been demonstrated that capsid is able to complement replication of an otherwise replication incompetent RV replicon containing an in-frame deletion of a 169 amino acid region in p150 (Tzeng and Frey, 2003). The amino terminal region of the capsid protein (amino acid residues 1-88) was found to be sufficient for complementation in *trans*. This region in p150 is of unknown function and resides between the Y domain and the proline hinge. It is not known how capsid complements this deletion mutant but it has been proposed that capsid might be involved in stabilizing RNA. Another recent study has shown that capsid protein is able to regulate replication of RV replicons (Chen and Icenogle, 2004). The effects of capsid were dependent on the levels of replicon RNA. At low levels of RNA, capsid enhanced replication of viral transcripts but with higher levels of RNA, capsid inhibited replication

of viral transcripts. The E2 signal peptide was necessary but not sufficient for trans complementation in this study. These results are consistent with the idea that capsid functions early in replication by enhancing replication of viral RNA possibly by stabilizing RNA.

Another interesting feature of RV capsid is that it displays multiple intracellular localizations. In cells transiently expressing all three structural proteins, a pool of capsid is localized to the Golgi region (Baron et al., 1992; Hobman et al., 1994; McDonald et al., 1991). In the absence of E2 and E1, capsid has been reported to associate largely with the ER (Baron et al., 1992). In addition, capsid has also been reported to localize to mitochondria and to RV replication complexes by immunogold electron microscopy and by indirect immunofluorescence (Beatch and Hobman, 2000; Lee et al., 1999). Colocalization of capsid with p150 by confocal microscopy has also been reported (Kujala et al., 1999). This localization of capsid with nonstructural proteins is unique among the RV structural proteins since E2 did not colocalize with p150 in this study. The presence of capsid at multiple cellular sites suggests that it has functions other than solely forming nucleocapsids.

#### **1.6.2.2. Envelope proteins**

E2 and E1 are type I membrane proteins which dimerize to form the spike complexes on the surface of the virion. The major functions of these spikes are to recognize receptors on the host cell and to mediate fusion with host cell membranes (Katow and Sugiura, 1988). The envelope proteins, E1 in particular, are also the major antigenic determinants against which neutralizing antibodies are directed (Waxham and Wolinsky, 1985).

E1 is 481 amino acid residues in length with an apparent molecular mass of 58 kDa on SDS-PAGE and contains three N-linked glycan moieties (Hobman et al., 1991). An amino terminal signal peptide facilitates translocation of E1 into the ER and a 22 amino acid hydrophobic sequence at its carboxy terminus mediates membrane association (Hobman et al., 1988). E1 also contains a carboxy terminal tail of 13 amino acids which is exposed to the cytoplasm (Figure 1.2).

E2 is 282 amino acid residues in length and contains two stretches of hydrophobic amino acid residues near its carboxy terminus: an 18 amino acid transmembrane domain which mediates membrane association and the E1 signal peptide (Baron et al., 1992; Clarke et al., 1987). These two hydrophobic domains are separated by a short, 7 amino acid loop containing a number of basic residues. Like E1, translocation of E2 into ER membranes is mediated by an amino terminal signal peptide (Hobman and Gillam, 1989) (Figure 1.2). E2 is heavily glycosylated and contains both N-linked and O-linked carbohydrates (Lundstrom et al., 1991; Qiu et al., 1992).

## **1.7. Rubella virus life cycle**

The RV life cycle is similar to that of alphaviruses in many respects but there are several major differences. As discussed above, RV replication is less efficient and much slower than that of alphaviruses (Hemphill et al., 1988). Also, the membrane association of the capsid protein is thought to confer several important differences between the replication of RV and alphaviruses. The consequences of these differences are discussed below. A schematic diagram of the RV life cycle is shown in Figure 1.4.

### **1.7.1. Attachment and internalization**

Attachment of the virus to cells is rapid although the host cell receptor for the virus remains unknown (Bardeletti et al., 1972). However, lipids are known to be important for virus binding since treatment of cells with phospholipases reduces virus infectivity (Mastromarino et al., 1990). Following binding to the cell, the virus is internalized by receptor-mediated endocytosis (Petruzzello et al., 1996). At low pH, the envelope glycoproteins become fusogenic and capsid undergoes a conformational change and becomes hydrophobic (Katow and Sugiura, 1988; Mauracher et al., 1991). These results suggest that the acidic environment of the endosome supports fusion of the viral envelope with cellular membranes and release of genomic RNA from the nucleocapsid.

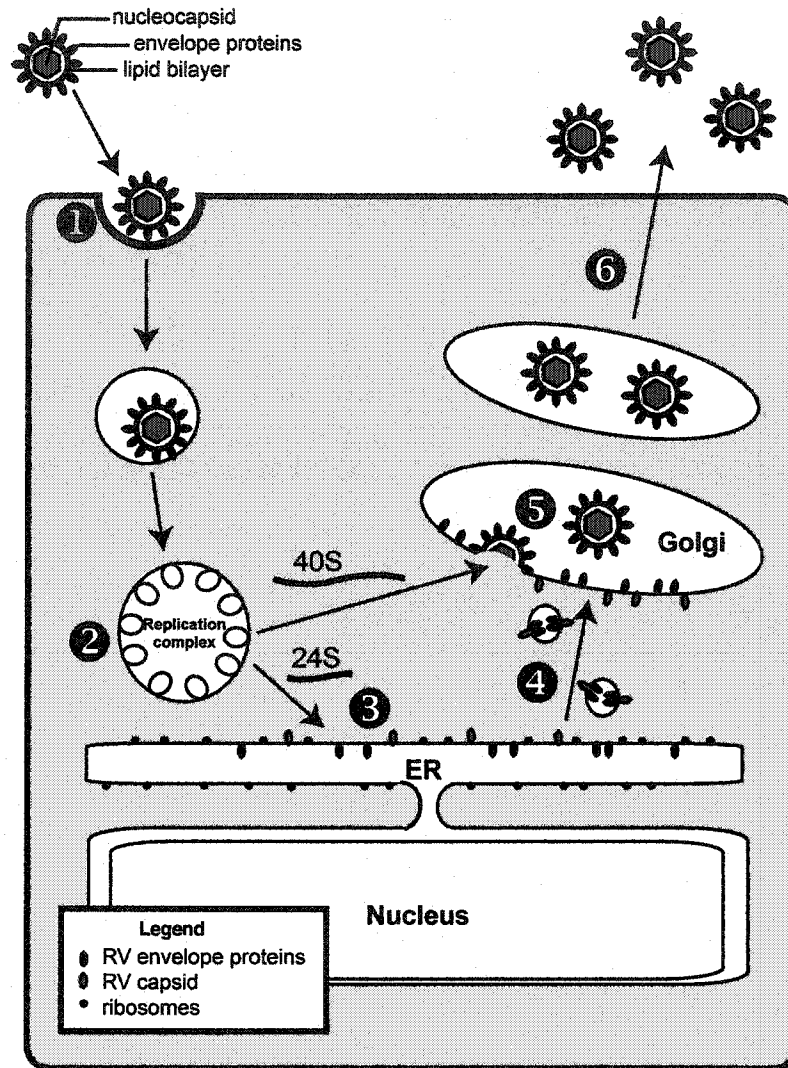


**Figure 1.4. The rubella virus life cycle.** 1) *Virus attachment and internalization.* Virions bind to an unknown host-cell receptor and enter the cell by receptor-mediated endocytosis. The low pH of endosomes induces fusion of the envelope proteins with cellular membranes and a conformational change in capsid which allows for the release of the genomic RNA. 2) *Virus replication.* Replication of the virus genomic RNA occurs at replication complexes derived from modified endosomes and lysosomes. 3) *Translation and processing of the structural proteins.* The structural proteins are translated from the subgenomic RNA (24S) as a polyprotein precursor and are cotranslationally processed by host cell signal peptidase at the ER. Individual structural proteins then undergo a series of post-translational modifications. 4) *Transport of structural proteins to the viral budding site.* Following processing, the structural proteins are targeted to the Golgi in a manner that requires the transmembrane domains of the structural proteins. 5) *Virus assembly.* Packaging of the genomic RNA (40S) and assembly of virus particles occurs at the Golgi. Formation of nucleocapsids is membrane associated and coincident with virus budding. Virions bud into the Golgi lumen. 6) *Virus secretion.* Following assembly, virions are secreted from the cell via exocytosis.

### 1.7.2. Replication

Togavirus replication occurs at specific intracellular sites in association with cellular membranes. Cytoplasmic vacuoles containing a series of irregularly shaped invaginations or spherules, approximately 60 nm in diameter, lining the internal face of the membrane are observed in RV infected cells (Lee et al., 1992). The spherules are connected to the vacuole via a thin membranous neck. Antibodies that recognize p150 and double stranded RNA label the spherules indicating that they are the sites of viral RNA synthesis (Kujala et al., 1999; Lee et al., 1994). The vacuoles colocalize with lysosomal markers suggesting that they are derived from endosomes or lysosomes (Magliano et al., 1998). These structures are referred to as cytopathic vacuoles, virus-modified lysosomes or replication complexes.

Similar replication complexes were previously identified in alphavirus infected cells (Froshauer et al., 1988; Peranen and Kaariainen, 1991). However, there are several important distinctions between the replication complexes of RV and alphaviruses. First, assembled nucleocapsids are rarely observed near replication complexes in RV infected cells whereas, in alphavirus infected cells, nucleocapsids are regularly observed surrounding the replication complexes. RV capsid has been detected at the cytoplasmic face of the replication complexes suggesting that nucleocapsid assembly may occur at these locations although this appears to be a rare event. In RV infected cells, formation of the replication complexes coincides with the rearrangement of other cellular structures. Specifically, rough ER and Golgi are found in close proximity to the virus-modified lysosomes and mitochondria cluster to regions of the cell containing replication complexes (Lee et al., 1996a; Lee et al., 1992; Risco et al., 2003). It has been suggested that mitochondria are relocalized in proximity to replication complexes since these are areas of high energy requirement. While mitochondrial aggregation to sites close to replication complexes also occurs in alphaviruses, the close association of the rough ER and Golgi with replication complexes is unique to RV infected cells. The reasons for the differences between RV and alphavirus replication complexes are not known but it is likely due to the fact that RV nucleocapsid assembly occurs in association with membranes whereas assembly of alphavirus nucleocapsids does not (see section 1.7.4.).

Recruitment of ER and Golgi membranes to the replication complexes is likely necessary to facilitate both rapid translation of the structural proteins and packaging of the genomic RNA. Possibly, the membrane association of capsid may be important for this feature of RV replication.

### **1.7.3. Targeting of structural proteins to the budding site**

Following synthesis of the subgenomic RNA, the RV structural proteins are cotranslationally inserted into ER membranes and the viral polyprotein is cleaved by signal peptidase at two sites to generate the three structural proteins (Hobman and Gillam, 1989; Hobman et al., 1988). The structural proteins are then post-translationally modified and transported to the Golgi complex which is the primary site of virus budding.

Processing and transport of the RV structural proteins, particularly the envelope proteins, has been well studied using coordinate and individual expression of these proteins. When co-expressed, E2 and E1 dimerize, form intramolecular disulphide bonds in the ER and are transported to, and retained in, the Golgi (Baron and Forsell, 1991; Hobman et al., 1993). However, when expressed alone, E1 does not target to the Golgi, but rather, is retained in a smooth ER-like compartment (Hobman et al., 1992). Thus, transport of E1 to the Golgi is dependent on coexpression of E2. The transmembrane domains of the structural proteins have important roles in regulating the localization and transport of these proteins. The carboxy terminal portion of E1, containing the transmembrane domain and the cytoplasmic tail, contains an ER retention signal which prevents passage of the protein through the ER (Hobman et al., 1997). Coexpression of E2 is able to mask the ER retention signal in E1 and allow transport of the E2-E1 heterocomplex from the ER to the Golgi. The transmembrane domain of E2, in turn, contains a Golgi retention signal which results in the retention of the E2-E1 heterodimer in this compartment (Hobman et al., 1995).

The specific regulation of RV glycoprotein transport appears to serve as a quality control mechanism. The half-life for transport of the RV glycoproteins to the Golgi is 60 to 90 minutes (whereas for alphavirus glycoproteins it is approximately 25 minutes)

(Hobman, 1993). Dimerization of E2 and E1 in the ER is not rate limiting since E2 and E1 associate rapidly following synthesis (Hobman et al., 1993). Rather, the rate-limiting step for transport of the glycoproteins is likely the slow maturation and folding of E1 in the ER since E2 achieves its mature conformation much faster than E1 (Hobman et al., 1993). E1 glycosylation mutants display decreased immunogenicity indicating that proper glycosylation is important to ensure proper folding of E1 (Hobman et al., 1991). Thus, the ER retention signal in E1 is thought to function by ensuring that E1 is retained in the ER until its proper conformation is achieved. Replacement of the E1 transmembrane domain with the VSV G transmembrane domain did not block transport of E2 or E1 to the Golgi but the rate of transport was faster (Garbutt et al., 1999b; Hobman et al., 1995). This suggests that the E1 transmembrane domain retains E1 in the ER until proper folding has been achieved. Once E1 achieves its proper conformation, E2 is able to mask the ER retention signal of E1 ensuring that only properly folded E2-E1 heterodimers are transported to the Golgi. The E2 Golgi retention signal, in turn, then holds the envelope proteins in the Golgi where budding occurs.

The E2 transmembrane and cytoplasmic domains are also important for physical interactions with E1 since replacement of the E2 transmembrane domain or arginine to alanine mutations in the cytoplasmic tail of E2 blocked binding of E2 to E1 (Garbutt et al., 1999b).

E2 also plays a crucial role in targeting of capsid to the Golgi. Expression of capsid alone in COS cells results in targeting of capsid to the ER but not to the Golgi. However, co-expression of capsid with E2 and E1 results in a large pool of capsid being targeted to the Golgi region (Baron et al., 1992; Hobman et al., 1990). The carboxy terminus of E2, including the transmembrane domain, plays a critical role in transport of capsid from the ER since replacement of this domain with the transmembrane domain of VSV G abrogates targeting of capsid and E2 to the Golgi (Garbutt et al., 1999b). Mutations in the cytoplasmic domain of E2 also reduced colocalization of capsid and E2. In contrast, replacement of the E1 transmembrane domain or cytoplasmic tail had no effect on targeting of capsid to the Golgi. Together, these results indicate that the E2 carboxy terminus containing the transmembrane region has an important role in

regulating the targeting of the RV structural proteins to the virus budding site.

The E2 signal peptide, which mediates the membrane association of capsid, is also necessary for proper intracellular targeting of capsid. Replacement of the E2 signal peptide with similar transmembrane regions from either VSV G or CD8 allowed membrane association of capsid but abrogated both targeting of capsid to the perinuclear region and formation of RLPs (Law et al., 2001). Thus, the E2 signal peptide is necessary for membrane association of capsid and contains specific information which is necessary for targeting of capsid to the Golgi. Presumably, the E2 signal peptide of capsid associates with the transmembrane regions of E2 and/or E1, a process that may facilitate transport of capsid from the ER to the Golgi by incorporation into transport vesicles.

#### **1.7.4. Virus assembly and secretion**

RV budding has been reported to occur at both the Golgi complex and the plasma membrane depending on cell type and the time postinfection (Bardeletti et al., 1979; von Bonsdorff and Vaheri, 1969). However, several lines of evidence suggest that the primary site for virus budding is at the Golgi complex. The presence of a Golgi retention signal in E2 results in colocalization of all three structural proteins at the Golgi when expressed together in tissue culture cells and, as a result, only a very small fraction of E2 or E1 reaches the plasma membrane (Baron et al., 1992; Hobman et al., 1990). Also, reports of budding at the plasma membrane typically occur late in infection suggesting that this is not the normal budding site. Furthermore, virion membrane composition is similar to that of intracellular membranes (Bardeletti and Gautheron, 1976).

Unlike alphavirus nucleocapsids, which are preformed in the cytoplasm of infected cells prior to budding, RV nucleocapsids form in association with cellular membranes co-incident with budding and are only rarely observed in the cytoplasm (Lee et al., 1999; Oshiro et al., 1969). It has been suggested that the membrane association of capsid is, at least partly, responsible for this feature of RV assembly (Suomalainen et al., 1990). Thus, RV must utilize a mechanism to prevent premature assembly of nucleocapsids. However, the exact mechanisms that regulate virus budding remain unknown. The transmembrane domains of the structural proteins are important for

targeting and may be involved in the regulation of budding. In addition, the carboxy terminal cytoplasmic loop of E2 contains a number of basic residues which may interact with acidic residues in the capsid protein. Mutation of these residues, to amino acids which reduced the net charge of this region, prevented assembly of RLPs (Garbutt et al., 1999b). It is also possible that interactions with host cell proteins may regulate budding.

Recently, a morphological study using freeze-substitution electron microscopy indicated that virions undergo a maturation process following budding into the Golgi (Risco et al., 2003). Interestingly, several lines of evidence suggest that the E1 transmembrane and cytoplasmic domains might have some function late in assembly. Replacement of the E1 transmembrane domain allows for proper assembly and budding of RLPs in the Golgi but secretion of RLPs was blocked indicating that this domain is necessary for secretion (Garbutt et al., 1999b). Furthermore, a point mutation in the E1 transmembrane domain reduced virus yield by 90% using an RV infectious clone (Yao and Gillam, 1999). Further examination revealed that mutation of specific amino acids in the E1 transmembrane and cytoplasmic domains allowed virion assembly and budding into the Golgi but blocked secretion of virions (Qiu et al., 2000; Yao and Gillam, 2000). Thus, it is possible that E1 is involved in a late stage maturation event that is necessary for virus secretion through the cellular secretory pathway. Alternatively, these results could suggest that the transmembrane and cytoplasmic domains of E1 are necessary for ensuring the proper conformation of the glycoproteins which is, in turn, necessary for secretion but not assembly.

## **1.8. Rubella virus cytopathic effects**

### **1.8.1. Effects of RV replication on cellular morphology**

The replication of positive strand RNA viruses occurs in association with membranes (Bienz et al., 1983; Carette et al., 2002a; Carette et al., 2002b; Egger et al., 2002; Froshauer et al., 1988; Kujala et al., 2001; Lee and Ahlquist, 2003; Miller et al., 2001). Thus, these viruses must possess mechanisms to modify cellular membranes and structures to facilitate virus replication. How this is accomplished, however, remains

poorly understood.

Several changes to cellular ultrastructure have been observed in RV infected cells. As described above, RV replication complexes are derived from modified lysosomes and are distinct from those of alphaviruses (see section 1.7.2) (Lee et al., 1992; Lee et al., 1994; Magliano et al., 1998). Changes in mitochondrial localization and morphology also occur in RV infected cells. As infection progresses, the numbers of mitochondria surrounding the replication complexes increase and mitochondria develop a club-shaped appearance and display a loss of cristae (Lee et al., 1996a). In addition, electron dense zones, 22-25 nm in thickness, between the membranes of various organelles are observed in RV infected cells (Lee et al., 1996a). Three types of confronting membranes have been identified: between the outer membrane of a mitochondrion and rough ER membranes, between the outer membranes of adjacent mitochondria, and between adjacent ER membranes. Interestingly, in SFV infected cells, mitochondria cluster to replication complexes but they remain normal in appearance. Furthermore, the formation of confronting membranes appears to be a unique feature of RV infection amongst togaviruses since these structures are not observed in SFV infected cells. The composition and function of these electron dense zones remains unknown. Lee *et al.*, were not able to detect virus structural proteins in the plaques but have localized capsid to mitochondria by immunogold electron microscopy. Changes in mitochondrial localization and formation of electron dense plaques are first detected approximately 12 hours post-infection and are maximal late in infection (48 to 72 hours post infection). Interestingly, these changes coincide with expression of the RV structural proteins. Together, these results suggest that RV structural proteins may have some role in mitochondrial aggregation and formation of confronting membranes (Lee et al., 1996a; Lee et al., 1999). Lee et al. (1996a) have suggested that mitochondrial aggregation to replication complexes might serve as a mechanism to increase the amount of energy available at sites of virus replication.

### 1.8.2 Cytopathic effect

RV typically causes limited cytopathology in most cultured cells. Cellular protein and RNA synthesis are not significantly impaired and little cell damage is observed when most cell lines are infected with RV at low MOIs (Hemphill et al., 1988; Maes et al., 1966; Vaheri and Cristofalo, 1967). In contrast, host cell protein and RNA synthesis is severely impaired in alphavirus infected cells and cell death from apoptosis often occurs 12 to 24 hours post infection (Kaariainen and Soderlund, 1978; Strauss and Strauss, 1994). In addition, RV can initiate persistent infections when cells are infected at low MOI (Stanwick and Hallum, 1974). This is likely due, in part, to the limited cytopathic effect and the inability of the virus to shut down host cell macromolecular synthesis.

Although cytopathology is typically minimal, RV infection has been shown to affect cell growth. In human fibroblasts, RV infection results in perturbation of cell cycle regulation leading to a slower growth rate (Plotkin et al., 1965; Plotkin and Vaheri, 1967). Reports of other abnormalities, which affect cellular growth, include inhibition of mitosis (Vaheri and Cristofalo, 1967), chromosomal breaks (Nusbacher et al., 1967), depolymerization of actin filaments (Bowden et al., 1987) and an altered growth response to EGF (Yoneda et al., 1986).

Several recent studies have demonstrated that RV is able to induce apoptosis in certain cultured cell lines. A portion of RK-13, Vero and BHK cells display cytopathic effect, round up and detach from the culture surface in response to RV infection. The majority of detached cells display characteristics of apoptosis including membrane blebbing, DNA laddering, nuclear condensation, TUNEL positive nuclei and relocalization of phosphatidylserine to the outer leaflet of the plasma membrane (Duncan et al., 1999; Hofmann et al., 1999; Pugachev and Frey, 1998). Treatment of cells with the caspase inhibitors z-VAD or zDEVD-fmk decreased the number of apoptotic cells indicating that the virus induced cell death occurs in a caspase dependent manner (Duncan et al., 1999; Pugachev and Frey, 1998).

Various cell lines display different sensitivity to RV infection (Duncan et al., 1999; Megyeri et al., 1999). For example, when infected with the same MOI (5 PFU / cell), 75% of RK-13 cells became detached from tissue culture dishes whereas 25% of

Vero and only 2 % of BHK became detached from tissue culture dishes at 48 hours post-infection (Duncan et al., 1999). The difference in the ability of RV to induce cytopathic effect in various cell lines has been suggested as an explanation for the ability of RV to selectively affect the organogenesis of specific organs in CRS fetuses (Duncan et al., 1999).

Apoptosis induced by RV is asynchronous and not all cells succumb to cell death. In Vero cells, all cells in a monolayer were found to be infected by 48 hours. However, up to 40% of cells remained viable and displayed no signs of apoptosis at 5 days postinfection (Pugachev and Frey, 1998). Similar results were found in RK-13 and BHK cells showing that not all cells are susceptible to RV induced apoptosis (Duncan et al., 1999). In addition, persistently infected cultures can be established. Persistently infected cells remain sensitive to chemical inducers of apoptosis such as staurosporine suggesting that these cells do not develop as a result of the selection of apoptosis resistant clones (Pugachev and Frey, 1998). It also suggests that RV does not possess anti-apoptotic mechanisms.

The mechanisms by which RV induces apoptosis are not clearly defined. One report showed that protein levels of the pro-apoptotic transcription factor p53 are upregulated in RV infected Vero cells and that expression of a dominant negative form of p53 resulted in decreased apoptosis in response to RV infection (Megyeri et al., 1999). This suggests that RV induced apoptosis may occur, at least partly, through a p53 dependent pathway. However, protein levels of p53 and p53-regulated Bcl family members were not changed during infection in another study, also using Vero cells (Hofmann et al., 1999). Conflicting roles over the involvement of Bcl family members in regulating apoptosis have also been reported. For instance, Bcl-X<sub>L</sub> protected BHK but not RK-13 cells from the apoptotic effects of RV (Duncan et al., 1999).

Signs of apoptosis are typically first observed in various cultured cell lines at 48 hours post-infection, when synthesis of virus proteins is maximal (Duncan et al., 1999; Hofmann et al., 1999; Pugachev and Frey, 1998). In addition, RLPs and UV inactivated virus are incapable of inducing apoptosis suggesting that virus replication is necessary for the induction of apoptosis (Duncan et al., 1999; Hofmann et al., 1999; Megyeri et al.,

1999). Together these results suggest that viral proteins, as opposed to viral RNA or a soluble factor in the medium, are involved in initiating the apoptotic pathway. However, there are conflicting reports regarding the involvement of the various viral proteins. Pugachev *et al.* mapped the cytopathic determinants to the nonstructural proteins using an infectious clone (Pugachev *et al.*, 1997) and apoptosis was not detected in Vero cells transfected with the RV structural proteins (Hofmann *et al.*, 1999) suggesting that the non-structural proteins are important for RV induced apoptosis. However, in another study, using RK-13 cells, it was determined that capsid is sufficient to induce apoptosis (Duncan *et al.*, 2000). The region of capsid important for induction of apoptosis was mapped to the amino terminal 170 amino acids. It was also determined that membrane association was important for the apoptotic effects of capsid. The reasons for the different abilities of RV structural and nonstructural proteins to induce apoptosis are unclear. The use of different cell types may account for the conflicting results.

Organs from CRS babies are often smaller than normal due to a reduced number of cells (Naeye and Blanc, 1965). It remains to be determined if reduced organ size is due to the reduced growth rate of RV infected cells or if apoptosis is responsible for the destruction of precursor cells early in organogenesis.

### **1.9. Multifunctional capsid proteins**

The RV capsid is multifunctional (see section 1.6.2.1). The main function of this protein is to oligomerize with itself and bind the genomic RNA to form the viral nucleocapsid. It also contains specific information that allows for targeting to the viral budding site in conjunction with the viral envelope proteins. In addition, capsid has been shown to complement replication of replicons containing a deletion in the nonstructural protein p150. Capsid has also been implicated in the induction of apoptosis in a manner that is dependent on its membrane association. Finally, capsid has been shown to exhibit several different subcellular localizations, including ER, Golgi, mitochondria and the virus replication complex.

The multifunctional nature of capsid is not surprising because virus genomes are under selective pressure to keep their genomes as small as possible. Small genomes

require less resources to package and having a smaller genome reduces the chances of incorporating deleterious mutations. As a consequence, virus proteins often have multiple functions and carry out these functions via interactions with host cell proteins. Capsid proteins are no exception and the capsids of several RNA viruses have been shown to possess functions in addition to packaging of the virus genome. For example, alphavirus capsid proteins, in addition to binding genomic RNA, contain a protease domain which separates the capsid from the polyprotein precursor (Melancon and Garoff, 1987). Alphavirus capsids also play an integral role in the regulation of virus assembly and disassembly. These capsids interact with the cytoplasmic domain of the E2 envelope glycoprotein to drive virus budding (Lopez et al., 1994; Zhao et al., 1994) and upon entry into a newly infected cell, nucleocapsids are disassembled and genomic RNA is released into the cytoplasm by binding of the capsid to ribosomes (Wengler, 1984).

A direct role for the nucleocapsid of mouse hepatitis virus (MHV) in replication of the virus genomic RNA has recently been demonstrated. The nucleocapsid protein of MHV colocalizes with the replicase proteins in infected cells (van der Meer et al., 1999) and replication of MHV genomic RNA is inefficient in the absence of the nucleocapsid (Baric et al., 1988; Compton et al., 1987) suggesting that this protein plays some role in replication of genomic RNA.

In addition to functions directly involved in virus replication and assembly, nucleocapsid proteins have been shown to regulate various cellular processes. For example, the hepatitis C virus (HCV) core protein is well studied and has several functions in addition to the binding of genomic RNA. Expression of HCV core in CHO or HepG2 cells results in the accumulation and targeting of core to lipid droplets in the cytoplasm suggesting that core affects cellular lipid metabolism (Barba et al., 1997). Several groups have also identified a role for the HCV core in the regulation of cellular gene expression. These include modulation of the activity of NF- $\kappa$ B, AP-1, p53 and p21 amongst others (Lu et al., 1999; Ray et al., 1997; Ray et al., 1998; Shrivastava et al., 1998). Regulation of transcription factors can affect processes such as cell cycle (Cho et al., 2001), cellular transformation (Jin et al., 2000) and apoptosis (Otsuka et al., 2002). Interestingly, HCV core has both pro- and anti-apoptotic properties. Core binds to the

death domain of the tumor necrosis factor receptor which sensitizes cells to TNF induced apoptosis (Ruggieri et al., 1997; Zhu et al., 1998). The anti-apoptotic functions attributed to core are due to up regulation of anti-apoptotic cellular proteins such as Bcl-XL and inhibitor of caspase-activated DNase (Otsuka et al., 2002; Sacco et al., 2003).

Thus, it has been clearly demonstrated that, in addition to their main function of packaging genomic RNA, the nucleocapsid proteins of RNA viruses often perform additional functions during virus replication. These include, the regulation of virus budding and replication, regulation of host cell pathogenic effect and the modulation of cellular functions such as cellular gene expression and lipid metabolism.

### **1.10. Project rationale**

The primary function of the RV capsid is to interact with virus genomic RNA and homo-oligomerize to form the nucleocapsid. In recent years, additional functions of capsid have been also been identified including: the regulation of virus budding; the ability to complement a deletion mutant in the nonstructural protein p150; and the ability to induce apoptosis in cultured cells. However, very little is known about how RV capsid may conduct these activities. It is highly likely that capsid mediates these functions via interactions with host cell proteins. At the time that this study was initiated, nothing was known regarding such interactions. We set out to identify capsid-binding proteins and determine the functions of these interactions on RV and host cell biology. We have found that capsid binds several host cell proteins and that capsid plays a role in rearrangement of mitochondrial localization which is important for virus replication.

## **CHAPTER 2. MATERIALS AND METHODS**

## 2.1. Reagents and Materials

### 2.1.1. Reagents

Reagents and supplies (Table 2-1) were used as recommended by the manufacturer unless otherwise mentioned.

**Table 2-1. Reagents**

Reagent	Source
40 % Acrylamide/Bis-acrylamide solution, 29:1	Bio-Rad
acetic acid	Fisher
adenosine triphosphate (ATP)	Sigma
agar	Difco
agarose A, electrophoresis grade	Rose Scientific Ltd.
ammonium persulphate	BDH
ampicillin	Sigma
baker's yeast tRNA	Roche
blasticidin S HCl	Invitrogen
bovine serum albumin (BSA)	Sigma
bromophenol blue	BDH
carbonyl cyanide <i>m</i> -chlorophenylhydrazone (CCCP)	Sigma
coenzyme A	Sigma
Complete™ EDTA-free protease inhibitor	Roche
coomassie Brilliant Blue	ICN
CSM-leu-his-trp-ade (complete supplement mixture minus leucine, histidine, tryptophan and adenine)	BIO 101
CSM-leu-his	BIO 101
cyanogen bromide-activated Sepharose 4B	Pharmacia
D-(+)-glucose	Sigma
dimethyl sulphoxide (DMSO)	Sigma
dithiothreitol (DTT)	ICN

Reagent	Source
doxycycline	Sigma
Dulbecco's modified Eagle's medium	Sigma
EPON resin (TAAB 812 resin)	Marivac
ethanol	Commercial Alcohols
ethylenediaminetetraacetic acid (EDTA)	Sigma
fetal bovine serum	Invitrogen
fibronectin	Sigma
formaldehyde, 37% (v/v)	BDH
glucose oxidase	Sigma
L-glutamine	Gemini Bio Products
glutaraldehyde, 25%	Ted Pella Inc
glutathione Sepharose 4B	Amersham Biosciences
glycerol	BDH
glycine	EM Science
HEPES	Invitrogen
hygromycin B	Invitrogen
hydrochloric acid	Fisher
kanamycin	Sigma
isopropanol	Fisher
luciferin	Luciferin
lead citrate	Fisher
magnesium carbonate	BDH
magnesium sulphate	Sigma
Mitotracker Red CMXRos	Molecular Probes
methanol	Fisher
minimal essential medium Eagle	Sigma
minimum essential medium lacking cysteine/methionine	ICN Biomedicals
neutral red solution	Sigma
N-Lauroyl-sarcosine	Sigma

Reagent	Source
N,N,N',N'-tetramethylethylenediamine (TEMED)	Invitrogen
paraformaldehyde	Fisher
OptiMEM	Invitrogen
osmium tetroxide	Fisher
penicillin – streptomycin solution (cell culture grade)	Gemini Bio Products
peptone	Difco
phenol, buffer-saturated	Invitrogen
phenylmethylsulphonylfluoride (PMSF)	Roche
phosphate-free medium	Invitrogen
propylene oxide	Fisher
protein A Sepharose	Amersham Biosciences
protein G Sepharose	Amersham Biosciences
Restore™ Western Blot Stripping Buffer	Pierce
salmon sperm DNA, sonicated	Sigma
Sf-900 II serum-free medium	Invitrogen
silver nitrate	BDH
sodium azide	Sigma
sodium chloride	Merck
sodium dodecyl sulfate (SDS)	Bio-Rad
sodium fluoride	Sigma
sodium hydroxide	BDH
sodium salicylate	EM Science
sodium orthovanadate	Sigma
sodium thiosulphate	Sigma
sorbitol	BDH
staurosporine	Sigma
sucrose	BDH
tetramethylrhodamine ethyl ester, perchlorate (TMRE)	Molecular Probes
translation grade <sup>35</sup> S methionine (1000 Ci/mmol)	Amersham Biosciences

Reagent	Source
tetrasodium pyrophosphate	Sigma
tumor necrosis factor- $\alpha$ (TNF $\alpha$ )	Calbiochem
Tris base	Roche
Triton X-100	BDH
Tween 20 (polyoxyethylenesorbitan monolaureate)	Caledon
uranyl acetate	Fisher
Vectashield mounting medium	Vector Laboratories
xylene cyanol FF	Sigma
yeast extract	Difco
yeast nitrogen base without amino acids and ammonium sulfate	Difco

### 2.1.2. Multicomponent systems

FuGENE 6 Transfection Reagent	Roche
<i>In vitro</i> toxicology assay kit – MTT based	Sigma
Matchmaker Two-Hybrid Systems 2 and 3	Clontech
MEGAscript kit	Ambion
mMessage mMachine <sup>TM</sup> High Yield Capped RNA Transcription kit	Ambion
Mobius 1000 Plasmid kit	Novagen
Platinum <i>Pfx</i> DNA polymerase	Invitrogen
<i>Pwo</i> polymerase	Roche
Perfectin transfection reagent	Gene Therapy Systems Inc
PROTEINscript II coupled transcription/translation kit	Ambion
QIAEX II Gel Extraction kit	Qiagen
QIAquick PCR purification kit	Qiagen
TNT coupled transcription/translation kit	Promega
Wizard Plus Minipreps DNA purification system	Promega

### 2.1.3. Modifying enzymes

calf intestinal alkaline phosphatase	Roche
DNA polymerase I, large fragment (Klenow)	Invitrogen
restriction endonucleases	NEB, Promega, Invitrogen
T4 DNA ligase	NEB

### 2.1.4. Radiochemicals

cytidine $\alpha$ - <sup>35</sup> S triphosphate (600 Ci/mmol)	ICN
H <sub>3</sub> <sup>33</sup> PO <sub>4</sub> (4,000 Ci/mmol)	ICN
<sup>35</sup> S methionine ( <i>in vitro</i> translation grade) (1,000 Ci/mmol)	Amersham Biosciences
Pro-mix <sup>35</sup> S methionine-cysteine (1,000 Ci/mmol)	Amersham Biosciences

### 2.1.5. Detection systems

Trans-Blot Transfer Medium - nitrocellulose membrane (0.45 $\mu$ m pore size)	Bio-Rad
Immobilon-P (PVDF) membranes	Millipore
Rx film	Fuji
Supersignal Westpico Chemiluminescent Substrate	Pierce
Kodak X-Omat AR film	Kodak

### 2.1.6. Molecular size standards

1 kb DNA ladder	NEB
<sup>14</sup> C-labeled protein standards	Amersham Biosciences
Prestained protein ladder, ~10-180 kDa	Fermentas
Prestained protein marker, broad range	BioLabs

## 2.2. Commonly used buffers

The composition of commonly used buffers is listed in Table 2.2.

**Table 2-2. Buffered Solutions**

Buffered Solution	Composition
2 X sample buffer	200 mM dithiothreitol, 4% SDS, 0.2% bromophenol blue, 20% glycerol, 100 mM Tris HCl, pH 6.8
6 X DNA gel loading dye	40% sucrose, 0.25% bromophenol blue, 0.25% xylene cyanol FF
FSB	10 mM KOAc, pH 7.5, 45 mM MnCl <sub>2</sub> , 10 mM CaCl <sub>2</sub> , 10 mM KCl, 3 mM hexaminecobalt chloride, 10% glycerol
Gel running buffer (SDS-PAGE)	250 mM glycine, 0.1% SDS and 100mM Tris Base
Lower gel buffer	0.1% SDS, 375 mM Tris HCl, pH 8.8
Luciferase assay buffer	20 mM tricine, 1.07 mM Mg-carbonate, 2.67 mM MgSO <sub>4</sub> , 0.1 mM EDTA, 33.3 mM dithiothreitol, 270 μM coenzyme A, 470 luciferin, 530 μM ATP
NP40 Lysis buffer	150 mM NaCl, 2 mM EDTA, 1% NP40, 20 mM Tris HCl pH 7.4
PBS	137 mM NaCl, 2.7 mM KCl, 8 mM Na <sub>2</sub> HPO <sub>4</sub> , 1.5 mM KH <sub>2</sub> PO <sub>4</sub> , pH 7.4
PBSCM	137 mM NaCl, 8 mM Na <sub>2</sub> HPO <sub>4</sub> , 1.5 mM KH <sub>2</sub> PO <sub>4</sub> , 0.5 mM CaCl <sub>2</sub> , 1 mM MgCl <sub>2</sub> , 0.05% sodium azide, pH 7.4,
RIPA	150 mM NaCl, 0.5% sodium deoxycholate, 0.1% SDS, 1% NP40, 50 mM Tris HCl, pH 8.0
TAE	40 mM Tris-Acetate, 1 mM EDTA, pH 8.0
Transfer buffer	200 mM glycine, 25 mM Tris base, 20% methanol
TBST	137 mM NaCl, 2.7 mM KCl, 24 mM Tris HCl, pH 7.4, 0.05% Tween 20
TE	1 mM EDTA, 10 mM Tris HCl, pH 7.5
Upper gel buffer	0.1% SDS and 250 mM Tris HCl, pH 6.8
Z buffer	60 mM Na <sub>2</sub> HPO <sub>4</sub> ·7H <sub>2</sub> O, 40 mM NaH <sub>2</sub> PO <sub>4</sub> ·H <sub>2</sub> O, 10 mM KCl, 50 mM MgSO <sub>4</sub> ·7H <sub>2</sub> O, 50 mM β-mercaptoethanol

## **2.3. Antibodies**

### **2.3.1. Primary antibodies**

Monoclonal antibodies to RV capsid (H15 C22) and E1 (B2) were gifts from Dr. John Safford (Abbott Laboratories, North Chicago, IL) and Dr. Barbara Pustowitz, (University of Leipzig, Leipzig, Germany) respectively. Rabbit antiserum to p32 was a gift from Dr. Willie Russell (University of St Andrews, St Andrews, UK). Rabbit polyclonal antiserum to Par-4 and rabbit anti-PKC $\zeta$  (C-20) were purchased from Santa Cruz Biotechnology Inc. The monoclonal antibody to HSP 60 (SPA-806) was purchased from StressGen. The mouse hybridoma 9E10, which secretes anti-cmyc antibodies, was purchased from the American Type Culture Collection.

### **2.3.2. Secondary antibodies**

Double-labeling grade Texas Red-conjugated goat anti-mouse IgG, Texas Red-conjugated donkey anti-goat IgG and FITC-conjugated donkey anti-rabbit IgG were purchased from Jackson ImmunoResearch Laboratories. Horseradish peroxidase (HRP)-conjugated goat anti-mouse IgG, goat anti-rabbit IgG and donkey anti-goat IgG were purchased from Bio-Rad.

## **2.4. Cell lines and viruses**

### **2.4.1. Cell lines**

Vero, COS-1, RK-13, BHK and HEK 293T cells were obtained from the American Type Culture Collection. The T-REx-293 cell line was obtained from Invitrogen.

### **2.4.2. Viruses**

The M33 strain of rubella virus and the pBRM33 infectious clone were obtained from Dr. Shirley Gillam (University of British Columbia, Vancouver, BC). Recombinant

baculovirus (OB504-1) encoding capsid was a gift of Dr. Christian Oker-Blom (University of Jyväskylä, Jyväskylä, Finland).

## **2.5. DNA analysis and modification**

### **2.5.1. Isolation of plasmid DNA from *E. coli***

Plasmid DNA was prepared using either the WizardPlus Miniprep kit (Promega) or the Mobius 1000 Plasmid kit (Novagen). These kits are based on a modified alkaline lysis protocol (Sambrook et al., 1989).

### **2.5.2. Restriction endonuclease digestion**

Restriction endonuclease digestion of DNA fragments was typically performed in 20  $\mu$ l reactions using 0.2-2  $\mu$ g of DNA (Sambrook et al., 1989).

### **2.5.3. Polymerase chain reaction**

DNA sequences were amplified using the polymerase chain reaction (PCR). *Pwo* or *Pfx* DNA polymerases were used according to manufacturer's instructions. Typical reactions included 2-4 U DNA polymerase, 100-500 ng plasmid DNA as template, forward and reverse oligonucleotide primers (15 pmol each), 10  $\mu$ M of each dNTP (dATP, dTTP, dCTP and dGTP) and 1 X reaction buffer in a volume of 100  $\mu$ l. Reactions were performed for 30 cycles in a Robocycler Gradient 40 (Stratagene) or a in a DeltaCycler II System (ERICOMP).

### **2.5.4. Agarose gel electrophoresis**

DNA samples were mixed with 6 X DNA gel loading buffer (Table 2-2) and fragments were separated by electrophoresis in agarose gels (0.8-2% agarose (w/v) in TAE) containing 0.5  $\mu$ g ethidium bromide/ml (Sambrook et al., 1989). Electrophoresis was performed at 10 V/cm in TAE and DNA was visualized using an ultraviolet

transilluminator (FisherBiotech Electrophoresis Systems) or a FluoroChem FC imaging system (Alpha Innotech Corporation).

#### **2.5.5. Purification of DNA**

PCR fragments to be subjected to endonuclease restriction digestion were purified from polymerases and nucleotides using the QIAquick PCR Purification Kit (Qiagen). Following restriction endonuclease digestion and agarose gel electrophoresis, DNA fragments were excised from agarose gels using a clean razor blade and purified using the QIAEX II Gel Extraction Kit (Qiagen).

#### **2.5.6. Dephosphorylation of 5' ends**

When necessary, the 5' ends of digested plasmid vectors were dephosphorylated to prevent self ligation using calf alkaline intestinal phosphatase (CIP) according to manufacturer's instructions.

#### **2.5.7. Filling in of 5' overhangs**

To create blunt-ended DNA fragments, the 5' overhanging ends of digested fragments were filled in using the Klenow fragment of DNA polymerase I. Reactions contained 1-2  $\mu\text{g}$  of DNA, 5 U enzyme and 25  $\mu\text{M}$  of each dNTP and were carried out for 30 min at 30 °C.

#### **2.5.8. Ligation of DNA fragments**

Purified DNA fragments were ligated together using 1 U of T4 DNA ligase in the buffer supplied by the manufacturer. The molar ratio of insert to vector was approximately 3:1 and was carried out in a 20  $\mu\text{l}$  volume for 1 h at room temperature or overnight at 4 °C. A portion of the ligation mixture was then transformed into either chemical competent or electrocompetent *E. coli* DH5 $\alpha$ .

### 2.5.9. Chemical transformation of DH5 $\alpha$

Chemical competent *E. coli* DH5 $\alpha$  were prepared as follows. Cells were grown to OD<sub>600</sub>=0.3-0.5 in 30 ml 2 X YT (1.6% bacto-tryptone, 1.6% bacto-yeast extract and 0.5% NaCl (w/v) in deionized water). Cells were then harvested by centrifugation at 4,000 x g for 15 min at 4°C and washed in 5 ml of ice-cold FSB (Table 2-2). Cells were pelleted again, divided into three 1 ml aliquots and incubated on ice for 15 min in FSB plus DMSO (35  $\mu$ l). The cells were then washed 2 X with ice-cold FSB, divided into 200  $\mu$ l aliquots, frozen in a dry ice-ethanol bath and stored at -80°C until needed.

Transformation of chemical competent DH5 $\alpha$  was carried out according to the method of Sambrook *et al.* (1989). Briefly, competent cells were thawed on ice and 5-10  $\mu$ l of a ligation mixture or 100-500 ng of plasmid DNA was added to 50  $\mu$ l of cells. This mixture was incubated on ice for 30 min followed by a 45 second heat-shock at 42 °C. One ml of LB was added to the transformed cells and cells were allowed to recover by incubation in a rotary shaker for 1 h at 37 °C. Cells were plated on LB agar plates (1% bacto-tryptone, 0.5% bacto-yeast extract, 1% NaCl and 1.5% agar (w/v) in deionized water) containing the appropriate antibiotic and incubated overnight at 37 °C.

### 2.5.10. Electroporation of DH5 $\alpha$

Electrocompetent *E. coli* DH5 $\alpha$  were prepared as follows. DH5 $\alpha$  were grown to OD<sub>600</sub>= 0.5-0.8 in 500 ml LB (1% bacto-tryptone, 0.5% bacto-yeast extract and 1% NaCl (w/v) in deionized water). Cells were harvested by centrifugation at 4,000 x g for 15 min at 4 °C, washed 2 X with 0.5 L of ice-cold sterile water and washed 1 X with 10 ml of ice cold 10% glycerol (v/v). Cells were then resuspended in 1 ml of ice cold 10% glycerol (v/v), divided into 50  $\mu$ l aliquots, frozen in a dry ice-ethanol bath and stored at -80 °C.

For electroporation, electrocompetent DH5 $\alpha$  were thawed on ice and 0.5-2  $\mu$ l of a ligation reaction or 0.2-1  $\mu$ g of plasmid DNA was added to 40  $\mu$ l of cells. This mixture was immediately transferred to an electroporation cuvette (Bio-Rad Gene Pulser cuvette, 0.2 cm gap) and submitted to an electrical pulse in a Bio-Rad MicroPulser (Bio-Rad). One ml of LB was added to the electroporated cells which were then allowed to recover

by incubation in a rotary shaker for 1 h at 37 °C before plating onto LB agar plates containing the appropriate antibiotic and incubated overnight at 37 °C.

#### 2.5.11. Automated DNA sequencing

Plasmids were sequenced using core facilities within the departments of Biological Sciences, Cell Biology and Biochemistry (University of Alberta). These facilities utilize fluorescently labeled dideoxy terminators which are randomly incorporated during elongation to determine the DNA sequence.

### 2.6. Recombinant plasmids

Recombinant plasmids were constructed as described below using standard subcloning techniques (Ausubel, 1992). When necessary, constructs were generated by PCR using the primers listed in Table 2-3. When PCR was used, constructs were sequenced to verify their authenticity and to ensure the absence of second site mutations.

#### 2.6.1. Constructs used in yeast two-hybrid analysis

**Capsid constructs:** The cDNA encoding amino acids 1-277 of capsid was amplified by PCR using the gene-specific primers Capsid-F and C-E2SP-R (containing an in frame stop codon). The *EcoR* I and *Bgl* II sites are underlined in the appropriate primers in Table 2-3. The PCR product was digested with *EcoR* I and *Bgl* II and ligated into the *EcoR* I and *BamH* I sites of pGBT9 (Clontech) to create **pGBT9-capsid**. To create **pGAD424-capsid**, the coding region of capsid was amplified and digested as per pGBT9-capsid and then subcloned into *EcoR* I / *Bgl* II digested pGAD424. Capsid deletion mutant cDNAs generated by PCR were digested with *EcoR* I and *Bgl* II and subcloned into the *EcoR* I and *BamH* I sites of pGBT9 or pGBKT7 (Clontech) as indicated. All constructs were subcloned in frame and contained stop codons which were introduced via the reverse primers. The primers used for each construct were: **pGBT9-C1-88**; Capsid-F and CM11, **pGBT9-C87-171**; CM12 and CM13, **pGBT9-C167-277**; CM14 and C-E2SP-R, **pGBKT7-C1-45**; Capsid-F and CR45, **pGBKT7-C46-89**;

**Table 2-3. Oligonucleotide Primers**

Name	Sequence*
<b>4mcFD</b>	5'-ATAGA <u>ATTCAGCC</u> ACCATGGAGCAAAGCTCATTCTGAAGAGGAC TTG GCGACCGGTGGCTACCG-3'
<b>4mcRV</b>	5'-CTAATCGATCTACCTGGTCAGCTGAC-3'
<b>5RAP</b>	5'-GCCGCGGCGCCTCGCAGTCGGCCGCGCCGGCCCCGCCGGCACAGG CCGACTCCAGCACCTCCG-3'
<b>6RAP2</b>	5'-GATCCGGGGCCCTGGACCAGTCCTTGCGCTGGCCAGCGCCCCGCGTTG CCGGCGGCGGCCCGCCGGCCCTCCGGAGTCACG-3'
<b>AV10</b>	5'-CAAGGCCAGGAGAGGCAC-3'
<b>AV10Cla</b>	5'-TTGATCATCGATGGGCACTGGAGTGGCAAC-3'
<b>AV11</b>	5'-TACGGTGGGAGGTCTATATAGC-3'
<b>AV11H</b>	5'-GATCCAAGCTTTACGGTGGGAGGTCTATATAGC-3'
<b>Capsid46</b>	5'-GGTCGAATTCAGCACCTCCGGAGATGAC-3'
<b>Capsid-F</b>	5'-CGCGAATTCATGGCTTCCACTACCC-3'
<b>Capsid-R</b>	5'-GGTCAGATCTCTAGGCGCGCGGTC-3'
<b>C-E2SP-R</b>	5'-ACTGAGATCTAGCGGATGCGCCAAGGATG-3'
<b>CGSTF</b>	5'-AGATCTGGATCCATGGCTTCCACTACCCCATC-3'
<b>CM11</b>	5'-GATCAGATCTCTAGCGACTTTCTTGCCGCTC-3'
<b>CM12</b>	5'-GATCGAATTCAGTCGCTCCCAGACTCCG-3'
<b>CM13</b>	5'-GATCAGATCTCTAGTCGACGCGGTAGAAGAC-3'
<b>CM14</b>	5'-GATCGAATTCATCCGCGTCGACCTG-3'
<b>CR45</b>	5'-GGTCAGATCTCTAGGAGTCGCGCTGTGCG-3'
<b>CR89</b>	5'-GGTCAGATCTCTAGGAGCGACTTTCTTGCCGC-3'
<b>GAD-PRV</b>	5'-GCATCGTGCACCATCTCAA-3'
<b>RVC30</b>	5'-GGTCGAATTCGGCGCCTCGCAGTCGC-3'
<b>RVC65R</b>	5'-GGTCAGATCTCTAGTTGCCGCGGCGGCGGC-3'
<b>RVC69R</b>	5'-GGTCAGATCTCTAGCCACGGCCCCGGTGC-3'
<b>RVC79R</b>	5'-GGTCAGATCTCTAGGGCGGGGCCCTGGAGTC-3'
<b>P32C1</b>	5'-GATCGAATTCATCCACCAACATTTGATGGTG-3'
<b>P32F2</b>	5'-GATCGAATTCATGCTACCTCTGCTGCGC-3'
<b>P32mG</b>	5'-GATCGAATTCCTGCACTGAAGGAGAC-3'
<b>P32N1</b>	5'-GATCGCGGCCGCTAATCAAATGTTGGTGGGATGC-3'
<b>P32R3</b>	5'-TGATCGGATCCTCTGCTGCTCTACTGGC-3'

\*Restriction endonuclease sites are underlined.

Capsid46 and CR89, **pGBKT7-C30-65**; RVC30 and RVC65R, **pGBKT7-C30-69**; RVC30 and RVC69R, **pGBKT7-C30-79**; RVC30 and RVC79R, **pGBKT7-C30-89**; RVC30 and CR89.

**p32 constructs:** **pGADT7-p32N** was created by amplifying the region of simian p32 encoding amino acids 1-138 of p32 by PCR using primers p32F2 and p32N1. The template used for PCR was pCB6<sup>+</sup>p32. The PCR fragment was digested with *Not* I, blunt ended using DNA polymerase Klenow fragment and then cut with *Eco*R I. This product was then subcloned, in-frame, into pGBKT7 which was digested with *Eco*R I and blunt ended at the *Bam*H I site. **pGADT7-p32C**, encoding amino acids 139-282 of p32, was also created by PCR. Primers p32C1 and GAD-PRV were used to amplify this region from clone 10 (isolated in the yeast two-hybrid screen). The PCR fragment was digested with *Eco*R I and *Bgl* II and subcloned, in-frame, into *Eco*R I and *Bam*H I cut pGBKT7.

### 2.6.2. Constructs for *in vitro* transcription/translation

The capsid cDNA was amplified by PCR from pCMV5-24S (Hobman et al., 1990) using the primers AV11 and C-E2SP-R and the resulting PCR product was blunt-end ligated into the *Eco*R V site of pBluescript-KS+ (Stratagene). The resulting plasmid, **pBLU-capsid**, contained RV capsid (minus the E2 signal peptide) under the transcriptional control of the T3 promoter. A plasmid containing green fluorescent protein (GFP) under the control of the T3 promoter **pBLU-GFP** was created by excising GFP from pEGFP-1 (Clontech) with *Eco* RI and *Not* I and ligating it into pBluescript-KS+.

### 2.6.3. Constructs for bacterial expression

The p32 coding region was subcloned, in-frame with glutathione S-transferase (GST), into the vector pGEX-4T1 (Pharmacia). The coding sequence for p32 was amplified from clone 10 (isolated in the yeast two-hybrid screen) using the gene-specific primer P32F2 and the vector-specific primer GAD-PRV. The PCR product was digested with *Eco* RI and *Not* I and ligated in-frame into pGEX4T1 to create **pGEX-p32**.

The capsid binding region of Par-4 was fused in-frame to GST by excising the *EcoR* I fragment from clone 11 (isolated in the yeast two-hybrid screen) and ligating it into pGEX-4T1 to create pGEX-Par-4. Restriction digestion was used to confirm that the insert was incorporated in the correct orientation.

#### 2.6.4. Constructs for mammalian expression

The RV expression plasmids pCMV5-24S (Clarke et al., 1987), pCMV5-E2E1 (Hobman and Gillam, 1989), pCMV5-CapE2SP (Law et al., 2001) and pCMV5-CapsidΔSP (Law et al., 2001) have been described previously. The expression plasmid pCB6<sup>+</sup>Par-4 encoding full length human Par-4 (Johnstone et al., 1996) was obtained from Dr Vivek Rangnekar (University of Kentucky, Lexington, KN).

**Capsid constructs:** pEBG-Capsid was created by amplifying the capsid cDNA (including the E2 signal peptide) from pCMV5-CapE2SP by PCR using primers CGSTF and AV10Cla. The PCR product was digested with *BamH* I and then ligated, in frame, to the 3' end of the glutathione S-transferase cassette in the mammalian expression vector pEBG (Mizushima and Nagata, 1990). pcDNA 5/T0-Capsid was created by amplifying the capsid cDNA, including the E2 signal peptide, from pCMV5-CapE2SP by PCR using primers AV11H and AV10. The PCR product was digested with *Hind* III and ligated into *Hind* III cut pcDNA 5/T0 (Invitrogen).

Arginine residues in the amino portion of capsid (which were thought to mediate capsid-p32 binding) were mutated to alanines as follows. Site-specific mutations were introduced into the capsid cDNA by PCR and the PCR products were subsequently used to replace analogous regions in both pCMV5-capsid and pCMV5-24S. pCMV5-C5RA was constructed using the forward primer 5RAP and the reverse primer Capsid-R. pCMV5-24S was used as the template for PCR. The PCR fragment was digested with *Nar* I and ligated into *Nar* I cut pCMV5-CapE2SP. pCMV5-C6RA was constructed using the forward primer AV11 and the reverse primer 6RAP2. pCMV5-24S was used as the template for PCR. The PCR fragment was digested using *EcoR* I and *Apa* I and ligated into pCMV5-CapE2SP digested with the same enzymes. pCMV5-C11RA was constructed with the forward primer 5RAP and the reverse primer Capsid-R. The

template for PCR was pCMV5-24S6RA. The PCR fragment was digested with *Nar* I and ligated into *Nar* I cut pCMV5-CapE2SP. To introduce the mutagenized regions of capsid into the 24S cDNA, the *Eco*RI / *Sph* I fragment of the mutant capsid was excised by endonuclease restriction digestion and used to replace the analogous region (*Eco*RI / *Sph* I) in pCMV5-24S

**p32 constructs:** pCB6<sup>+</sup>p32 was created by excising the *Eco*RI / *Not* I fragment from pGEX-p32 and ligating it into pCB6<sup>+</sup> (Patwardhan et al., 1991). pEGFP-p32m was created by fusing the region encoding mature p32, in-frame, to the C-terminus of GFP. The cDNA sequence encoding mature p32 was amplified by PCR from pCB6<sup>+</sup>p32 using primers p32mG and p32R3. The PCR product was digested with *Eco*RI and *Bam*HI and subcloned into pEGFP-C1 (Clontech) cut with the same restriction enzymes.

**Par-4 constructs:** To create pCB6<sup>+</sup>mycPar-4, the complete coding region of human Par-4 was amplified by PCR using the primers 4mcFD and 4mcRV from pCB6<sup>+</sup>Par-4. 4mcFD contains a Kozak consensus sequence (Kozak, 1987) upstream of a c-myc tag which is in frame with the coding region of Par-4. The PCR product was subcloned into pCB6<sup>+</sup> using the restriction sites *Eco*RI and *Cla*I.

### 2.6.5. Introduction of RA mutations into the infectious clone

The arginine to alanine mutations in capsid were introduced into the rubella virus M33 strain infectious clone (pBRM33) (Yao and Gillam, 1999) by replacing the *Nco*I and *Sph*I fragments from the capsid encoding region of pBRM33 with the similar region from constructs containing the desired mutations (pCMV5-C5RA, pCMV5-C6RA or pCMV5-C11RA).

## 2.7. Protein gel electrophoresis and protein detection

### 2.7.1. SDS-PAGE

Protein samples were resolved using 10 % sodium dodecyl sulfate-polyacrylamide gel electrophoresis (SDS-PAGE) (Ausubel, 1992). Briefly, proteins were denatured by boiling in 2 X gel sample buffer (Table 2-2) for 5 min. Samples were then

separated by discontinuous gel electrophoresis (4% stacking gel followed by 10% resolving gel) in gel running buffer (see Table 2-2) at 80-160 V using the Bio-Rad Mini-Protean II or the Bio-Rad Mini-Protean III systems. Gels were then processed for fluorography, silver staining or Western blotting as described below (see sections 2.7.2. to 2.7.4.).

### **2.7.2. Fluorography**

To visualize radiolabeled proteins, gels were processed for fluorography following electrophoresis. Gels were fixed in 25% (v/v) isopropanol and 10% (v/v) acetic acid for 30 min, rinsed in deionized water and then incubated in 100 mM sodium salicylate containing 0.01% (v/v)  $\beta$ -mercaptoethanol for 30 min. Gels were dried and exposed to Kodak XAR film at  $-80^{\circ}\text{C}$ .

### **2.7.3. Silver staining**

Following SDS-PAGE, gels were fixed in 50% (v/v) methanol and 10% (v/v) acetic acid for 30 min at room temperature, sensitized in 0.02% (v/v) sodium thiosulfate for 1 min at room temperature and then treated with 0.1% (w/v) silver nitrate for 25 min at  $4^{\circ}\text{C}$ . Gels were developed in 2% (w/v) anhydrous sodium carbonate, 0.02% (v/v) formaldehyde for 5-10 min at room temperature. Development was stopped by immersing gels in a 1.4% (w/v) EDTA sodium salt solution.

### **2.7.4. Western blotting**

Following SDS-PAGE, proteins were transferred to PVDF membranes for immunoblotting. Gels and PVDF membranes (rinsed in methanol) were equilibrated in transfer buffer (Table 2-2) for 15 min prior to transfer which was carried out at 240 mA for 1 h in transfer buffer using a Mini Trans-Blot Electrophoretic Transfer Cell apparatus (Bio-Rad). Following transfer, membranes were washed 1 X with TBST (Table 2-2), blocked with TBST containing 5% non-fat milk for 30 min and then incubated with the appropriate antibodies diluted in TBST plus 5% non-fat milk for 1 h. Membranes were

washed 3 X with TBST followed by incubation with secondary antibodies conjugated to HRP (used at 1:3000 dilution) in TBST plus 5% non-fat milk for 1 h. Membranes were washed as above and treated for ECL using Supersignal Westpico Chemiluminescent Substrate. Signal was detected using Fuji RX film.

## **2.8. Culture and transfection of mammalian cell lines**

### **2.8.1. Mammalian cell culture**

Unless otherwise indicated, cells were incubated at 37 °C in a humidified atmosphere with 5% CO<sub>2</sub> in the following growth media. COS, Vero, HEK293T and BHK cells were cultured in Dulbecco's modified Eagle medium containing 10% fetal bovine serum, 2 mM glutamine, 10 mM HEPES and the antibiotics penicillin (100 U/ml) and streptomycin (100 U/ml). RK-13 cells were cultured in minimal essential medium containing 10% fetal bovine serum, 2 mM glutamine, 10 mM HEPES and the antibiotics penicillin (100 U/ml) and streptomycin (100 U/ml).

### **2.8.2. Transient transfection of cell cultures**

COS and Vero cells were transiently transfected with the indicated amounts of plasmid DNA using FuGENE 6 or Perfectin transfection reagents exactly as described by the manufacturers. Transfected cells were used for experiments 24–48 h post-transfection.

### **2.8.3. Generation of HEK 293T-REx cells inducibly expressing capsid**

To create stable cell lines expressing capsid, subconfluent T-REx 293 cells (1 x 10<sup>6</sup> cells/60 mm dish) stably expressing the tetracycline repressor protein (pcDNA6/TR) in the T-REx inducible expression system were transfected with 8 µg pcDNA5T/0-capsid. At 48 h post-transfection, cells were split 1:10 and cultured in normal HEK culture medium containing hygromycin B (5 µg/ml) and blasticidin (100 µg/ml). When colonies became visible they were picked using cloning rings. Inducible expression of capsid was determined by immunofluorescence and by immunoblot analysis of lysates

from cells grown in the presence or absence of 1  $\mu\text{g/ml}$  doxycycline. Multiple clones were analyzed, but clone 293TRC 2B was used for all experiments described in this thesis.

## **2.9. Immunoprecipitation and radioimmunoprecipitation**

### **2.9.1 Immunoprecipitation**

Immunoprecipitations were carried out using lysates from transfected COS cells as described previously (Hobman et al., 1993). Briefly, transfected cells were washed 2 X with ice-cold PBS 24-48 h post-transfection, lysed with RIPA (Table 2-2) for 5 min on ice and lysates were cleared with a 14,000 x g spin for 5 min at 4 °C. Immunoprecipitation from the supernatants was carried out using the indicated antibodies for 1 h with rotation at 4 °C followed by the addition of protein A- or G-Sepharose beads for 1 h with rotation at 4 °C. Immune-complexes were washed 3 X with RIPA and then proteins were eluted from the Sepharose beads by boiling for 5 min in the presence of 2 X gel loading buffer.

### **2.9.2. Metabolic labeling and radioimmunoprecipitation**

To identify protein complexes, transfected COS cells or infected Vero cells were metabolically labeled with  $^{35}\text{S}$ -methionine/cysteine prior to immunoprecipitation. Confluent cells were washed 1 X with PBS and then incubated in medium lacking cysteine and methionine for 30 min at 37 °C to deplete intracellular stores of cysteine and methionine. Cells were then labeled with 100  $\mu\text{Ci}$  of  $^{35}\text{S}$ -Pro-mix /ml medium for 2-16 h. Cells were washed 3 X with ice-cold PBS and radioimmunoprecipitation was carried in a manner similar to the immunoprecipitation protocol described above (see section 2.9.1.) with the following modifications to preserve protein-protein interactions. NP40 lysis buffer (Table 2-2) containing Complete EDTA-free protease inhibitors was used to lyse cells instead of RIPA and immune complexes were washed with PBS containing 0.1% TritonX-100 instead of RIPA. Following SDS-PAGE, proteins were visualized using fluorography.

## **2.10. Identification of capsid interacting proteins by yeast two-hybrid screening**

Yeast strain HF7c was sequentially transformed with pGBT9-capsid and then with a CV1 cDNA library in the vector pGAD10 (Clontech). Approximately  $7 \times 10^6$  transformants were screened. Plasmids were isolated from His<sup>+</sup> LacZ<sup>+</sup> colonies and then re-transformed with or without pGBT9-capsid into yeast strain SFY526 followed by testing for  $\beta$ -galactosidase activity. Plasmid clones that activated LacZ only in the presence of pGBT9-capsid were characterized by DNA sequencing or restriction endonuclease mapping.

Interactions between capsid deletions (subcloned into pGBT9 or pGBKT7) and p32 or Par-4 (in pGAD10) were assayed by co-transfecting AH109 cells and testing for growth on media lacking adenine, histidine, leucine and tryptophan. Plates were incubated at 30 °C and assayed for growth 3-4 days post-transformation.

All transformation, screening and plasmid isolation techniques, media and  $\beta$ -galactosidase assays were performed according to the protocols described in the MATCHMAKER Two-Hybrid System II and III (Clontech).

## **2.11. Identification of capsid interacting proteins by GST pulldown**

COS or HEK 293T cells ( $9 \times 10^5$ /100 mm dish) were transiently transfected with 6  $\mu$ g of either pEBG or pEBG-Capsid. Forty-eight h post-transfection, cells were lysed in 1% NP40 lysis buffer containing Complete protease inhibitors on ice for 5 min. Lysates were cleared by centrifugation (10,000 x g) and the supernatants were incubated with glutathione Sepharose beads overnight at 4 °C. Beads containing protein complexes were then washed 3 X with lysis buffer followed by elution by boiling the beads for 5 min in 2 X gel sample buffer. Following SDS-PAGE, proteins were visualized by silver staining or Western blotting.

Bands which were unique to the GST-capsid lane were excised from silver stained gels with a clean razor blade and subjected to in-gel digestion and MALDI-TOF mass spectrometry at the Institute for Biomolecular Design (Department of Biochemistry,

University of Alberta). Sequence was analyzed using the Mascot search engine (<http://www.matrixscience.com/>).

## **2.12. *In vitro* binding interactions**

### **2.12.1. Purification of GST fusion proteins from bacteria**

For *in vitro* binding assays, GST fusion proteins were purified from *E. coli* using a method described previously (Frangioni and Neel, 1993). *E. coli* BL21 cells containing GST fusion vectors were grown to  $OD_{600}=0.5-2$  in 2 X YT and IPTG was added to a final concentration of 0.1 mM to induce expression of the GST fusions. Following the addition of IPTG the cells were incubated in a rotary shaker at 37 °C for 3 h. Cells were then pelleted at 7,000 x g for 7 min. Pellets were resuspended in 3 ml STE buffer (10 mM Tris, pH 8.0, 150 mM NaCl, 1 mM EDTA) containing 100 µg/ml lysozyme and incubated on ice for 15 min. Dithiothreitol (to 5 mM) and *N*-laurylsarcosine (to 1.5%) were added to the cell suspension and cells were sonicated briefly using a Branson Sonifier 250. Lysates were clarified by centrifugation at 10,000 x g for 5 min at 4 °C. Supernatants were mixed with glutathione Sepharose 4B beads for 1-4 h with rotation at 4 °C. Beads were washed 3 X with ice-cold PBS prior to use in *in vitro* binding experiments.

### **2.12.2. Conjugation of glucose oxidase to CNBr activated beads**

Glucose oxidase was coupled to cyanogen bromide (CNBr) activated Sepharose 4B beads following the manufacturer's protocol. CNBr activated Sepharose 4B beads were resuspended in 1 mM HCl for 30 min followed by 5 washes with 1 mM HCl. Beads were then washed 2 X with coupling buffer (0.1 M NaHCO<sub>3</sub>, 0.5 M NaCl, pH 8.3). The washed CNBr beads were incubated with 10 mg of glucose oxidase (50 mg/ml in coupling buffer) for 2 h at room temperature. Beads were washed 2 X in coupling buffer and remaining active groups were blocked by incubating with 0.2 M glycine overnight at 4 °C. Beads were washed 3 X with coupling buffer before use in *in vitro* binding assays.

### **2.12.3. *In vitro* binding assay**

*In vitro* binding assays were used to confirm protein-protein interactions identified using the yeast two-hybrid screen. Capsid and GFP were synthesized in the presence of <sup>35</sup>S-methionine using coupled transcription/translation systems (Promega or Ambion) according to the manufacturer's instructions. To confirm the capsid-p32 interaction, 5  $\mu$ l of the <sup>35</sup>S-labeled translation reactions were incubated with Sepharose beads coated with GST, GST-p32 or glucose oxidase in 1 ml PBS containing 0.1% TX-100. To confirm the capsid-Par-4 interaction, 5  $\mu$ l of the <sup>35</sup>S-labeled translation reactions were incubated with Sepharose beads coated with GST or GST-Par-4 in 1 ml PBS containing 0.1% TX-100. The mixtures were incubated on a rotating device overnight at 4 °C. The beads were collected by centrifugation at 500 x g for 5 min and then washed 3 X with PBS containing 0.1% Triton-X100 and the bound proteins were eluted by boiling in SDS-PAGE sample buffer for 5 min. Samples were analyzed by SDS-PAGE and fluorography.

## **2.13. Microscopy**

### **2.13.1. Immunofluorescence microscopy**

Vero cells grown on coverslips were processed for indirect immunofluorescence microscopy 24 h after transfection. To visualize mitochondria, Mitotracker Red CXMRos was added to the cell culture medium at a final concentration of 30 ng/ml for 20 min at 37 °C prior to fixation. Cells were washed 2 X with PBS and then fixed in 3% paraformaldehyde for 20 min followed by quenching with 50 mM ammonium chloride. The samples were washed 2 X with PBS containing Ca<sup>2+</sup> and Mg<sup>2+</sup> (PBSCM). Plasma membranes were permeabilized by the addition of 25  $\mu$ g/ml digitonin for 5 min followed by washing with PBSCM. To permeabilize the intracellular membranes, cells were treated with 0.1% TritonX-100 for 10 min before incubation with primary and secondary antibodies. Samples were examined using a Zeiss 510 confocal microscope. Images from optical sections (0.8  $\mu$ m) were processed using Adobe Photoshop 7.0. Alternatively,

samples were examined using a Zeiss Axioskop 2 and images were captured using a digital camera (Diagnostic Laboratories Inc.).

### **2.13.2. Electron microscopy**

HEK 293TRC 2B cells were induced to express capsid by the addition of 1  $\mu\text{g/ml}$  doxycycline to the growth medium. Uninduced HEK 293TRC 2B cultures served as the negative controls. Cells were processed for electron microscopy 45 h post-induction. Cells were washed 1 X with PBS and then fixed in 2% paraformaldehyde, 2.5% glutaraldehyde in 0.1 M cacodylate buffer (pH 7.4) for 10 min at room temperature. Cells were scrapped off the dish, pelleted by centrifugation at 1,000 x g for 5 min and then the pellets were fixed overnight in the same fixative at 4 °C. Pellets were washed 3 X with 0.1 M cacodylate buffer, post-fixed with 1% osmium tetroxide in phosphate buffer for 45 min on ice and then washed 3 X with deionized water. Pellets were dehydrated with increasing percentages of ethanol solutions (60%, 80%, 95% and 100%) followed by 3 washes (5 min each) with propylene oxide. Pellets were then infiltrated with a 1:1 mixture of propylene oxide and EPON embedding medium for 1 h followed by pre-embedding in 100% EPON for 4 h and then embedded in fresh 100% EPON resin. The resin was allowed to polymerize at 60 °C for 48 h. Thin sections (70 nm) were collected on 300 mesh copper grids (EM Science), stained with uranyl acetate and lead citrate and then examined on an EM 410 electron microscope (Phillips) at 80 kV. Images were captured using a Megaview 3 CCD camera (Soft Imaging System).

## **2.14. Virus infection, propagation and titering techniques**

### **2.14.1. Infection of Vero cells with rubella virus**

For immunoprecipitation experiments, Vero cells were infected with the M33 strain of rubella virus (MOI of 1 PFU/cell) for 2 h. Virus inoculum was removed and cells were then incubated at 35 °C for 2 days before use in radioimmunoprecipitation experiments.

#### **2.14.2. One step growth curves**

To determine one-step growth curves, Vero cells were infected with rubella virus (MOI of 5 PFU/cell) as follows. Medium containing virus collected from electroporated BHK cells was added to subconfluent Vero cells ( $2 \times 10^5$ /35mm dish) for 2 h at 35 °C. Cells were washed 1 X with PBS and then incubated for 1 h in normal growth medium. Fresh medium was then added and cells were incubated at 35 °C. Medium was removed at 12 h intervals, stored at -80 °C and titered by plaque assay (see section 2.14.4.).

#### **2.14.3. Synthesis of infectious viral RNA and production of mutant virus**

Plasmids containing full length RV cDNA clones were linearized with *Hind* III and used as templates for transcription of capped RNAs (mMessage mMachine kit). RNAs were quantitated by electrophoresis and by spectroscopy at 260 nm. RNA was introduced into BHK cells by electroporation as follows. Subconfluent BHK cells were trypsinized, resuspended at  $1 \times 10^7$  cell/ml in PBS and equal amounts of wild type and mutant viral RNAs (10 µg) were added to 0.5 ml aliquots of cell suspensions. The cell-RNA mixtures were transferred to a 0.2 mm gap electroporation cuvette and incubated on ice for 10 min. Cells were electroporated using a 500 V, 100 µF pulse in an Electro Cell Manipulator ECM600 (BTX Electronic Genetics). Immediately following the pulse, 1 ml of culture medium was added to the cuvettes. These mixtures were then diluted to 20 ml with culture medium and incubated in 100 mm tissue culture dishes at 35 °C. Virus containing culture media were collected at various timepoints. Media were clarified at  $7,000 \times g$  for 10 min before storage at -80 °C. Virus titers were determined by plaque assay as described below (see section 2.14.4.).

#### **2.14.4. Plaque assay**

Plaque assay was used to determine the titer of virus in the medium of electroporated BHK cells or infected Vero cells. To determine virus titers, RK-13 cells ( $1.8 \times 10^5$ ) in 6 well tissue culture dishes were washed 1 X with PBS and then infected with serial dilutions of virus stocks for 2 to 4 h. Cells were allowed to recover for 1 h in

fresh culture medium and then overlaid with 0.5% agarose in culture medium for 6 days at 35 °C. To visualize plaques, cells were stained with 4% neutral red solution (Sigma) for 4 h.

## **2.15. Generation of polyclonal antibodies**

### **2.15.1. Generation of polyclonal antibodies to capsid**

To generate antigen, capsid protein was expressed in lepidopteran *Spodoptera frugiperda* cells (Sf9) using a recombinant baculovirus containing the coding sequence for capsid fused to a 6X His sequence (Schmidt et al., 1998). Briefly, Sf9 cells (approximately  $1 \times 10^6$  cells per ml) were infected with recombinant virus (MOI=1 PFU/cell) and cultured in suspension at room temperature with rotation (130 rpm). Seventy-two h post-infection, cells were pelleted at 500 x g. The (His)<sub>6</sub>-tagged capsid was purified by separating the insoluble fraction (10,000 x g pellet) from infected Sf9 cells lysed with lysis buffer (0.5 M NaCl, 10 mM HEPES, 10% (v/v) glycerol, 0.1 mM EDTA, 5 mM imidazole, 75 µg/ml PMSF, 1% Triton X-100, pH 7.8) by SDS-PAGE. Proteins were visualized by staining with ice-cold 250 mM KCl and the capsid band was excised and electroeluted into dialysis membrane (14 kDa exclusion size) for 48 h at 20 mA in 40 mM Tris-acetate, pH 8.4, 0.02% SDS. The electroeluted capsid protein was dialyzed against 200 mM sodium bicarbonate/0.1% SDS. Rabbits were immunized with 70 µg of capsid protein followed by booster injections (70 µg) at four week intervals. The antiserum used in this study is 7W7.

### **2.15.2. Generation of polyclonal antibodies to p32**

GST-p32 was induced in *E. coli* and purified on glutathione Sepharose beads as described above (see section 2.12.1.). Protein was eluted from beads by the addition of 20 mM reduced glutathione in 0.1% Triton X-100, 150 mM NaCl, 50 mM Tris-HCl (pH=8.5). A total of 4 elution steps were carried out. Eluates were pooled and dialyzed (14 kDa exclusion size) against PBS and then concentrated using a Centrprep Centrifugal Filter Unit with a molecular mass cut off of 10 kDa (Millipore). A total of 0.5

mg GST-p32 (170  $\mu\text{g/ml}$ ) was sent to Chemicon for the generation of goat anti-p32 antiserum.

## **2.16. Analysis of the effects of capsid on mitochondrial membrane potential and cell growth**

### **2.16.1. MTT assay**

The *in vitro* Toxicology Assay Kit (Sigma) was used to estimate relative cell numbers as a function of mitochondrial activity. Vero or RK-13 cells ( $8 \times 10^4$  cells/well in a 96 well dish containing 100  $\mu\text{l}$  culture medium) were infected at an MOI of 5 PFU/cell. Forty-eight h post-infection, 10  $\mu\text{l}$  MTT solution (5 mg/ml) was added to culture medium. Cultures were then incubated for 4 h followed by solubilization of MTT formazan crystals by the addition of 100  $\mu\text{l}$  Solubilization Solution (0.1 N HCl in anhydrous isopropanol plus 10% Triton X-100). Absorbance was measured at 570 nm and the background at 690 nm was subtracted. Plates were read using a VersaMax microplate reader (Molecular Devices).

### **2.16.2. Flow cytometry**

HEK 293TRC 2B cells were cultured under either induced or non-induced conditions for the indicated amounts of time (2-5 days) before use in flow cytometry experiments. The mitochondrial membrane potential sensitive dye TMRE (0.5 mM) was added to growth medium to stain active mitochondria for 30 min before analysis. Loss of membrane potential was induced by the addition to the culture medium of 10 mM CCCP for 15 min or 2  $\mu\text{M}$  staurosporine for 4-5 h prior to analysis. Following treatment, cells were washed 2 X in PBS, and then detached from dishes by treatment with 1 X trypsin EDTA solution. Cells were washed 3 X with PBS containing 1% FBS and then analyzed by flow cytometry. Analysis was conducted using a Becton Dickson FACScan flow cytometer. Data were acquired in the FL2 channel and 10,000 events per sample were analyzed. Results were analyzed using CellQuest software.

## **2.17. Analysis of capsid arginine to alanine mutants**

### **2.17.1. Virion assembly (RLP) assay**

COS cells ( $1.5 \times 10^5$ /35 mm dish) were transiently transfected with 2  $\mu$ g of the pCMV5-24S constructs containing either wild type capsid or capsid with the indicated mutations. Media was collected from transfected cells 48 h post-transfection and cells were lysed. Media was precleared by centrifugation at 10,000 x g and RLPs were pelleted from the precleared media by centrifugation at 100,000 x g for 1 h. The presence of capsid in the cellular lysate and in the 100,000 x g pellet was detected by subjecting samples to SDS-PAGE and immunoblotting with anti-capsid antibodies (7W7).

### **2.17.2. $^{33}\text{P}$ labeling of capsid**

COS cells were transiently transfected with 2  $\mu$ g of plasmid DNA. Twenty-four h post-transfection, cells were washed 1 X with PBS and then incubated in phosphate-free medium for 30 min prior to the addition of 100  $\mu$ Ci of  $\text{H}_3^{33}\text{PO}_4$ . Cells were radiolabeled with phosphate for 12 h at 37 °C, washed 1 X with cold PBS and then lysed with RIPA buffer containing phosphatase inhibitors (1mM sodium orthovanadate, 50 mM sodium fluoride, 5 mM tetrasodium pyrophosphate). Lysates were immunoprecipitated as described above (section 2.10.1.) using antibody 7W7. All solutions contained phosphatase inhibitors. Samples were resolved by SDS-PAGE and subjected to fluorography.

### **2.17.3. *In vitro* RNA binding assay**

COS cells were transiently transfected with 2  $\mu$ g of various capsid constructs. Forty-eight h post-transfection, capsid proteins were immunoprecipitated using antibody 7W7 as described above (section 2.10.1.). To enhance capsid binding to RNA, proteins were dephosphorylated by incubation overnight at 37 °C in the presence of 100 U of calf alkaline intestinal phosphatase in dephosphorylation buffer (1mM EDTA, 0.05 Tris-HCl, pH 8.5). Samples were resolved by SDS-PAGE and transferred to nitrocellulose membranes (240 mA for 1 h). Membranes were washed in probe buffer (50 mM NaCl,

1 mM EDTA, 1 X Denhardt's solution, 10 mM Tris HCl pH 7.5) for 10 min and then blocked for 1 h in probe buffer containing 250  $\mu$ g/ml of baker's yeast tRNA.

The MEGAscript kit was used to generate the non-capped RNA probe using the *BamH* I linearized pSK-RNAII as the template. This plasmid contains the RV genomic RNA packaging signal (nucleotides 1 to 4,211) and has been described previously (Law et al., 2003). Transcription reactions (20  $\mu$ l) contained 1  $\mu$ l of  $\alpha$ -<sup>35</sup>S-labeled CTP (10  $\mu$ Ci). Membranes were incubated with the probe in probe buffer for 1 h at room temperature and then washed 3 X in probe buffer and exposed to a PhosphorImager plate. Protein levels were determined by Western blotting using a mouse anti-capsid antibody (C1 (Waxham and Wolinsky, 1985)).

## 2.18. Luciferase assay

The Mercury Pathway Profiling System (Clontech) was used to determine the effects of capsid and its binding partners on candidate cellular signaling pathways. To determine the effects on NF- $\kappa$ B or AP-1 signaling, HEK 293 cells were transiently transfected as follows. Cells were seeded into fibronectin coated culture dishes (6 x 10<sup>5</sup> cells/35 mm dish) and then transiently transfected the next day as indicated. The following amounts of plasmid DNA were used for transfection: pCMV5-CapE2SP (1  $\mu$ g); pCB6+p32 (1  $\mu$ g); pCB6+Par-4 (1  $\mu$ g); luciferase reporter plasmid (pTAL- NF- $\kappa$ B or pTAL-AP-1)(0.5  $\mu$ g). Cells were also transfected with a plasmid encoding  $\beta$ -galactosidase (pCH110 (0.5  $\mu$ g)) to control for transfection efficiency. The total amount of plasmid DNA per transfection was 3  $\mu$ g. To ensure that equal amounts of plasmid DNA were transfected, cells were also transfected with the plasmid vector pCMV5 when necessary. After 24 h, cells were serum starved for 20 h. Activation of the NF- $\kappa$ B signaling pathway was induced by the addition of TNF- $\alpha$  (50 ng/ml) to the growth medium for 6 h. Activation of the AP-1 signaling pathway was induced by the addition of normal growth medium containing 10% serum for 6 h. Cells were then washed 3 X with PBS and then lysed in 100  $\mu$ l NP40 lysis buffer (0.5% NP-40, 100 mM Tris, pH 7.8) for 20 min at room temperature and then subjected to a freeze thaw at -80 °C. Lysates were cleared at 10,000 x g. To determine luciferase activity, 100  $\mu$ l of luciferase assay buffer

(Table 2.2) was added to 40  $\mu\text{l}$  of lysate and luminescence was measured in a black 96 well plate using a Fluoroskan Ascent FL plate reader (ThermoLabsystems) and data were analyzed using Ascent Software version 2.4.2.

To normalize for transfection efficiencies,  $\beta$ -galactosidase assays were conducted on all cell lysates as follows. Lysates (50  $\mu\text{l}$ ) were added to 500  $\mu\text{l}$  Z buffer (Table 2-2) and 100  $\mu\text{l}$  ONPG (4 mg/ml) and incubated at 30 °C for approximately 2 h. Reactions were stopped by the addition of 250  $\mu\text{l}$  of 1 M  $\text{Na}_2\text{CO}_3$  and the absorbance was read at  $\text{OD}_{420}$ .

### **CHAPTER 3. IDENTIFICATION AND CHARACTERIZATION OF CAPSID- INTERACTING HOST CELL PROTEINS**

Data from this chapter have been published in "**Beatch, M. and T. Hobman. 2000. Rubella virus capsid associates with host cell protein p32 and localizes to mitochondria. J. Virology. 74(12):5569-5576.**" Used with permission from The American Society for Microbiology.

### 3.1. Overview

The main function of the RV capsid is to homo-oligomerize and bind the virus genomic RNA to form the nucleocapsid. In addition, capsid has also been implicated in the regulation of other processes such as virus budding, virus genome replication and apoptosis (Chen and Icenogle, 2004; Duncan et al., 1999; Suomalainen et al., 1990). The mechanisms by which capsid carries out these diverse functions remain unknown. However, it is likely that interactions between host cell proteins and capsid are required to mediate these events. Our goal in this study was to identify host cell proteins that interact with the RV capsid. To identify candidate capsid-binding proteins, a yeast-two hybrid screen and GST pulldown experiments were conducted. Using these methods, we identified four capsid-binding proteins. Interactions between capsid and two of these proteins, p32 and Par-4 were confirmed in further detail using *in vitro* binding assays and *in vivo* co-immunoprecipitation experiments. The intracellular localizations of these interactions were determined by indirect immunofluorescence. Finally, the interacting regions of capsid and these host cell proteins were mapped using the yeast two-hybrid system. Our data indicate that the amino terminal portion of capsid interacts with at least two cellular proteins at distinct subcellular sites.

### 3.2. Identification of capsid-binding proteins

#### 3.2.1. Yeast two-hybrid screen

The yeast two-hybrid system was used to identify potential host cell capsid-binding proteins. This method was chosen since it is able to detect both transient and stable interactions between proteins (Guarente, 1993). Vero cells are one of the few types of cultured cells in which RV is able to establish a productive infection but yeast two-hybrid Vero cDNA libraries are not commercially available. As an alternative, we chose to screen a cDNA library prepared from CV1 cells which, like Vero cells, are derived from African green monkey kidney cells. Bait (capsid) and prey (CV1 cDNA) plasmids were sequentially transformed into the yeast strain HF7c. Plasmids were isolated from transformants that grew on media lacking leucine, tryptophan and histidine. These

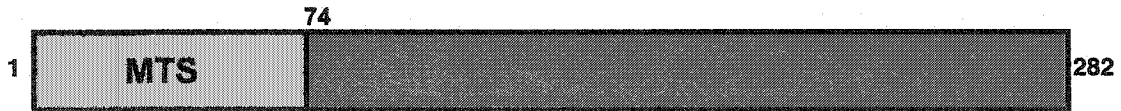
plasmids were then re-transformed into the yeast strain SFY526 and assayed for  $\beta$ -galactosidase activity as a secondary test. Plasmids which were positive in the  $\beta$ -galactosidase assay were subjected to nucleotide sequencing to determine the identity of the insert cDNAs.

Of 32 positive clones obtained from the screen, 16 were characterized in further detail. Fifteen of these plasmid clones were found to encode the full-length cDNA for a previously characterized protein, p32 (Figure 3.1A and B). P32 is a highly conserved protein that is ubiquitously expressed in all eukaryotes. The amino terminus of human p32 contains a 74 amino acid mitochondrial targeting sequence and several studies have shown that under normal circumstances p32 is largely, if not entirely, located in the mitochondrial matrix in both yeast and vertebrates (Dedio et al., 1998; Muta et al., 1997; Seytter et al., 1998). During mitochondrial import, the mitochondrial targeting sequence of p32 is cleaved and mature subunits assemble into homotrimers (Jiang et al., 1999).

The function of p32 remains the subject of speculation. Despite the ubiquitous expression of p32, the protein is not necessary for survival in *Saccharomyces cerevisiae*. Strains in which the gene encoding MAM33p, the yeast homolog of p32, is knocked out are viable but display a growth defect on glycerol suggesting that MAM33p may play a role in oxidative phosphorylation (Muta et al., 1997; Seytter et al., 1998). A trypanosome homolog of p32 was shown to regulate the ability of RBP16, a protein involved in mitochondrial RNA editing, to bind guide RNA (Hayman et al., 2001). The function of p32 in the mitochondrial matrix of higher eukaryotes, however, remains unknown. P32 has been shown to interact with a number of non-mitochondrial cellular proteins. For instance, p32 binds nuclear splicing factors and is able to regulate RNA splicing (Krainer et al., 1991; Petersen-Mahrt et al., 1999). In addition, p32 has also been shown to bind to and regulate the kinase activity of a number of Protein Kinase C (PKC) isoforms (Robles-Flores et al., 2002; Storz et al., 2000). Binding of p32 to a number of viral proteins has also been reported. The majority of these proteins, like the RV capsid, are arginine rich, nucleic acid binding proteins. The reported functional significance of these interactions include the modulation of RNA binding and stability, transcriptional regulation and protein translocation (see Table 3-1). Typically, these interactions involve the

**Figure 3.1. The structure and sequence of p32.** A) Schematic diagram of human p32. P32 is 282 amino acid residues in length and contains a mitochondrial targeting sequence (MTS) in its amino terminal 74 amino acids. All numbers refer to amino acid residues. B) Nucleotide and predicted amino acid sequences of clone 10 which encodes simian p32. The numbers on the left correspond to nucleotides; the numbers on the right correspond to amino acid residues. Residues that differ from the published human sequence are shown in bold with the corresponding human sequence below. The arrow indicates the site of cleavage of the mitochondrial targeting leader sequence in human p32. Vector sequences are in lower case and the stop codon is indicated by an asterisk. The predicted amino acid sequence of simian p32 is 95.4% identical to human p32.

# A



# B

```

-20 gaa ttc gcg gcc gcg tcg acT TGT CCT TTG CAT CCG CAC GTG TTC GCA GTG GAT TCC GCG
41 ATG CTA CCT CTG CTG CGC TGC GTG CCC CGT GTG CTG GGC TCC GCC GTC CCC AGC CTC CGC
  M L P L L R C V P R V L G S A V P S L R 20
                                     S A
101 CCT GCC GCG CCC GCC TCG CCT TTC CGG CAG CTC CTG ACG CCG GGG CCC CGG CTG TGC GCC
  P A A P A S P F R Q L L T P G P R L C A 40
  A Q A T
161 CGG CCC TTC GGG CTG CTC AGC GTG CGC GCA GGT TCC GAG CGG CGG CCG GGC CTC CTG CGG
  R P F G L L S V R A G S E R R P G L L R 60
221 CCT CGA GGA CCC TGC GCC TGT GGC TGT GGC TGC GGC TTG CTG CAC ACT GAA GGA GAC AAA
  P R G P C A C G C G C G L L H T E G D K 80
                                     S D
281 GCT TTT GTT GAT TTC CTA AAT GAT GAA ATT AAG GAG GAA AGA AAA ATC CAG AAG CAT AAA
  A F V D F L N D E I K E E R K I Q K H K 10
                                     S
341 ACC CTC CCT AAG ATG TCT GGA GGT TGG GAG CTG GAA CTG AAT GGG ACA GAA GCG AAA TTA
  T L P K M S G G W E L E L N G T E A K L 120
401 ATG CGG AAA GTT GCC GGG GAA AAA ATC ACT GTC ACT TTC AAC ATT AAC AAC AGC ATC CCA
  M R K V A G E K I T V T F N I N N S I P 140
  V
461 CCA ACA TTT GAT GGT GAG GAG GAA CCC ACG CAA GGG CAG AAG GTT GAA GAA CAG GAG CCT
  P T F D G E E E P T Q G Q K V E E Q E P 160
                                     S
521 GAA CTG ACA TCA ACT CCC AAT TTC GTG GTT GAA GTT ATA AAG AAT GAT GAT GGC AAG AAG
  E L T S T P N F V V E V I K N D D G K K 180
581 GCC CTT GTG TTG GAC TGT CAT TAT CCA GAG GAT GAG GTT GGA CAA GAA GAC GAG GCT GAG
  A L V L D C H Y P E D E V G Q E D E A E 200
641 AGT GAC ATC TTC TCT ATC AGG GAA GTT AGC TTT CAG TCC AGT GGG GAG TCT GAA TGG AAG
  S D I F S I R E V S F Q S S G E S E W K 220
                                     T
701 GAT ACT AAT TAC ACA CTC AAC ACA GAT TCC TTG GAC TGG GCC TTA TAT GAC CAC CTG ATG
  D T N Y T L N T D S L D W A L Y D H L M 240
761 GAT TTC CTT GCG GAC CGA GGG GTG GAC AAC ACT TTT GCA GAT GAG TTG GTG GAG CTC AGC
  D F L A D R G V D N T F A D E L V E L S 260
821 ACA GCC CTG GAG CAC CAG GAG TAC ATT AGT TTT CTT GAA GAC CTC AAG AGT TTT GTC AAG
  T A L E H Q E Y I S F L E D L K S F V K 280
                                     T
881 AGC CAG TAG AGC AGA CAG ACG CTG AAA GCC TTA GTT TCA CGG CAG GCT CTG GCC AGT GAA
  S Q * 282
941 CAA GTC CTA CTC TGA AGC TAG ACA TGT GCT TTG AAA TGA TAT CGT CCT AAT ATC ATG GGG
1001 AAA AAC ACC AAA TTT AAA TTA TAT GTT TTG CGC TCT CAT TTA TTA TCA TTT TTC CTG TAC
1061 AAA TCT ATT ATT TCT AGA TTT TTG TAT AAC ATG ATA GAC ATA AAA TTG GTT TAT CTC CTC
1121 CAA AAA AAA AAA AAA AAA AAA AAg tcg acg cgg ccg cga att c
  
```

**Table 3-1. p32 interacting proteins**

<b>Cellular Proteins</b>		
<b>p32 interacting protein</b>	<b>Function</b>	<b>References</b>
<b>ASF/SF2 cell splicing factor</b>	p32 "sequesters" ASF/SF2 into an inhibitory complex. p32 inhibits phosphorylation of ASF/SF2. p32 inhibits binding of ASF/SF2 to RNA.	Krainer et al., 1991 Honore et al., 1993 Peterson-Mahrt et al., 1999
<b>Lamin B receptor</b>	No function determined.	Simos and Georgatos, 1994 Mylonis et al., 2003
<b>C1q Complement protein</b>	Receptor for globular domain of complement (C1q).	Ghebrehiwet et al., 1994
<b>Transcription Factor IIB</b>	No function determined.	Yu et al., 1995a
<b>Kininogen</b>	No function determined.	Herwald et al., 1996
<b>Vitronectin</b>	No function determined.	Lim et al., 1996
<b>Cytochrome b2 (Saccharomyces cerevisiae)</b>	MAM33p (p32 homolog) Binds sorting signal of cytochrome b2 but not essential for sorting of cytochrome b2 to mitochondrial intermembrane space. MAM33 knockout strain is viable.	Seytter et al., 1998
<b><math>\alpha_{1\beta}</math>-adrenergic receptor</b>	p32 retains $\alpha_{1\beta}$ -adrenergic receptor in intracellular region and prevents surface expression.	Xu et al., 1999
<b>Protein Kinase C<math>\mu</math></b>	p32 binds kinase domain of PKC (PKC $\mu$ ). p32 inhibits kinase activity of PKC $\mu$	Storz et al., 2000
<b>RB16 (Trypanosoma brucei)</b>	p22 (p32 homolog) stimulates the guide RNA binding capacity of RBP16.	Hayman et al., 2001
<b>Protein Kinase C (various isoforms)</b>	p32 is a general PKC binding protein (binds $\alpha, \beta, \delta, \epsilon, \theta, \mu$ and $\zeta$ isoforms). p32 binding stimulates kinase activity of $\theta$ and $\delta$ isoforms.	Robles-Flores et al., 2002
<b>Membrane type 1 metalloproteinase</b>	No function determined.	Rozaanov et al., 2002
<b>Fibrillarlin</b>	No function determined.	Yanagida et al., 2004
<b>Hrk</b>	Interaction of Hrk with p32 necessary for Hrk induced apoptosis.	Sunayama et al., 2004

**Table 3-1. p32 interacting proteins cont'd**

<b>Viral Proteins</b>		
<b>p32 interacting protein</b>	<b>Function</b>	<b>References</b>
<b>Human immunodeficiency virus* Tat</b>	No function determined.	Yu et al., 1995a Yu et al., 1995b
<b>Human immunodeficiency virus* Rev</b>	P32 de-commits HIV pre-mRNA from splicing pathway to promote transport of incompletely spliced HIV RNA from nucleus.	Tange et al., 1996 Luo et al., 1994
<b>*HIV function</b>	Human p32 relieves a post-transcriptional block to HIV replication in murine cells	Szabo et al., 2001 Zheng et al., 2003
<b>Herpes simplex virus type 1 ORF P</b>	No function determined.	Bruni and Roizman, 1996 Randall et al., 1997
<b>Epstein-Barr virus EBNA-1</b>	Translocates EBNA-1 from nucleus into cytoplasm. p32 binds bipartite arginine rich region. p32 binding region necessary for replication of an oriP containing plasmid.	Wang et al., 1997 Chen et al., 1998 Van Scoy et al., 2000
<b>Adenovirus V protein</b>	No function determined. p32 targeted to nucleus.	Matthews and Russell, 1998
<b>Herpes simplex virus type 1 IE63</b>	IE63 targets p32 to nucleus. P32 binds bipartite R rich region. No function determined.	Bryant et al., 2000
<b>Rubella virus Capsid protein</b>	Increased p32 expression correlates with increased RV infectivity. Also see this thesis.	Beatch and Hobman, 2000 Mohan et al., 2002
<b>Hepatitis C virus Core protein</b>	No function determined.	Kittlesen et al., 2000
<b>Herpesvirus saimiri ORF 73</b>	Translocates p32 to nucleus. p32 binds bipartite arginine rich region. p32 binding domain necessary for ORF 73 transactivation.	Hall et al., 2002
<b>Hepatitis B virus p22</b>	Translocates p32 to nucleus. No function determined.	Laine et al., 2003

relocalization of p32 from the mitochondria to alternate subcellular localizations such as the cytoplasm or the nucleus. A complete list of viral and cellular proteins which have been determined to interact with p32 is presented in Table 3-1.

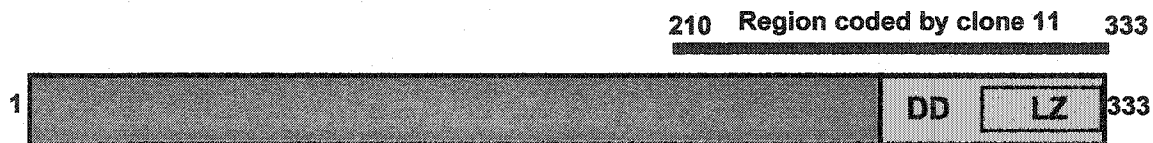
Sequencing of the cDNA encoding simian p32 (isolated from the CV1 yeast two-hybrid cDNA library) confirmed that the protein is highly conserved between primates (Figure 3.1B). The full-length cDNA sequence for simian p32 was submitted to GenBank (accession number AF238300). The predicted amino acid sequence of simian p32 is 95.4% identical to human p32 overall (Honore et al., 1993). In the region encoding the mitochondrial targeting signal the sequence is 90.4% identical to human p32 whereas in the mature sequence the identity is 97.1%.

We also identified Par-4 as a cellular capsid-binding protein in the yeast two-hybrid screen. A single plasmid clone encoding the carboxy-terminal region of Par-4 fused in-frame with the DNA binding domain of GAL4 was isolated (Figure 3.2A and B). This cDNA encoded amino acid residues 210 to 342 of Par-4 (Johnstone et al., 1996). In this region, the predicted amino acid sequence of simian Par-4 is 98.5% identical to human Par-4. Par-4 was originally isolated in a screen to identify proteins upregulated during apoptosis in prostate cells (Sells et al., 1994). Subsequently, Par-4 was found to sensitize cells to apoptotic stimuli by blocking the anti-apoptotic effects of NF- $\kappa$ B (Camandola and Mattson, 2000; Chang et al., 2002; Chendil et al., 2002). Inhibition of NF- $\kappa$ B is achieved through the ability of Par-4 to bind to and inhibit PKC $\zeta$ , a protein which is able to activate NF- $\kappa$ B (Diaz-Meco et al., 1996).

### **3.2.2. GST pulldown experiments**

GST pulldown experiments were utilized as an alternate method of identifying novel capsid-interacting proteins, and to confirm interactions detected in the yeast two-hybrid system. This method was used since it is able to purify endogenous protein complexes from cells; a distinct advantage over the yeast two-hybrid system, which requires nuclear targeting of bait and prey interacting proteins. In addition, proteomic analysis can be used to easily and rapidly determine the identity of proteins that co-purify with the GST-fusion proteins. For these experiments, the entire coding region of capsid was fused, in frame, to the carboxy terminus of GST (pEBG-capsid). COS or HEK

**A**



**B**

1	GAT CCA GGC AGT TCC TAT CTG CTA CAG GAG CCA CCT AGA ACA GTT TCA GGC AGA TAT AAA	
	D P G S S Y L L Q E P P R T V S G R Y K	20
61	AGC ACA ACC AGT GTC TCT GAA GAA GAT GTC TCA AGT AGA TAT TCT CGA ACA GAT AGA AGT	
	S T T S V S E E D V S S R Y S R T D R S	40
121	GGG TTC CCT AGA TAC AAC AGG GAT GCA AAT GTT TCA GGT AAT CTG GTT TCA AGT AGC ACA	
	G F P R Y N R D A N V S G <b>N</b> L V S S S T	60
		<b>T</b>
181	CTG GAA AAG AAA ATT GAA GAT CTT GAA AAG GAA GTA GTA CGA GAA AGA CAA GAA AAC CTA	
	L E K K I E D L E K E V V <b>R</b> E R Q E N L	80
		<b>T</b>
241	AGA CTT GTG AGA CTG ATG CAA GAT AAA GAG GAA ATG ATT GGA AAA CTC AAA GAA GAA ATT	
	R L V R L M Q D K E E M I G K L K E E I	100
301	GAT TTA TTA AAT AGA GAC CTA GAT GAC ATA GAA GAT GAA AAT GAA CAG CTA AAG CAG GAA	
	D L L N R D L D D I E D E N E Q L K Q E	120
361	AAT AAA ACT CTT TTG AAA GTT GTT GGT CAG CTG ACC AGG TAG	
	N K T L L K V V G Q L T R *	133

**Figure 3.2. The structure and sequence of simian Par-4.** A) Schematic diagram of human Par-4. Par-4 is 333 amino acid residues in length and contains death domain (DD) and leucine zipper (LZ) motifs in its carboxy terminus. The region of simian Par-4 encoded by clone 11 (corresponding to amino acid residues 210 to 333 of human Par-4) is indicated by a solid black line. B) Nucleotide and predicted amino acid sequences of the coding region of clone 11 which encodes the carboxy terminus of simian Par-4. The numbers on the left correspond to nucleotides; the numbers on the right correspond to amino acid residues. Residues that differ from the published human sequence are shown in bold with the corresponding human sequence below. The predicted amino acid sequence of simian Par-4 is 98.5% identical to human Par-4. Only the coding sequence is shown. The stop codon is indicated by an asterisk.

293T cells were transiently transfected with plasmids encoding either GST or GST-capsid. Forty-eight hours post-transfection, cells were lysed and GST proteins were bound to glutathione Sepharose beads. Beads were washed and proteins were eluted from the beads and separated by SDS-PAGE. Proteins were silver stained and proteins which specifically bound to GST-capsid, but not to GST alone, were excised from the gels (Figure 3.3A). To determine the identity of the capsid-binding proteins, proteins were subjected to in gel digestion and MALDI-TOF mass spectrometry. Using this method, two capsid-interacting proteins were identified. The first was p32, which further confirms our earlier finding that p32 interacted with capsid in the yeast two-hybrid system. The other protein was identified as the cytoplasmic poly(A)-binding protein (isoform 4). The poly(A)-binding protein binds poly(A) tracts at the 3' end of eukaryotic mRNAs and enhances translation and RNA stability (Gallie, 1998). A protein with an apparent molecular mass of approximately 80 kDa also bound to GST-capsid (Figure 3.3A, arrow) but we were unable to determine the identity of this protein using mass spectrometry.

Immunoblotting was also used to identify proteins that bound to capsid in the GST pulldown assay. Using this method, we found that both p32 and Par-4 specifically bound to GST-capsid but not to GST alone (Figure 3.3B), confirming our previous findings that p32 and Par-4 interact with capsid. We also investigated whether PKC $\zeta$  bound to GST-capsid. This interaction was examined since both p32 and Par-4 are known to interact with various isoforms of PKC (Diaz-Meco et al., 1996; Robles-Flores et al., 2002; Storz et al., 2000). In particular, Par-4 negatively regulates the kinase activity of PKC $\zeta$ . Furthermore, a protein with the same apparent molecular mass as PKC $\zeta$  (80 kDa, Figure 3.3A, arrow) was observed in GST-capsid pulldowns. We were unable to determine the identity of this protein by mass spectrometry, however, immunoblotting indicated that PKC $\zeta$  was present in GST-capsid pulldowns but not in GST pulldowns (Figure 3.3B).

In summary, we have identified four novel capsid-interacting proteins using two different methodologies. These proteins were p32, Par-4, PKC $\zeta$  and the poly(A) binding protein. Due to time limitations, only the interactions between capsid and p32 and Par-4 were investigated in further detail.

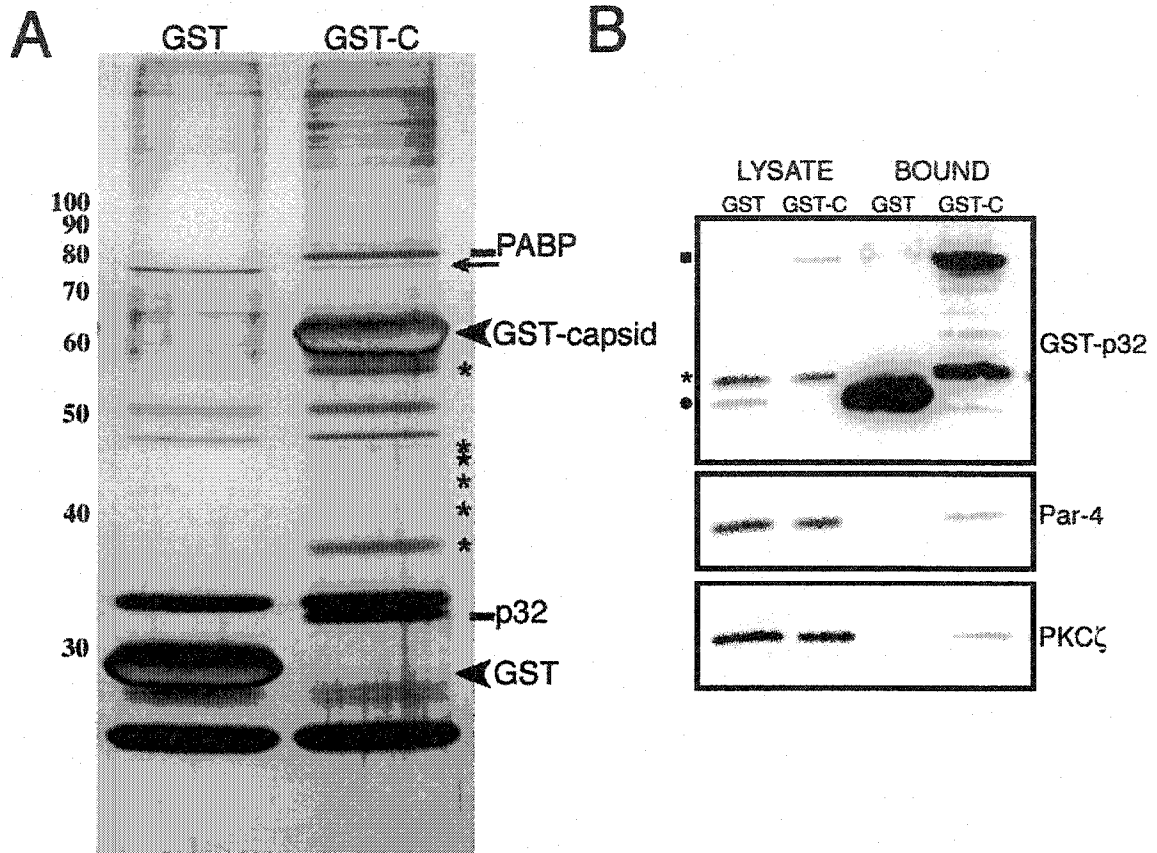


**Figure 3.3. Identification of capsid-binding proteins by GST pull-down.** A) COS cells were transiently transfected with plasmids encoding GST or GST-capsid (GST-C). Forty-eight hours post-transfection, cells were lysed and lysates were mixed with glutathione Sepharose beads. Beads were washed and bound proteins were eluted and subjected to SDS-PAGE. The gel was silver stained and proteins that bound to GST-capsid but not GST were excised and identified by MALDI-TOF mass spectrometry. GST and GST-capsid are indicated with arrowheads. Bands which were identified as p32 and the poly(A) binding protein (PABP) are indicated. Bands that were determined to be degradation products of GST-capsid are indicated by an asterisk. The identity of the band indicated by a small arrow was not determined. The location of molecular mass markers is indicated to the left of the gel. B) Western blotting was also used to identify proteins which bound to GST-capsid. GST pull-downs were conducted as described in A and lysates and eluates from the beads were subjected to Western blotting using the antibodies indicated to the left of the panel. The asterisk indicates the band corresponding to p32, the solid circle indicates the band corresponding to GST and the triangle indicates the band corresponding to GST-capsid in the p32 immunoblot.

### **3.3. Confirmation and characterization of the capsid-p32 interaction**

#### **3.3.1. Capsid and p32 interact *in vitro***

Previous studies showed that the majority of p32 localizes to the mitochondrial matrix (Muta et al., 1997). We were therefore surprised to find that the capsid would interact with this type of protein. To further investigate the capsid-32 interaction, we employed an *in vitro* binding assay to measure the interaction of radiolabeled capsid with p32 immobilized on Sepharose beads. <sup>35</sup>S-labeled capsid (lacking the E2 signal peptide) or GFP were incubated with either GST or GST-p32 pre-bound to glutathione Sepharose beads. The beads were washed and bound proteins were eluted and analyzed by SDS-PAGE and fluorography. In this assay, <sup>35</sup>S-labeled capsid was bound by GST-p32 but not by GST (Figure 3.4, lanes 2 and 3). <sup>35</sup>S-labeled GFP, which served as a negative control, did not bind to either GST-p32 or GST (Figure 3.4, lanes 6 and 7). We were concerned that the interaction between capsid, which contains a large basic region, and p32, which is rich in acidic residues, might be the result of non-specific electrostatic interactions. This was shown not to be the case since capsid did not bind to glucose oxidase which, like p32, is an acidic soluble protein (Figure 3.4, lane 4). Together, these results demonstrate that the interaction of capsid with p32 is specific.

#### **3.3.2. Capsid and p32 interact *in vivo***

Co-immunoprecipitation studies were used to determine if capsid interacts with p32 *in vivo*. COS cells were co-transfected with expression vectors encoding p32 and either 24S (capsid, E2 and E1) or E2E1 (E2 and E1). Alternatively, cells were transfected with the 24S or p32 expression vectors alone. Forty hours post-transfection cells were biosynthetically labeled with <sup>35</sup>S-methionine and cysteine and cell lysates were prepared using non-denaturing conditions. Lysates were subjected to radioimmunoprecipitation with antibodies specific for capsid or p32 and the immune-complexes were analyzed by SDS-PAGE and fluorography. Capsid-p32 complexes were co-immunoprecipitated from transfected cells using antibodies to capsid or p32 (Figure 3.5A, lanes 2, 3 and 9). Neither capsid nor p32 were immunoprecipitated by pre-immune rabbit serum (Figure 3.5A, lane

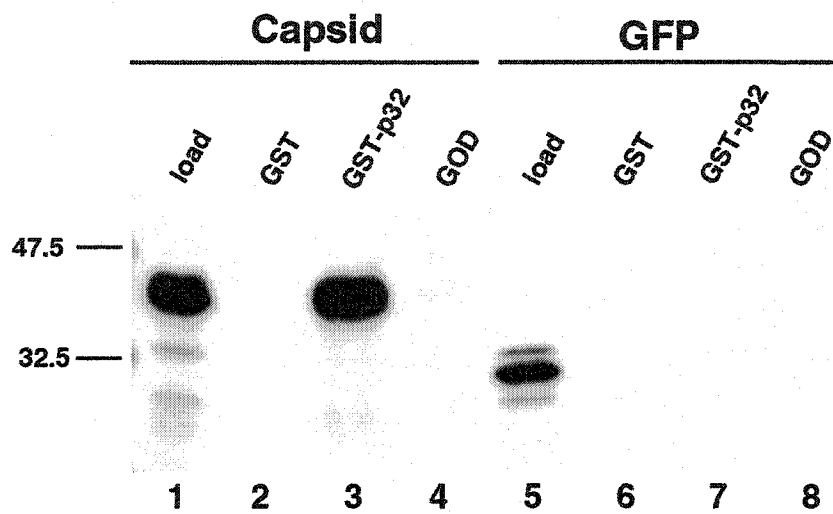


**Figure 3.4. Capsid binds to p32 *in vitro*.** Sepharose beads coated with GST (lanes 2 and 6), GST-p32 (lanes 3 and 7), or glucose oxidase (GOD) (lanes 4 and 8) were mixed with <sup>35</sup>S-labeled capsid (lanes 2-4) or GFP (lanes 6-8). The beads were washed and bound proteins were eluted and visualized by SDS-PAGE and fluorography. An equivalent amount of starting material as used in the binding assays was loaded in lanes 1 and 5.

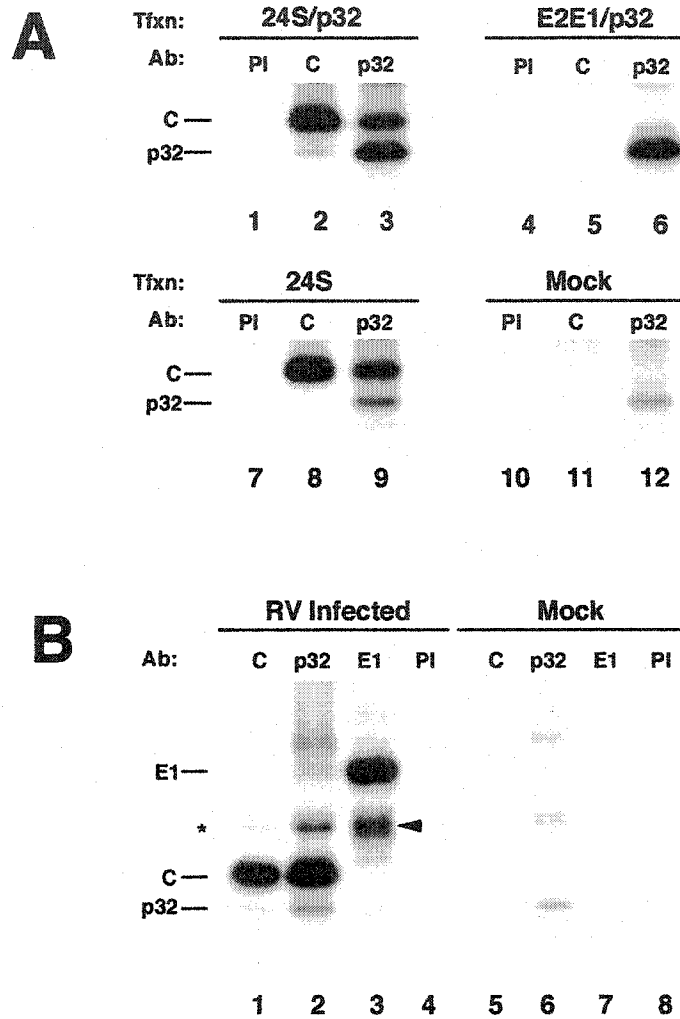


**Figure 3.5. Coimmunoprecipitation of capsid and p32.** A) COS cells were transfected (Tfxn) with expression vectors encoding the RV structural proteins (24S) and p32 (lanes 1-3), the RV envelope proteins (E2E1) and p32 (lanes 4-6), 24S alone (lanes 7-9), or mock transfected (lanes 10-12). Forty hours post-transfection the cells were biosynthetically labeled with  $^{35}\text{S}$ -methionine/cysteine, lysed and then subjected to immunoprecipitation with pre-immune serum (PI, lanes 1, 4, 7, 10), or antibodies (Ab) specific for capsid (lanes 2, 5, 8, 11) or p32 (lanes 3, 6, 9, 12). Immune-complexes were subjected to SDS-PAGE and fluorography. The positions of capsid (C) and p32 are indicated to the left of gels. B) Vero cells were infected or mock-infected with rubella virus at MOI=1 PFU/cell. Forty-eight hours post-infection, the cells were biosynthetically labeled with  $^{35}\text{S}$ -methionine/cysteine. Immunoprecipitations were performed using lysates from infected cells (lanes 1-4) and mock-infected cells (lanes 5-8) as above using antibodies (Ab) specific for capsid (lanes 1, 5), p32 (lanes 2, 6), E1 (lanes 3, 7) or pre-immune serum (lanes 4, 8). The positions of E1, capsid (C) and p32 are indicated to the left of gels. E2, which co-precipitates with E1 (lane 3) is indicated with an arrowhead. The asterisk denotes an unknown protein that co-migrates with E2 in lanes 1, 2, and 4).

1). For negative controls, the immunoprecipitations were performed on E2E1/p32-transfected and mock-transfected COS cells (Figure 3.5A, lanes 4-6 and 10-12). Capsid was not immunoprecipitated from these lysates and p32 was only immunoprecipitated using anti-p32 (Figure 3.5A, lanes 6 and 12). To confirm that the capsid-p32 interaction is relevant in the context of viral infection, immunoprecipitations were repeated using lysates prepared from RV-infected Vero cells. Similar to the results obtained using transfected cells, capsid and p32 were co-immunoprecipitated using antibodies specific for capsid or p32 in a reciprocal fashion from infected cells, but not from mock-infected cells (Figure 3.5B, lanes 1,2,5 and 6). In addition, neither capsid nor p32 were immunoprecipitated by pre-immune rabbit serum or a monoclonal antibody specific for E1 (Figure 3.5B, lanes 3,4,7 and 8). Although capsid and p32 co-immunoprecipitated in a reciprocal fashion, the amount of p32 immunoprecipitated with anti-capsid antibodies was much lower than the amount of capsid immunoprecipitated with anti-p32 antibodies. One possibility is that binding of the polyclonal antibodies to capsid results in disruption of the capsid-p32 complexes.

To determine the intracellular localization of the capsid-p32 interaction, indirect immunofluorescence microscopy was used to analyze transiently transfected cells. In cells expressing RV structural proteins and p32, a significant proportion of capsid co-localized with p32 to cytoplasmic vesicular structures in the perinuclear region (Figure 3.6 A, B arrowheads). These structures were identified as mitochondria since p32 co-localized with the mitochondria-specific dye Mitotracker Red CMXRos (Figure 3.6 C, D). No co-localization was observed between p32 and the RV envelope protein E1 (Figure 3.6 E, F). Interestingly, the mitochondria in cells expressing RV structural proteins were more spherical and were clustered in the perinuclear region in contrast to those in non-transfected cells which were more lacy and peripherally localized (Figure 3.6 B, F).

To determine whether p32 and capsid are interacting on the cytoplasmic surface or within the matrix of the mitochondria, cells were fixed and treated with digitonin to permeabilize only the plasma membrane or with digitonin followed by TritonX-100 to permeabilize intracellular membranes. Using this method, mitochondrial staining of

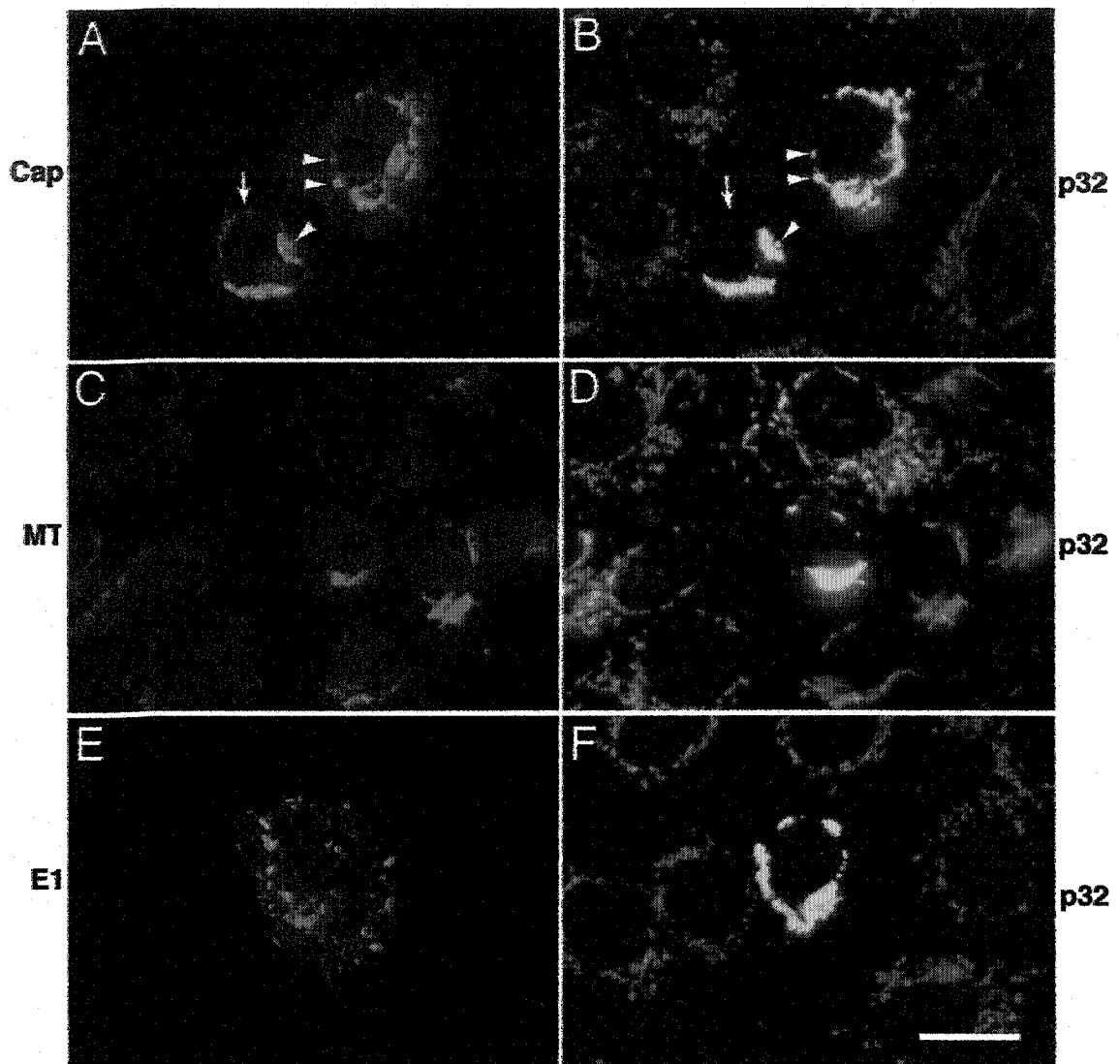


**Figure 3.6. Capsid colocalizes with p32 at the mitochondria.** Vero cells were transfected with expression vectors encoding the RV structural proteins (24S) and p32. Cells were incubated with antibodies to capsid (Cap) (A), p32 (B, D, F) or E1 (E) as indicated. For samples shown in C and D, mitochondria were labeled, prior to fixation, with Mitotracker Red CMXRos (MT) (C) followed by staining with anti-p32. Primary antibodies were detected with Texas Red-goat anti-mouse IgG and FITC-donkey anti-rabbit IgG. The Texas red channel is shown on the left (A, C, E) and the FITC channel is shown on the right (B, D, F). Areas of colocalization are shown by arrowheads whereas the arrow denotes a perinuclear pool of capsid which does not overlap with p32. Bar = 20  $\mu\text{m}$ .

capsid was observed in both digitonin and digitonin/TritonX-100 permeabilized cells (Figure 3.7 A, C). In contrast, p32 was only detected in digitonin/TritonX-100 treated cells. These results indicate that p32, but not capsid is translocated into the mitochondria and can potentially explain why the distributions of these two proteins are slightly different (Figures 3.6 and 3.7.). This conclusion is supported by confocal scanning microscopy analysis which showed that anti-capsid and anti-p32 antibodies stained different regions of the mitochondria (Figure 3.7 E, F and G). Capsid staining was often localized to the periphery of mitochondria (Figure 3.7 E) whereas p32 staining was more central and extended into the interior of these structures (Figure 3.7 G).

### **3.3.3. The amino-terminus of capsid binds the carboxy-terminus of p32**

We used the yeast two-hybrid system to identify the region of capsid that binds p32. Initially, three different, but similarly sized regions of the capsid cDNA were amplified by PCR and sub-cloned into pGBT9. The capsid constructs were co-transformed with clone 10 (pGAD-p32) into AH109 cells and tested for the ability to grow on media lacking adenine, leucine, tryptophan and histidine. These interactions were further tested using the  $\beta$ -galactosidase filter assay. Full-length capsid and the amino terminal region of capsid (amino acids 1-88) interacted strongly with p32 in these assays (Figure 3.8 A). In contrast, the middle and carboxy terminal regions of capsid (amino acids 87-171 or 167-277 respectively) did not interact with p32. The amino terminal 88 amino acid residues of capsid was then subdivided into two smaller regions and tested using the same assay. No growth was observed on media lacking adenine, leucine, tryptophan and histidine when AH109 were cotransformed with constructs encoding p32 and capsid residues 1-45. In contrast, a weak interaction between amino acids 46-89 of capsid and p32 was detected. AH109 cotransformed with constructs encoding p32 and capsid residues 46-89 developed small, slow-growing colonies. These results indicate that the minimal region of capsid which can interact with p32 is located within amino acids 46-89 but that the participation of amino acids outside of this region are important to achieve the full binding potential. To further characterize the binding region, constructs encoding capsid amino acids 30-65, 30-69, 30-79 and 30-89 were

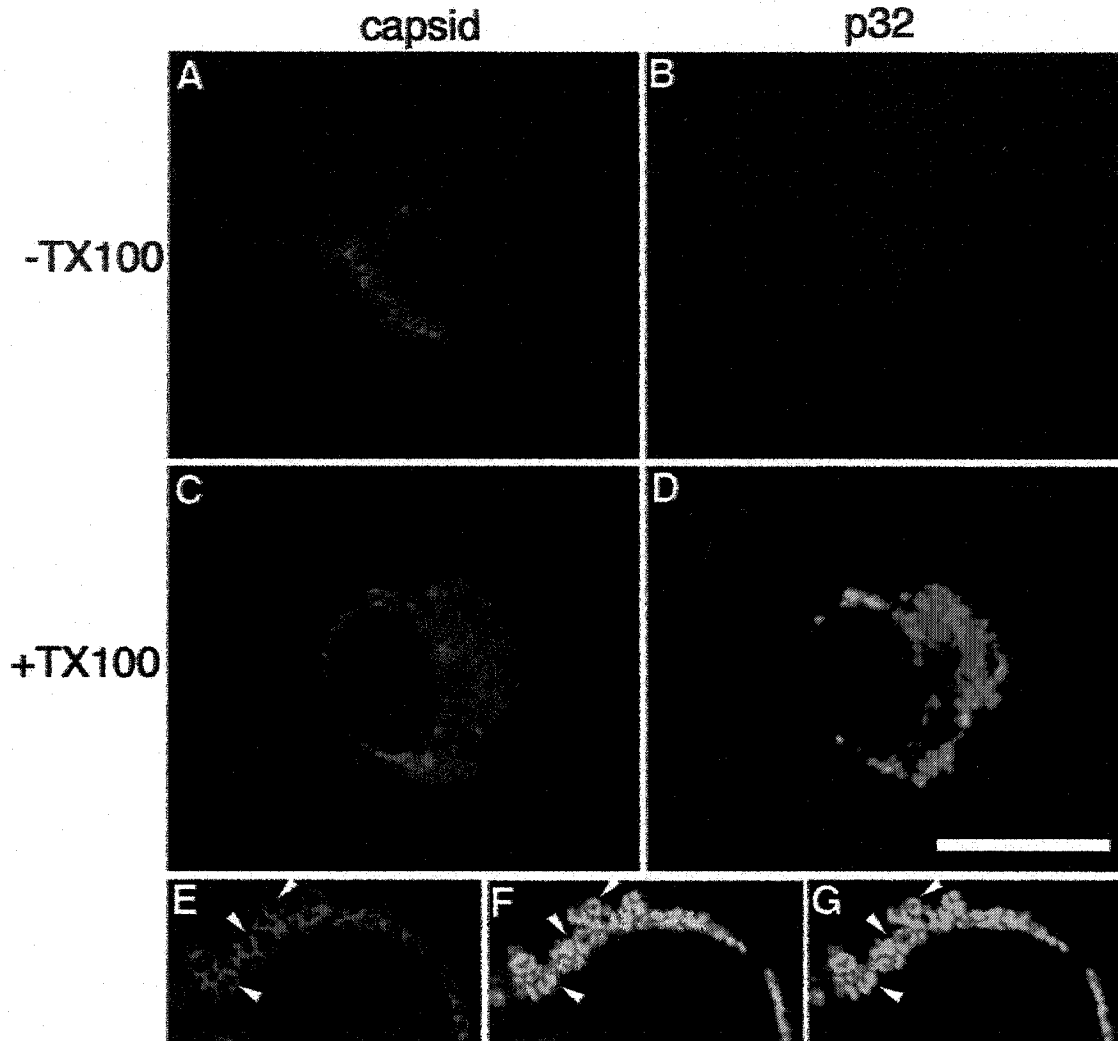


**Figure 3.7. Capsid is associated with the cytoplasmic surface of mitochondria.** Vero cells were transfected with expression vectors encoding the RV structural proteins (24S) and p32, and cells were fixed with 3% paraformaldehyde. Plasma membranes were permeabilized with digitonin only (-TX100) (A and B). To permeabilize intracellular membranes, cells were treated with TritonX-100 (+TX100) (C and D). Cells were double-labeled with antibodies specific for capsid (A and C) or p32 (B and D). Primary antibodies were detected with Texas Red-goat anti-mouse IgG and FITC-donkey anti-rabbit IgG. The Texas red channel is shown on the left (A and C) and the FITC channel is shown on the right (B and D). Bar = 20  $\mu$ m. (E to G) Confocal images of Triton X-100 treated cells. The arrowheads indicate capsid staining at the periphery of mitochondria which does not coincide with p32 staining (G). Panel F is a merge of the images shown in panels E and G.

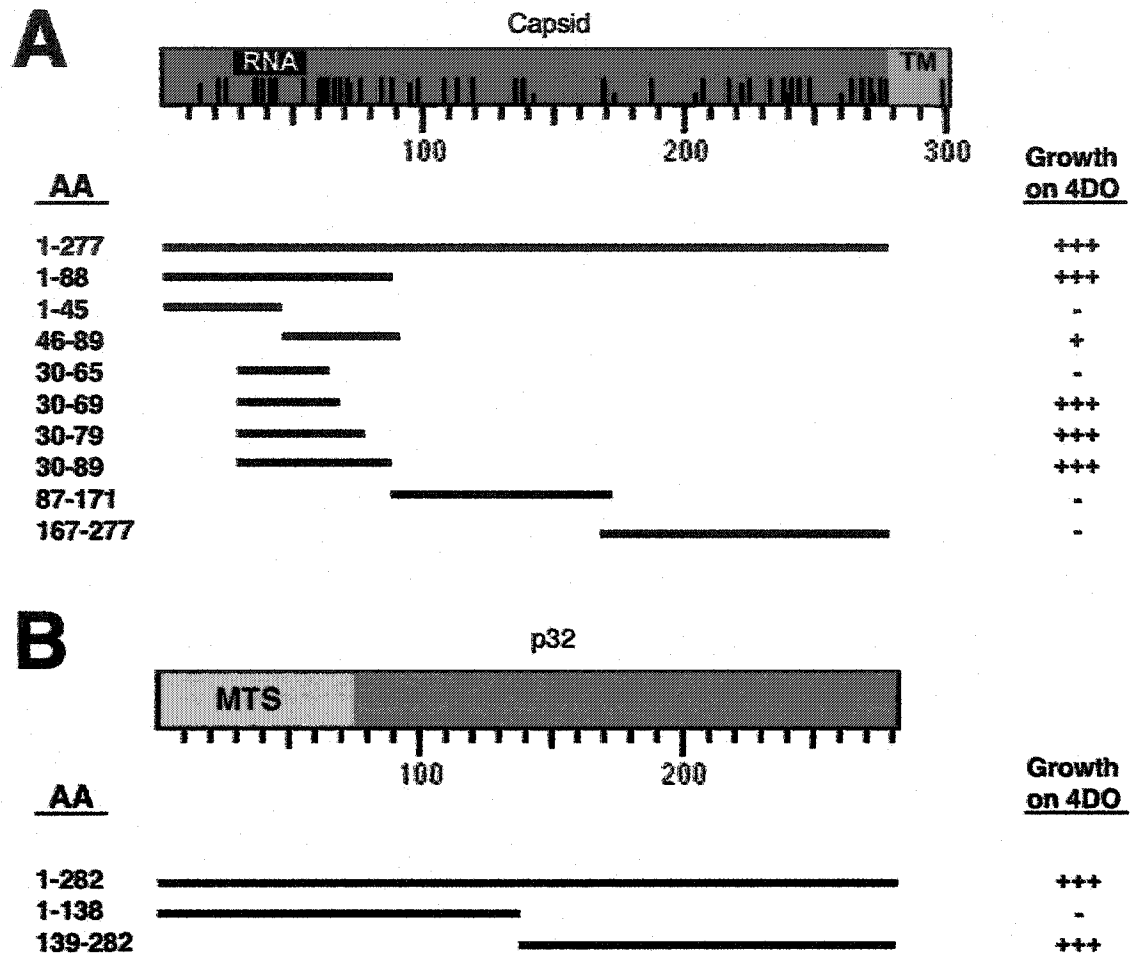


**Figure 3.8. Characterization of the capsid-p32 binding regions using the yeast two-hybrid system.** A) The p32-binding site is located in the amino terminal region of capsid. AH109 yeast cells were transformed with pGAD-p32 and various plasmids encoding capsid (amino acid residues 1-277) or portions of capsid fused to the GAL4 binding domain. The capsid constructs are named according to the amino acid residues (AA) in capsid which they encode. For example, 1-45 is the coding region for amino acid residues 1-45 of capsid fused to the GAL4 binding domain. The region of capsid encoded by each construct is indicated by a solid line underneath the capsid schematic. Transformants were plated onto media lacking tryptophan, leucine, histidine and adenine (4DO) and growth was scored visually in relation to positive and negative controls as follows: (-) no growth, (+) weak growth, (+++) strong growth. The positive control was a Clontech system control that utilizes two strongly interacting proteins, p53 (in pGBKT7) and SV40 large T antigen (in pGAD). As a negative control (-), AH109 were transformed with two plasmids encoding proteins which do not interact (pGBKT7-p53 and pGAD-ABP280). Growth on the 4DO plates within 4 days was interpreted as evidence of a positive interaction. B) The carboxy terminal half of p32 binds capsid. AH109 yeast cells were transformed with pGAD424-capsid and either pGBKT7-p32 (encoding amino acid residues 1-282), pGBKT7-p32N (encoding amino acid residues 1-138) or pGBKT7-p32C (encoding amino acid residues 139-282) and scored as in A.

tested for binding to p32 as described above. In contrast to amino acids 46-89, which interacted weakly with p32, amino acids 30-69, 30-79 or 30-89 but not 30-65 interacted as strongly as full-length capsid with p32. Together, these results indicate that the region of capsid which interacts with p32 is located within amino acids 30-69.

The yeast two-hybrid system was also used to determine the region of p32 which interacts with capsid. PCR was used to amplify the 5' and 3' terminal halves of the p32 cDNA and these constructs were then sub-cloned, in frame with the GAL4 DNA binding domain, into pGBKT7. AH109 yeast cells were transformed with pGAD424-capsid and either pGBKT7-p32N (amino acids 1-138 of p32) or pGBKT7-p32C (amino acids 139-282 of p32) and tested for growth on media lacking adenine, leucine, tryptophan and histidine (Figure 3.8 B). The carboxy terminal half of p32 was found to interact strongly with capsid whereas no growth was observed when the amino half of p32 was transformed into AH109 together with capsid. These results indicate that the region of p32 which interacts with capsid is located in the conserved carboxy terminus of p32.

### **3.4. Confirmation and characterization of the capsid –Par-4 interaction**

#### **3.4.1. Capsid and Par-4 interact *in vitro***

We also wanted to confirm the interaction of capsid with the host cell protein Par-4. To do this, we employed *in vitro* binding experiments similar to those used to confirm the capsid-p32 interaction. GST or GST-Par-4 were immobilized on glutathione Sepharose beads which were then incubated with <sup>35</sup>S-methionine labeled capsid (lacking the E2 signal peptide) or GFP. Following incubation, beads were washed and bound proteins were eluted. Eluates were analyzed by SDS-PAGE and fluorography. In this assay, <sup>35</sup>S-labeled capsid specifically bound to GST-Par-4 but not to GST alone (Figure 3.9, lanes 2 and 3). <sup>35</sup>S-labeled GFP was used as a negative control and did not bind to either GST or GST-Par-4 (Figure 3.9, lanes 5 and 6). These results suggest that capsid specifically interacts with Par-4.

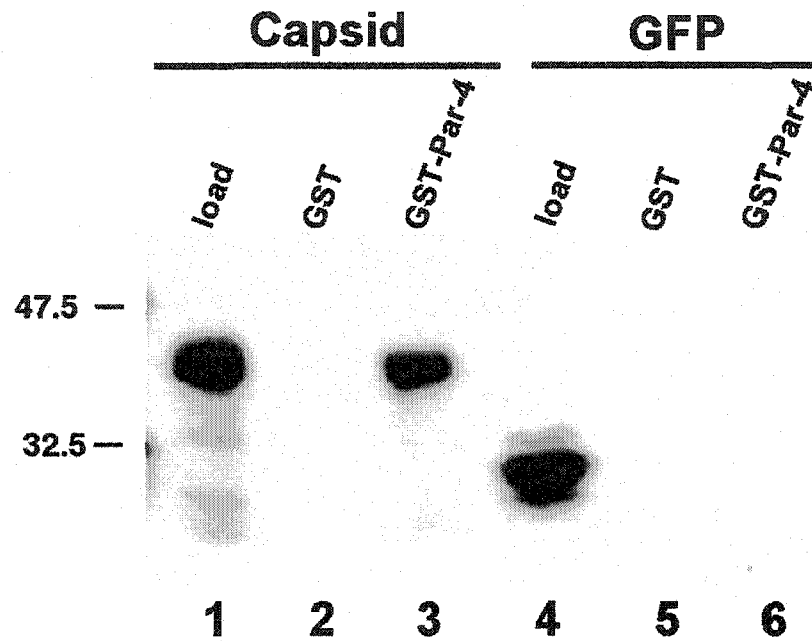


**Figure 3.9. Capsid binds to Par-4 *in vitro*.** Sepharose beads coated with GST (lanes 2 and 5) or GST-Par-4 (lanes 4 and 6) were mixed with <sup>35</sup>S-labeled capsid (lanes 1-3) or GFP (lanes 4-6). The beads were washed and bound proteins were eluted and visualized by SDS-PAGE and fluorography. An equivalent amount of starting material as used in the binding assays was loaded in lanes 1 and 4.

### 3.4.2. Capsid and Par-4 interact *in vivo*

To determine if capsid and Par-4 interact *in vivo*, coimmunoprecipitation experiments were conducted. COS cells were transiently cotransfected with expression vectors encoding capsid and c-myc tagged Par-4. Forty hours post-transfection, cells were biosynthetically labeled with <sup>35</sup>S-methionine-cysteine and cell lysates were prepared using non-denaturing conditions. Antibodies specific for either the c-myc tag or for capsid were used for radioimmunoprecipitation. Immune complexes were analyzed by SDS-PAGE and fluorography. Capsid was coimmunoprecipitated with anti-c-myc from cells expressing both capsid and c-myc tagged Par-4 (Figure 3.10, lane 3). As a negative control, to confirm that this interaction was not due to non-specific interaction of capsid with the c-myc antibody, cells were transiently cotransfected with vectors encoding capsid and Par-4 lacking the c-myc tag (Figure 3.10, lane 7-8). In this instance, capsid was not immunoprecipitated with the c-myc antibody (Figure 3.10, lane 7). Interaction of capsid and Par-4 was dependent on the membrane association of capsid since capsid lacking the E2 signal peptide did not coimmunoprecipitate with anti-c-myc (Figure 3.10, lane 5). This result was interesting since the capsid used in the *in vitro* binding assay did not possess the E2 signal peptide but was found to stably bind to Par-4. Together, these results suggest that retention of the E2 signal peptide on capsid is necessary for membrane association of capsid and not for binding to Par-4 *per se*. Interestingly, capsid also did not coimmunoprecipitate with anti-c-myc when cells were cotransfected with vectors encoding the RV structural proteins and c-myc tagged Par-4 (Figure 3.10, lane 1). These results suggest that retention of capsid in specific intracellular membranes, presumably ER, is necessary for the interaction of capsid with Par-4.

It was difficult to reciprocally confirm the capsid-Par-4 immunoprecipitation due to a band that comigrated with Par-4 using the anti-capsid serum (Figure, 3.10, lanes 2,4, 6 and 8). However, Par-4 did not appear to coimmunoprecipitate with capsid when anti-capsid antibodies were used. It is possible that polyclonal antibodies to capsid interfere with the interaction of these two proteins. In support of this, it is worth noting again that Par-4 bound to GST-capsid in GST pulldown experiments (see Figure 3.3B). Together, these results indicate that capsid interacts with Par-4 *in vivo*.

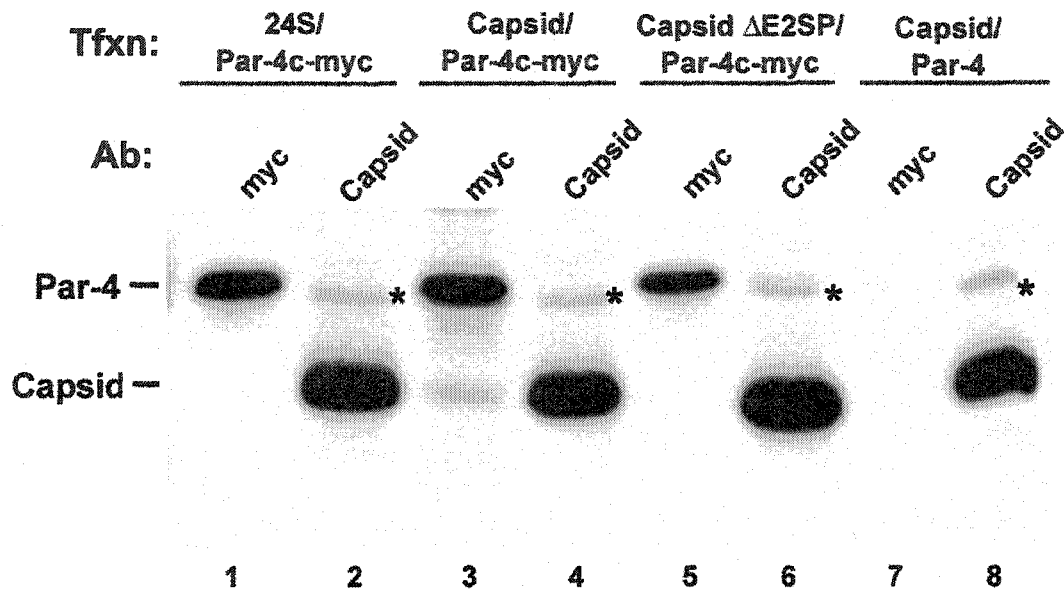


**Figure 3.10. Coimmunoprecipitation of capsid and Par-4.** COS cells were transfected (Tfxn) with expression vectors encoding c-myc tagged Par-4 (lanes 1 to 6) and either the RV structural proteins (24S) (lanes 1 and 2), capsid (lanes 3 and 4), or capsid minus the E2 signal peptide (capsid ΔE2SP) (lanes 5 and 6). Alternatively, cells were cotransfected with capsid and Par-4 lacking the c-myc tag (lanes 7 and 8). Forty hours post-transfection, the cells were biosynthetically labeled with <sup>35</sup>S-methionine-cysteine, lysed and then subjected to immunoprecipitation (IP) with a monoclonal antibody (Ab) to the c-myc tag (myc) (lanes 1, 3, 5 and 7), or rabbit polyclonal antibodies specific for capsid (lanes 2, 4, 6 and 8). Immune-complexes were subjected to SDS-PAGE and fluorography. The positions of Par-4 and capsid are indicated to the right of the gel. The asterisk indicates a nonspecific band which migrates at the same size as Par-4.

### **3.4.3. Capsid and Par-4 co-localize at intracellular membranes**

Indirect immunofluorescence microscopy was used to determine the intracellular sites at which capsid interacts with Par-4. COS cells were transiently cotransfected with expression vectors encoding the RV structural proteins and c-myc-Par-4. Twenty-four hours post-transfection, cells were fixed and processed for indirect immunofluorescence microscopy. Samples were stained using monoclonal antibodies to c-myc (9E10) and either rabbit polyclonal antibodies to capsid (7W7) or mouse monoclonal antibodies to E1 (1B9). A large proportion of capsid was found to colocalize with the c-myc tagged Par-4 at intracellular membranous structures that resembled peripheral ER (Figure 3.11 A-C). In contrast, very little E1 was observed to colocalize with tagged Par-4 (Figure 3.11 D-E). These results are in accordance with the previously reported localization of capsid to ER membranes (Baron et al., 1992; Hobman et al., 1990) and suggest that the capsid-Par-4 interaction occurs at these sites.

### **3.4.4. Identification of the Par-4 binding region of capsid**

The capsid constructs described previously (see section 3.3.3.) were used to determine the region of capsid involved in the interaction with Par-4. AH109 cells were co-transformed with various capsid constructs fused to the GAL4 binding domain and the cDNA encoding the capsid binding region of Par-4 (clone 11 identified in the original yeast two-hybrid screen) fused to the GAL4 activation domain. The ability of transformants to grow on media lacking adenine, leucine, tryptophan and histidine was then tested. The Par-4 binding region of capsid was first mapped to the amino terminus of capsid since constructs encoding amino acid residues 1-88 of capsid interacted strongly with Par-4 whereas constructs encoding amino acid residues 87-171 or 167-277 did not (Figure 3.12). As with the p32 interaction, constructs encoding amino acid residues 46-89 interacted weakly with Par-4 but constructs encoding amino acid residues 1-45 did not interact. Constructs encoding amino acid residues 30-65, 30-69, 30-79 and 30-89 were also tested for binding to Par-4. Using these constructs, the minimal region for the interaction was amino acid residues 30-79, which interacted with Par-4 as strongly as

full-length capsid. These results indicate that the region of capsid which interacts with Par-4 resides between amino acid residues 30-79. Interestingly, this region overlaps with the p32 binding region but is distinct since the minimal region for p32 binding resides within amino acid residues 30-69 of capsid.

### **3.5. Summary**

Two independent methods of identifying protein interactions were used to identify four host cell proteins (p32, Par-4, PKC $\zeta$  and the poly(A) binding protein) that interact with the RV capsid. The interactions with p32 and Par-4 were characterized in greater detail using a variety of *in vitro* and *in vivo* methods. Capsid was shown to interact specifically with the mitochondrial matrix protein, p32, at the cytoplasmic face of the mitochondria. In addition, Par-4, a protein which sensitizes cells to apoptosis, bound specifically to capsid and colocalized with capsid at intracellular membranes. The regions of capsid responsible for the interactions were mapped to overlapping, but distinct, regions in the amino terminal portion of capsid.

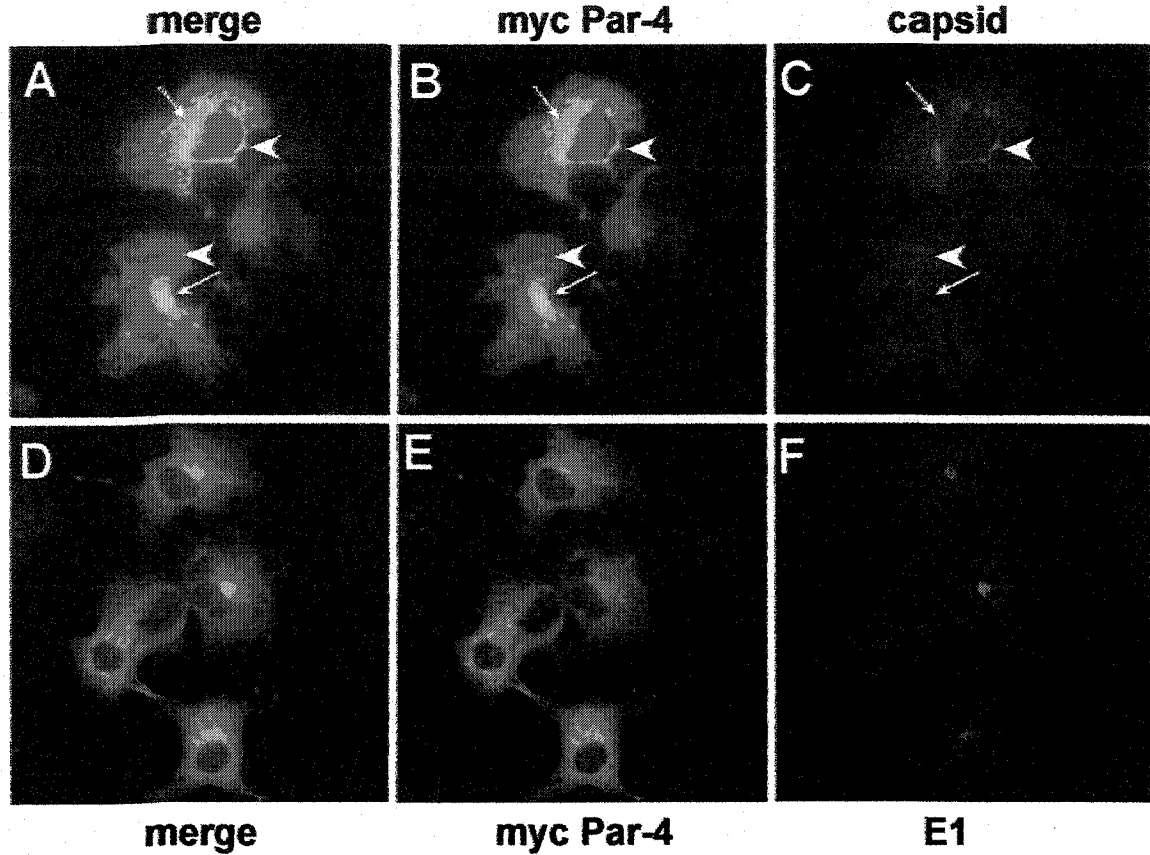


**Figure 3.11. Capsid colocalizes with Par-4 at intracellular membranes.** COS cells were cotransfected with plasmids encoding the RV structural proteins (24S) and c-mycPar-4. Twenty-four hours post-transfection, cells were fixed, permeabilized and incubated with antibodies to the c-myc tag (A, B, D, E), capsid (A, C), or E1 (D, F). Primary antibodies were detected with Texas Red-goat anti-mouse IgG and FITC-donkey anti-rabbit IgG. The FITC channel is shown in panels B and E and the Texas Red channels is shown in panels C and F. Panels A and D show both channels. Areas of colocalization are indicated with arrowheads. Areas where staining patterns do not overlap are indicated with arrows.

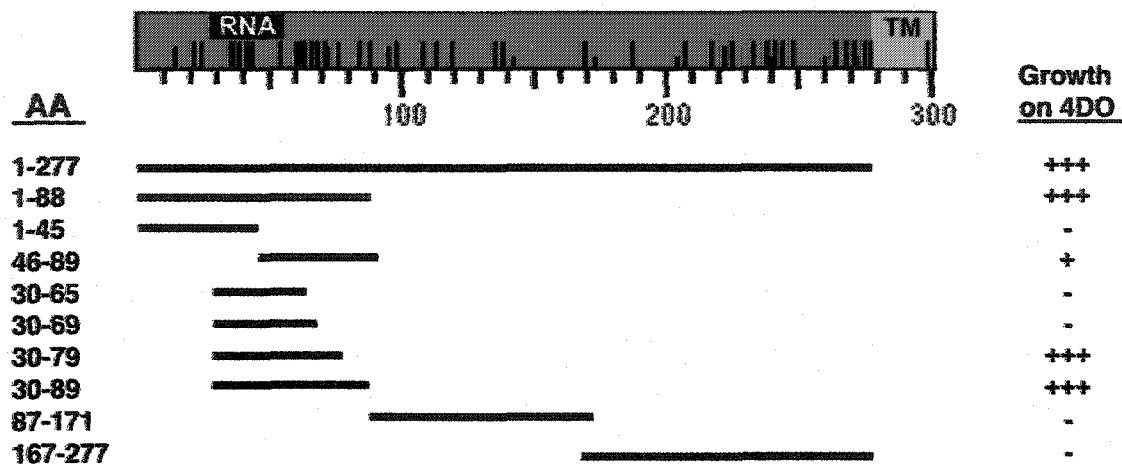


**Figure 3.12. Identification of the Par-4 binding region of capsid using the yeast two-hybrid system.** AH109 cells were transformed with clone 11 (encoding the carboxy terminus of Par-4 fused to the GAL4 activation domain) and various plasmids encoding capsid (amino acid residues 1-277) or portions of capsid fused to the GAL4 binding domain. The capsid constructs are named according to the amino acid residues (AA) in capsid which they encode. For example, 1-45 is the coding region for amino acid residues 1-45 of capsid fused to the GAL4 binding domain. The region of capsid encoded by each construct is indicated by a solid line underneath the capsid schematic. Transformants were plated onto media lacking tryptophan, leucine, histidine and adenine (4DO) and growth was scored visually in relation to positive and negative controls as follows: (-) no growth, (+) weak growth, (+++) strong growth. The positive control was a Clontech system control that utilizes two strongly interacting proteins, p53 (in pGBKT7) and SV40 large T antigen (in pGAD). As a negative control (-), AH109 was transformed with two plasmids which do not interact; pGBKT7-p53 and pGAD-ABP280. Growth on the 4DO plates after 4 days was interpreted as evidence of a positive interaction.

**CHAPTER 4. INTERACTIONS BETWEEN CAPSID AND p32 ARE  
IMPORTANT FOR VIRAL REPLICATION**

#### **4.1. Overview**

Here we show that expression of the RV capsid has direct effects on mitochondrial localization and morphology in cultured cells. Specifically, expression of capsid results in perinuclear clustering of mitochondria and the formation of electron dense zones between opposing mitochondria. We previously identified a minimal region of the capsid (amino acid residues 30 to 69) which is responsible for the interaction between capsid and the mitochondrial matrix protein p32. Two clusters of arginine residues within this minimal region are required for stable binding of capsid and p32. Mutations in the p32-binding region of capsid resulted in decreased mitochondrial clustering indicating that interactions with p32 are required for capsid-dependent reorganization of mitochondria. Despite the dramatic effects of capsid on mitochondrial distribution, capsid expression neither decreased mitochondrial membrane potential nor protected mitochondria from the effects of pro-apoptotic drugs. Recombinant viruses encoding arginine to alanine mutations in the p32-binding region of capsid exhibited altered plaque morphology and replicated to lower titers in a one-step growth curve. Together, these results suggest a role for the capsid-p32 interaction in reorganization of mitochondria during infection and that this process is beneficial for viral replication.

#### **4.2. Analysis of the capsid-p32 interacting domain.**

In the previous chapter, we identified a minimal region of capsid that is necessary for binding of capsid to the host-cell protein, p32. To further investigate the importance of the capsid-p32 interaction for virus replication and pathogenic effect, we set out to identify specific amino acid residues in capsid that are necessary for this interaction. The goal of this analysis was to create capsid mutants that do not interact with p32 for the purpose of examining virus replication in the absence of the capsid-p32 interaction. The p32-binding region of capsid (amino acids 30 to 69) contains a number of arginine residues which reside in two clusters: an amino proximal cluster containing five arginine residues and a carboxy proximal cluster containing six arginine residues (Figure 4.1). Since the p32-binding domains of several other p32-interacting proteins

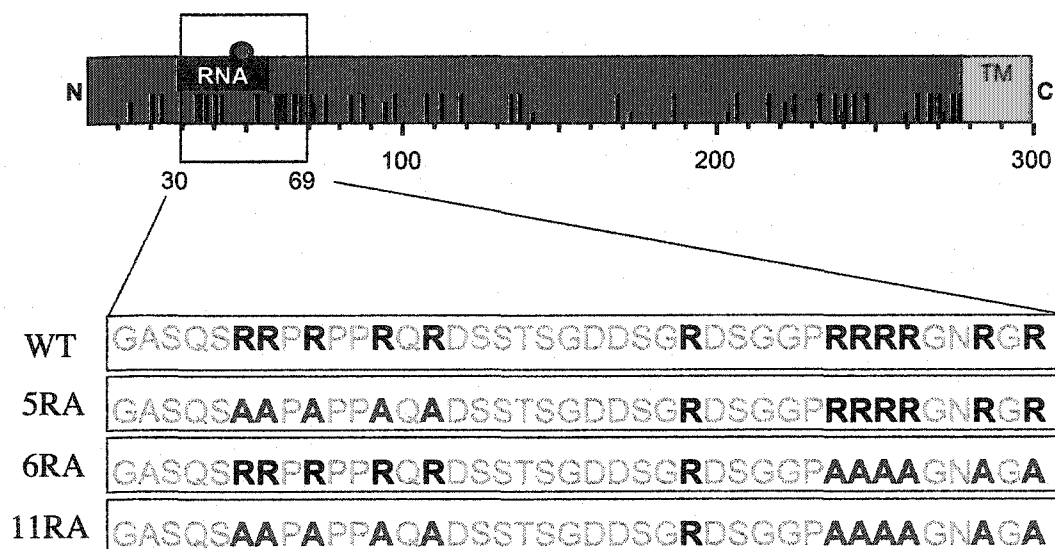


**Figure 4.1. The p32 binding region of capsid.** The p32-binding region of capsid (amino acid residues 30-69) (boxed) contains two clusters of arginine residues. The wild-type (WT) sequence of the M33 strain of RV is indicated below the capsid schematic. Arginines are in black bold type. Arginines in each cluster were mutated to alanine residues (red bold type) as indicated and designated 5RA, 6RA or 11RA. The RNA binding region (RNA), the E2 signal peptide (TM), positive charged residues (vertical lines), and serine 46 (red circle) are indicated on the capsid schematic.

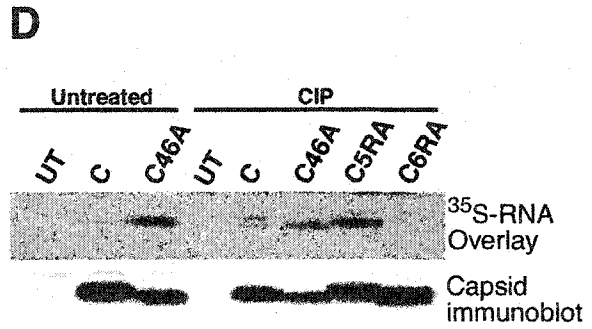
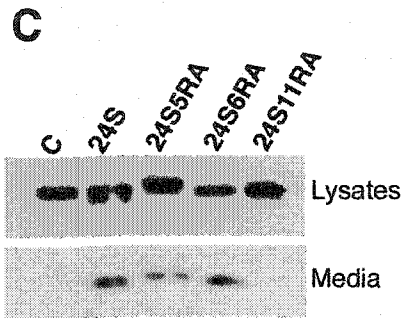
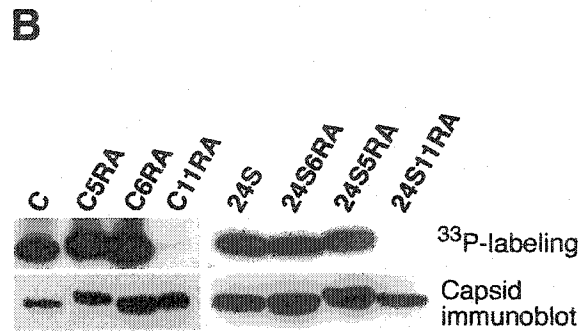
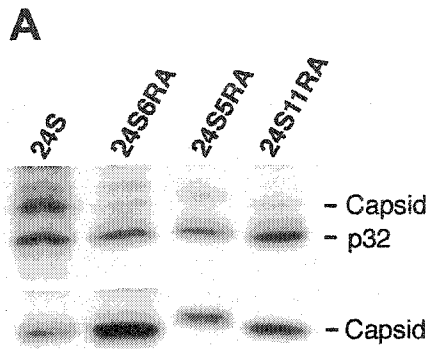
contain arginine-rich regions (Bryant et al., 2000; Hall et al., 2002; Luo et al., 1994; Nikolakaki et al., 1996; Wang et al., 1997), we focused our studies on the arginine residues in this region of capsid. Arginines in the p32-binding region were changed to alanine residues by site-directed mutagenesis. The resulting capsid constructs were named 5RA, 6RA and 11RA, as indicated in figure 4.1.

Coimmunoprecipitation studies were used to determine if the arginine residues in the p32-binding domain of capsid are required for binding to p32. COS cells were transiently transfected with expression vectors encoding RV E2, E1 and wild type or mutant capsids. At 40 h post-transfection, cells were biosynthetically labeled with <sup>35</sup>S-methionine-cysteine and cell lysates were prepared using non-denaturing conditions. Goat anti-p32 serum was used to immunoprecipitate p32 from the lysates and immune complexes were analyzed by SDS-PAGE and fluorography. As expected, wild type capsid co-immunoprecipitated with p32 (Figure 4.2 A, upper panel). In contrast, capsids containing the 5RA, 6RA or 11 RA mutations did not coimmunoprecipitate with p32 as efficiently (Figure 4.2 A, upper panel). To ensure that the mutant capsid constructs were stable when expressed in transfected cells, capsid was also immunoprecipitated from cellular lysates using rabbit anti-capsid serum (Figure 4.2 A, lower panel). Interestingly, the 5RA capsid consistently ran slower than wild type capsid possibly due to a conformational change in the capsid protein. Together, these experiments indicated that the mutant capsid constructs are all stable and that both arginine clusters within the p32-binding domain are necessary for stable binding of capsid to p32. This was not unexpected since our results obtained using the yeast two-hybrid system indicated that portions of capsid containing the amino proximal arginine cluster (amino acids 1 to 45) or the carboxy proximal arginine cluster (amino acids 46 to 89) were unable to bind p32 strongly, whereas amino acids 30 to 69, which contains both arginine clusters in their entirety, bound to p32 as strongly as full-length capsid.

Various assays were conducted to determine if these mutations had any adverse effects on capsid function. First, the phosphorylation state of the capsid mutants was examined. This was of interest since the mutated regions of capsid are in close proximity to serine 46, which is the primary phosphorylated residue in capsid (Law et al., 2003).

**Figure 4.2. Two clusters of arginines in capsid are required for binding to p32, but not for phosphorylation of capsid, assembly of virus-like particles, or RNA binding.**

**A) Coimmunoprecipitation of capsid arginine to alanine mutants with p32.** COS cells were transfected with expression vectors encoding the RV structural proteins (24S), or the RV structural proteins containing arginine to alanine mutations in the capsid. Cells were biosynthetically labeled with  $^{35}\text{S}$ -methionine-cysteine prior to lysis and immunoprecipitation with either goat anti-p32 serum (upper panel) or rabbit anti-capsid serum (lower panel). Samples were subjected to SDS-PAGE and fluorography. The positions of capsid and p32 are indicated to the right of the gels. **B) Capsid Phosphorylation.** COS cells were transfected with expression vectors encoding capsid (C), the RV structural proteins (24S), or constructs containing arginine to alanine mutations (5RA or 6RA). Cells were labeled with  $\text{H}_3^{33}\text{PO}_4$  and capsid was immunoprecipitated from lysates. Samples were subjected to SDS-PAGE and fluorography (upper panel). The relative expression levels of capsid were determined by immunoblot of cell lysates (lower panel). **C) Assembly of virus-like particles (RLPs).** COS cells were transfected with expression vectors encoding capsid (C), the RV structural proteins (24S), or the RV structural proteins containing arginine to alanine mutations in the capsid. RLPs were collected from the medium by centrifugation at  $100,000 \times g$  (Media) and cellular lysates were prepared (Lysates). Samples were subjected to SDS-PAGE and immunoblotting for capsid. The presence of capsid in the media indicates that capsid is incorporated into RLPs. **D) RNA binding assay.** COS cells were transfected with expression vectors encoding wild type capsid (C), the capsid RA mutants (C5RA or C6RA) or hypophosphorylated capsid (C46A). Transfected and untransfected (UT) cells were lysed and capsid was isolated by immunoprecipitation. Following SDS-PAGE, proteins were transferred to nitrocellulose membranes (Untreated). Alternatively, samples were treated with calf intestinal alkaline phosphatase to dephosphorylate capsid following immunoprecipitation (CIP). Membranes were incubated with a  $^{35}\text{S}$ -labeled RV-specific RNA, washed and binding was detected by exposure to a PhosphorImager (upper panel). Relative capsid expression levels were determined by stripping the membranes and then immunoblotting using a mouse monoclonal antibody to capsid (lower panel).



Any changes to the consensus sequence necessary for phosphorylation may result in loss of phosphorylation and improper binding of capsid to genomic RNA. COS cells were transiently transfected with constructs encoding either the wild type or the mutant capsids. Cells were labeled with  $H_3^{33}PO_4$  for 12 h, then lysed, immunoprecipitated using anti-capsid serum and proteins were separated by SDS-PAGE. Wild type capsid and capsids containing either the 5RA or the 6RA mutations were phosphorylated to the same extent as wild type capsid whether they were expressed alone or together with E2 and E1 (24S cDNA)(Figure 4.2 B, upper panel). In contrast, the 11RA mutant was not stably phosphorylated to the same extent. Immunoblot analysis showed that all of the mutant capsid constructs were stable when over-expressed in transfected cells (Figure 4.2 B, lower panel).

Structural changes to capsid caused by the arginine to alanine mutations might also affect the ability of capsid to assemble into virions. To rule out this possibility, virus assembly assays were conducted. Coordinated expression of the RV structural proteins results in the formation of rubella virus-like particles (RLPs), which resemble native virions in terms of morphology, antigenicity and immunogenicity (Hobman et al., 1994; Qiu et al., 1994). These assays have previously been used in our lab to study virus assembly and secretion (Garbutt et al., 1999a; Garbutt et al., 1999b; Hobman et al., 1994; Law et al., 2001). Wild type and mutant capsids containing the arginine to alanine mutations were coexpressed with or without E2 and E1 in COS cells and RLPs were isolated from the media by ultracentrifugation at 100,000 x g. Pellets were resuspended in gel loading buffer and separated by SDS-PAGE. The presence of capsid in the media indicates that RLPs have been assembled and secreted. When coexpressed with the RV glycoproteins, wild type capsid and capsid containing the 5RA or the 6RA mutations were able to support assembly and secretion of RLPs (Figure 4.2 C, lower panel). Comparable amounts of each capsid were detected in the media suggesting that all three of these constructs are able to form particles with similar efficiencies. RLPs were not formed when capsid was expressed alone, or when the capsid 11RA mutant was coexpressed with E2 and E1. The presence of intracellular capsid in the transfected cells was determined by immunoblotting of cellular lysates and confirmed that capsid

constructs were expressed in transfected cells (Figure 4.2 C, upper panel).

Since the p32-binding region of capsid overlaps with the RNA binding domain, the ability of capsid mutants to bind genomic RNA was also determined using an *in vitro* RNA binding assay (Law et al., 2003). Capsid proteins were expressed in COS cells and then immunoaffinity purified. Purified capsids were then dephosphorylated using calf intestinal alkaline phosphatase (CIP) to increase their RNA binding activities, or left untreated. Capsids were then separated by SDS-PAGE, transferred to nitrocellulose membranes and overlaid with a <sup>35</sup>S-labeled RNA probe. The probe consisted of the portion of the RV genomic RNA containing the capsid-binding packaging signal (Liu et al., 1996). As expected from our previously published results (Law et al., 2003), treatment with CIP was necessary for efficient binding of the RNA probe to wild type capsid (Figure 4.2 D, upper panel). A non-phosphorylated capsid mutant (46A) bound the RNA probe efficiently independent of phosphatase treatment, also as expected. Interestingly, capsid containing the 5RA mutations bound the RNA probe more efficiently than wild type capsid, while capsid containing the 6RA mutations did not bind the RNA probe at detectable levels. This result was unexpected since, intuitively, the 5RA mutant is more likely to display impaired binding because the 5RA mutations occur within the previously described RNA binding region of capsid. In contrast, the 6RA mutations occur outside of this region. However, these results indicate that capsid containing the 5RA mutations is still able to bind genomic RNA. One possible explanation for the inability of the 6RA mutant to efficiently bind genomic RNA is that these assays likely underestimate the RNA binding capacity of capsid due to a lack of sensitivity. Indirect evidence will be presented later suggesting that capsids containing both the 5RA and the 6RA mutations are able to package genomic RNA (see Figure 4.10). Immunoblotting with a capsid monoclonal antibody (C1) showed that all capsid constructs were stable when expressed (Figure 4.2 D, lower panel). The 11RA mutant was not tested for RNA binding since it was not phosphorylated and did not form RLPs.

Together, these results suggest that, although capsid proteins containing specific mutations of arginines to alanine residues (5RA or 6RA) do not interact with p32, they are phosphorylated and are able to assemble into RLPs as efficiently as wild type capsid.

In addition, the above results also suggest that the capsid-p32 interaction does not regulate phosphorylation. This is a significant finding since p32 has been shown to regulate the kinase activity of PKC isoforms (Robles-Flores et al., 2002; Storz et al., 2000). Finally, these results also indicate that capsid-p32 interactions are not necessary for RLP formation or, presumably, for formation of virions.

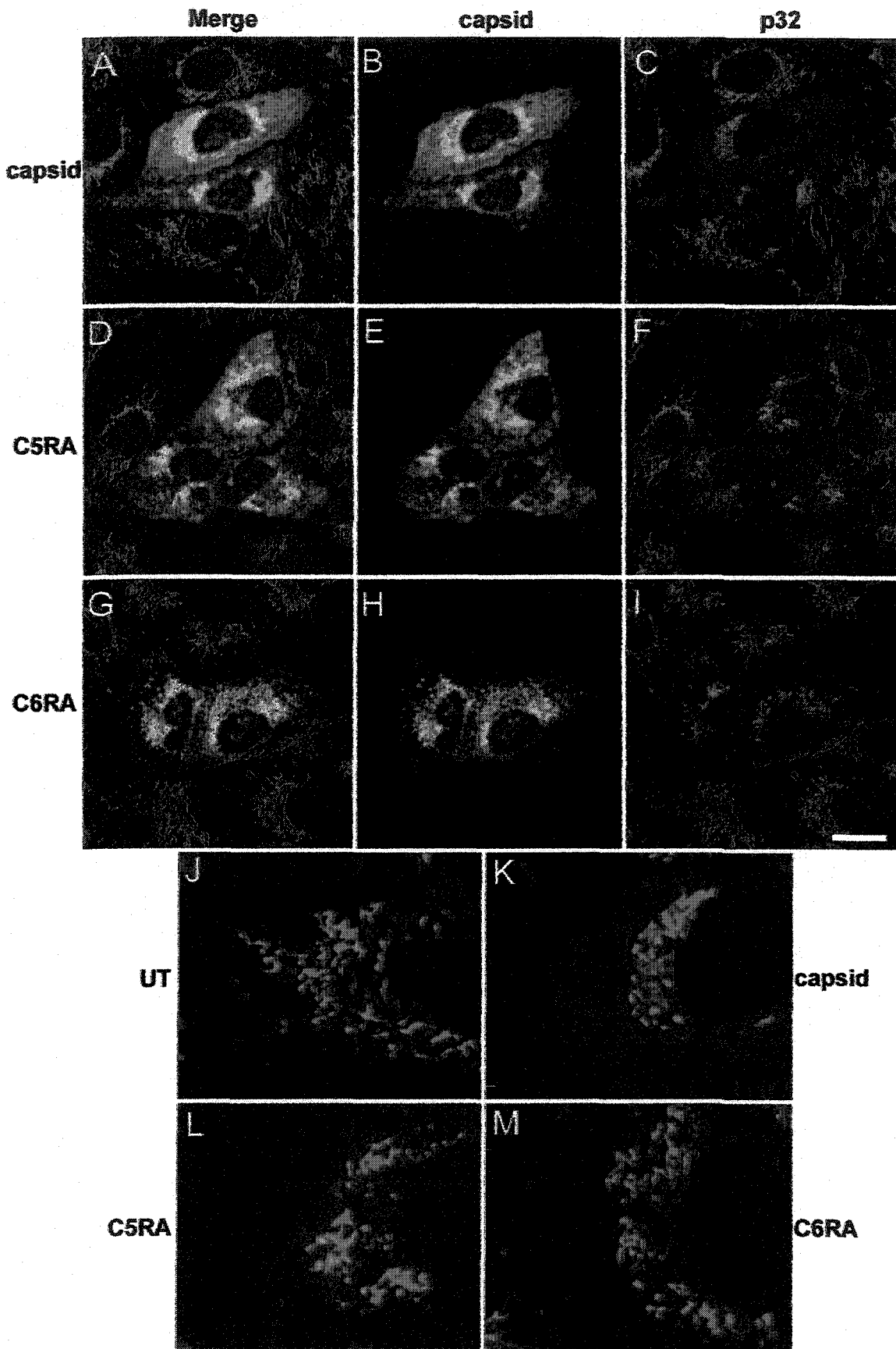
### **4.3. Effects of the capsid-p32 interaction on mitochondrial aggregation**

#### **4.3.1. The arginine rich regions of capsid are necessary for clustering of mitochondria**

Clustering of mitochondria to the juxtannuclear location in transfected cells expressing the RV structural proteins was reported in the previous chapter. To investigate the role of capsid in this phenomenon, capsid was expressed in Vero cells, in the absence of the RV envelope glycoproteins. Twenty-four hours post-transfection, cells were fixed and processed for indirect immunofluorescence. Samples were stained with antibodies to capsid and p32 and then examined by confocal microscopy. Antibodies to p32 were used to label mitochondria. A significant proportion of capsid was found to associate with mitochondria (Figure 4.3 A-C). In contrast to untransfected control cells where p32 exhibited a lacy pattern throughout the cytoplasm, mitochondria in capsid expressing cells were found to tightly cluster to a juxtannuclear region (Figure 4.3 J-K). This indicates that expression of capsid alone is sufficient to induce relocalization of mitochondria to the juxtannuclear region.

Since we previously demonstrated that capsid interacts with the mitochondrial protein p32, and localizes to the cytoplasmic surface of mitochondria, the importance of the capsid-p32 interaction in mitochondrial clustering was examined. Vero cells were transiently transfected with vectors encoding the capsid arginine to alanine mutations and processed as described above. In cells expressing the capsid 5RA (Figure 4.3 D-F and L) or 6RA (Figure 4.3 G-I and M) mutants, mitochondrial staining was more punctate and slightly more condensed into a juxtannuclear region than in untransfected control cells. However, mitochondrial aggregation was not as extensive as in cells expressing wild type

**Figure 4.3. Capsid expression results in clustering of mitochondria.** Vero cells were transfected with expression vectors encoding wild type capsid (A-C), or capsid containing arginine to alanine mutations C5RA (D-F) or C6RA (G-I). Cells were fixed, permeabilized and double labeled with a mouse monoclonal antibody to capsid (H15 C22) and a goat polyclonal antiserum to p32. Primary antibodies were detected with FITC-conjugated donkey anti-mouse IgG and Texas Red-conjugated donkey anti-goat IgG. Samples were examined by confocal microscopy. Merged images are shown on the left (A, D, G), the FITC channel is shown in the middle (B, E and H) and the Texas Red channel is shown on the right (C, F and I). Images A-I: Bar, 20  $\mu\text{m}$ . Panels J-M are enlarged images of mitochondria from untransfected cells (UT), or cells expressing capsid (K), C5RA (L) or C6RA.



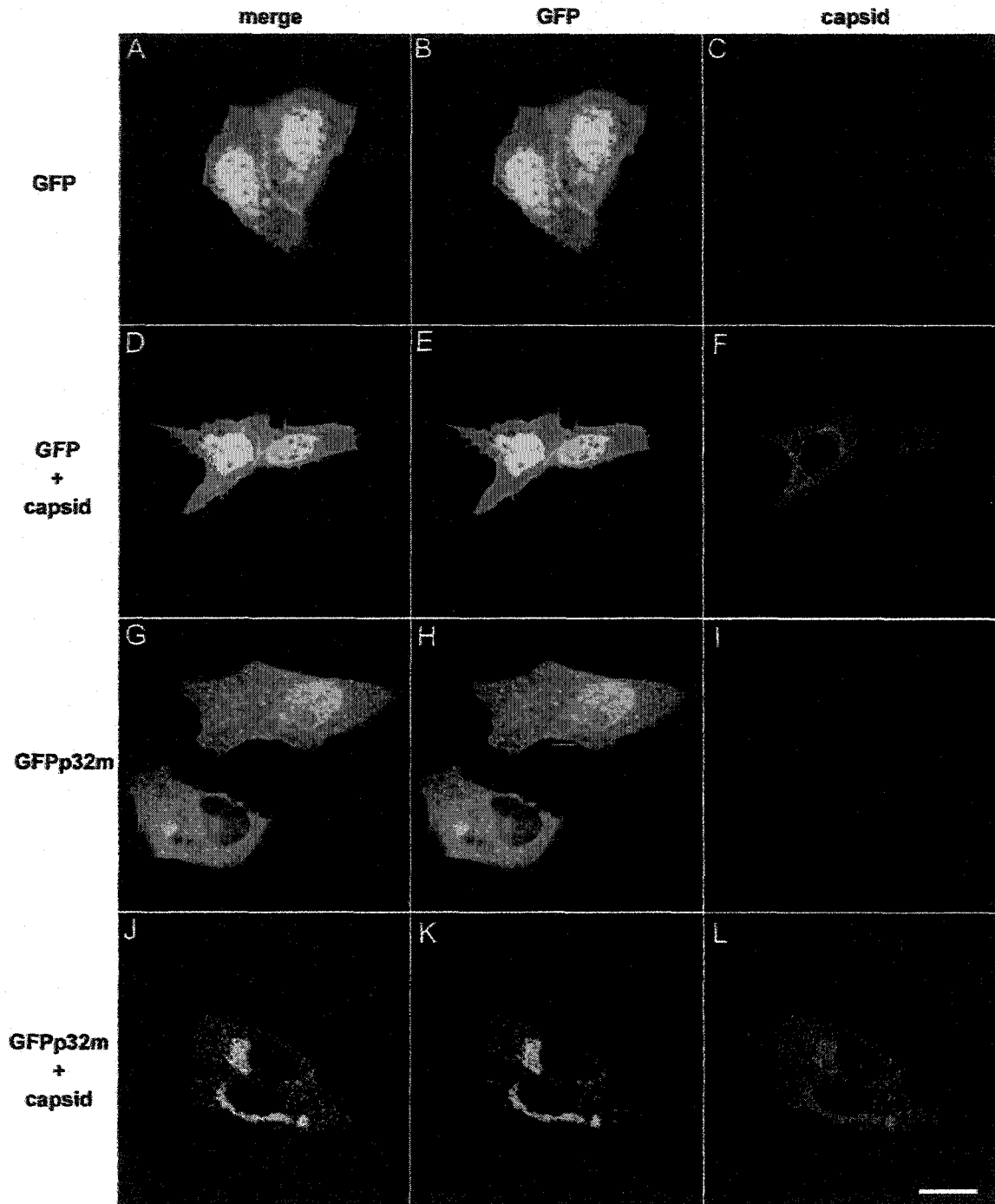
capsid. These results suggest that the interaction of capsid with p32 may facilitate the recruitment of mitochondria to the juxtannuclear region.

#### **4.3.2. Capsid recruits p32 lacking the amino terminus to mitochondria**

Association of capsid with mitochondria was intriguing since, at the time that this work was conducted, there was no obvious mechanism for targeting of this protein to the cytoplasmic surface of this organelle. One potential mechanism would be for capsid to bind to a protein which is naturally targeted to the mitochondria. This hypothesis was quite attractive since capsid was shown to interact with the carboxy terminus of p32 which would be expected to leave the mitochondrial targeting sequence of p32 unobstructed and functional. To test this hypothesis, the mitochondrial targeting sequence of p32 was replaced with GFP (GFPP32m). It was expected that GFPP32m would act in a dominant negative fashion and abrogate targeting of capsid to mitochondria. Vero cells were transiently transfected with plasmids encoding GFP or GFPP32m either alone or together with capsid. When coexpressed with GFP, capsid displayed a characteristic, juxtannuclear localization, while GFP was diffuse throughout the cytoplasm (Figure 4.4 D-E). In addition, the localization of GFP was not altered by the expression of capsid, demonstrating that these two proteins do not interact (Figure 4.4 A-C). When expressed alone, GFPP32m was largely diffuse throughout the cytoplasm and in punctate structures (Figure 4.4 H). The punctate pattern could be aggregates of p32 forming in the cytoplasm since p32 is a multimeric protein. As expected, coexpression of capsid with GFPP32m resulted in the colocalization of GFPP32m with capsid (Figure 4.4 J-L). However, much to our surprise, coexpression of these proteins resulted in a dramatic relocation of GFPP32m from a diffuse cytoplasmic pattern throughout the cytoplasm to condensed juxtannuclear structures. This staining pattern resembled that of mitochondrially targeted capsid (see Figure 3.6).

To confirm that the capsid-GFPP32m interaction was occurring at mitochondria, Vero cells were transfected with plasmids encoding either GFPP32m alone or GFPP32m and capsid. Mitotracker Red CMXRos was used to visualize mitochondria for these experiments. When expressed alone, GFPP32m was largely diffuse throughout the

**Figure 4.4. Capsid recruits GFPp32m to a juxtannuclear region.** Vero cells were transfected with expression vectors encoding GFP (A-C), GFP and capsid (D-F), GFPp32m (G-I) or GFPp32m and capsid (J-L). Cells were fixed with paraformaldehyde and permeabilized. Capsid was stained with a monoclonal antibody specific to capsid (H15C22) followed by Texas Red-conjugated donkey anti-mouse IgG. Samples were examined by confocal microscopy. Merged images are shown on the left (A, D, G and J), the GFP channel is shown in the middle (B, E, H and K) and the Texas Red channel is shown on the right (C, I F and L). Bar, 20  $\mu$ m.



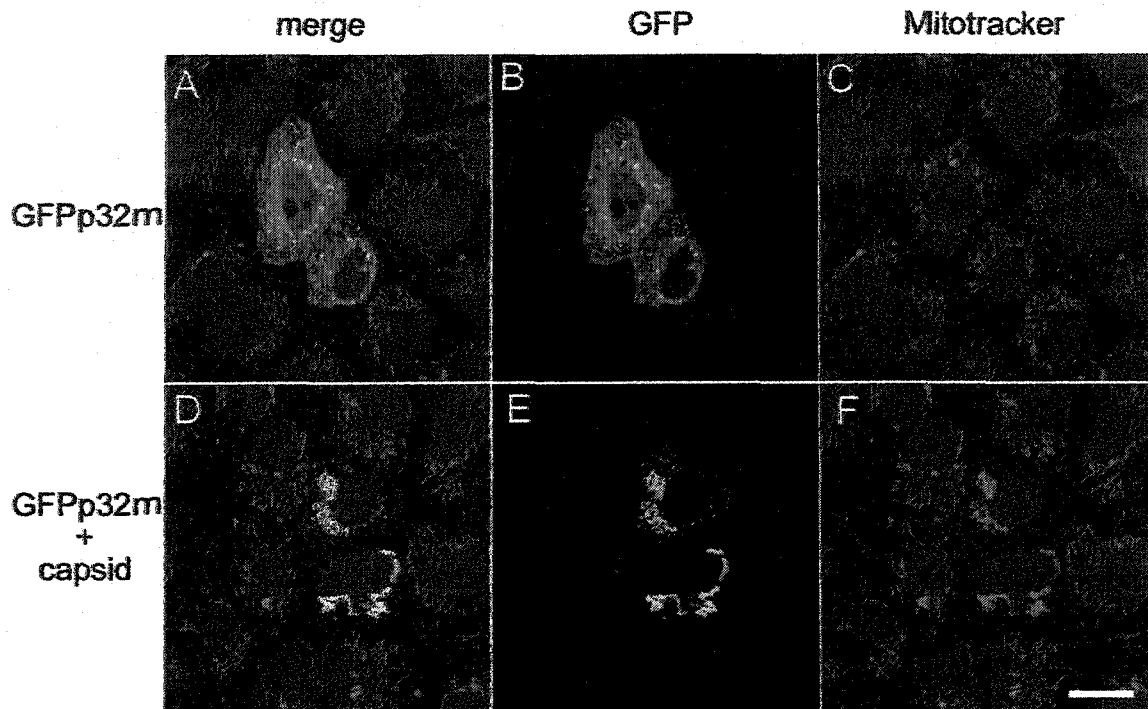
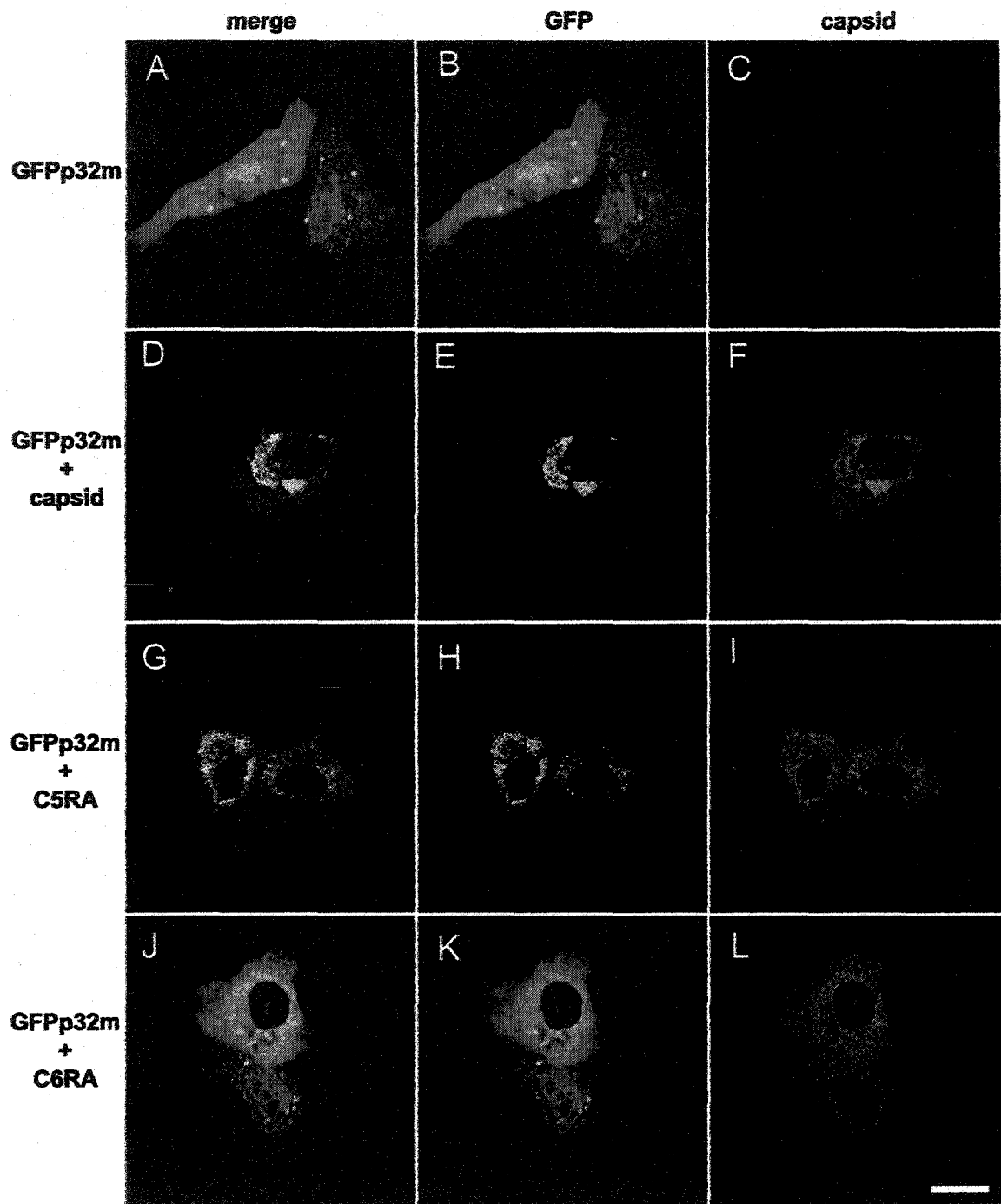


**Figure 4.5. Co-localization of capsid and GFPp32m occurs at mitochondria.** Vero cells were transfected with expression vectors encoding GFP and capsid (A-C) or GFPp32m and capsid (D-F). Cells were stained with Mitotracker Red CMXRos (30 ng/ml) for 30 minutes prior to fixation with paraformaldehyde. Samples were examined by confocal microscopy. Merged images are shown on the left (A and D), the GFP channel is shown in the middle (B and E) and the Mitotracker channel is shown on the right (C and F). Bar, 20  $\mu$ m.

cytoplasm and mitochondria appeared identical to those in untransfected control cells (Figure 4.5 A-C). In contrast, when GFPp32m was coexpressed with capsid, GFPp32m displayed a juxtannuclear localization which colocalized with Mitotracker (Figure 4.5 D-F). These results further confirm that capsid and p32 interact on the cytoplasmic face of the mitochondria. In addition, these results also suggests that capsid is targeted to mitochondria by a mechanism that is independent of the p32 mitochondrial targeting sequence. However, we cannot rule out the possibility that endogenous p32 (or another cellular protein) is responsible for targeting of capsid and p32 to mitochondria. In this scenario, p32 could target both p32 and capsid to mitochondria where capsid is responsible for retaining GFPp32m at the cytoplasmic surface of the mitochondrion.

The ability of the capsid 5RA and 6RA mutants to recruit GFPp32m to the juxtannuclear region was also examined (Figure 4.6). Coexpression of GFPp32m with the capsid 5RA mutant resulted in a colocalization of these two proteins at punctate structures in the perinuclear region (Figure 4.6 G-I). Coexpression of GFPp32m with the capsid 6RA mutant resulted in colocalization of these two proteins but GFPp32m remained diffuse and punctate throughout the cytoplasm (Figure 4.6 J-L). The colocalization of the capsid mutants with GFPp32m is somewhat unexpected since we do not expect these proteins to interact stably with p32. One possibility, suggested by the punctate nature of the colocalization, is that the capsid RA mutants are forming non-specific aggregates with GFPp32m. Alternatively, the capsid RA mutants may bind weakly to GFPp32m *in vivo* and partial colocalization may occur as a result. Whatever the nature of the interaction, it is important to note that the colocalization patterns of the RA mutants with GFPp32m differ from that of wild type capsid and GFPp32m. For example, wild type capsid colocalizes with GFPp32m in a tightly condensed, juxtannuclear region (Figure 4.6 D-F). In contrast, capsid 5RA and 6RA colocalize with GFPp32m in a more punctate pattern in the perinuclear region. Neither of the mutant capsids were observed to cause juxtannuclear condensation of GFPp32m to the same degree as wild type capsid. Together, these data suggest that stable interaction of capsid with p32 is necessary for the relocation of GFPp32m to the juxtannuclear

**Figure 4.6. Capsid arginine to alanine mutants are unable to efficiently target GFPp32m to the juxtannuclear region.** Vero cells were transfected with vectors encoding GFPp32m (A-C), GFPp32m and capsid (D-F), GFPp32m and C5RA (G-I), or GFPp32m and C6RA (J-L). Capsid was stained with a monoclonal antibody specific to capsid (H15C22) followed by Texas Red-conjugated donkey anti-mouse IgG. Samples were examined by confocal microscopy. Merged images are shown on the left (A and D), the GFP channel is shown in the middle (B and E) and the Texas Red channel is shown on the right (C and F). Bar, 20  $\mu$ m.



region. Furthermore, these data suggest that the interaction of capsid with p32 may be involved in mitochondrial clustering.

#### **4.4. Capsid expression induces the formation of mitochondrial plaques**

Our data indicate that the capsid-p32 interaction may be directly involved in the rearrangement of mitochondrial localization observed in RV infected cells (Lee et al., 1996a). Furthermore, the interaction of these two proteins at the cytoplasmic surface of mitochondria also raises the possibility that capsid may play a role in the formation of confronting membranes which are observed between opposing mitochondria in RV infected cells. To further examine the effects of capsid on mitochondrial morphology, a stable cell line in which capsid expression was under control of the tetracycline repressor was created (HEK 293TRC 2B). These cells inducibly expressed capsid when cultured in the presence of the tetracycline analog, doxycycline (DOX) (Figure 4.7 A). Capsid expression was induced in the HEK 293TRC 2B cell line and, 48 h later, cells were processed for transmission electron microscopy. Induced and non-induced cells were examined for equal amounts of time. Electron dense structures were observed between opposing mitochondria in eight capsid-expressing cells (Figure 4.7 C-E) but were never observed in uninduced cells (Figure 4.7 B). These structures closely resembled the confronting membranes which occur in RV infected cells (Lee et al., 1996a). The width of these structures in RV infected cells was reported to be 22-25 nm. In accordance with this, the average width of the electron zones in capsid expressing cells was 24 nm ( $\pm 2.3$  nm,  $n=4$ ). These results indicate that expression of the RV capsid is sufficient to induce the formation of confronting membranes, a hallmark of RV infection.

#### **4.5. Effects of capsid expression on mitochondrial membrane potential**

Since we found that the RV capsid has such striking effects on mitochondrial localization and morphology (reported in this thesis), and since capsid has previously been reported to induce apoptosis in cultured cells (Duncan et al., 2000), the effects of capsid on mitochondrial membrane potential were examined. For these experiments, we used the same cell line that displayed the formation of electron dense zones in response

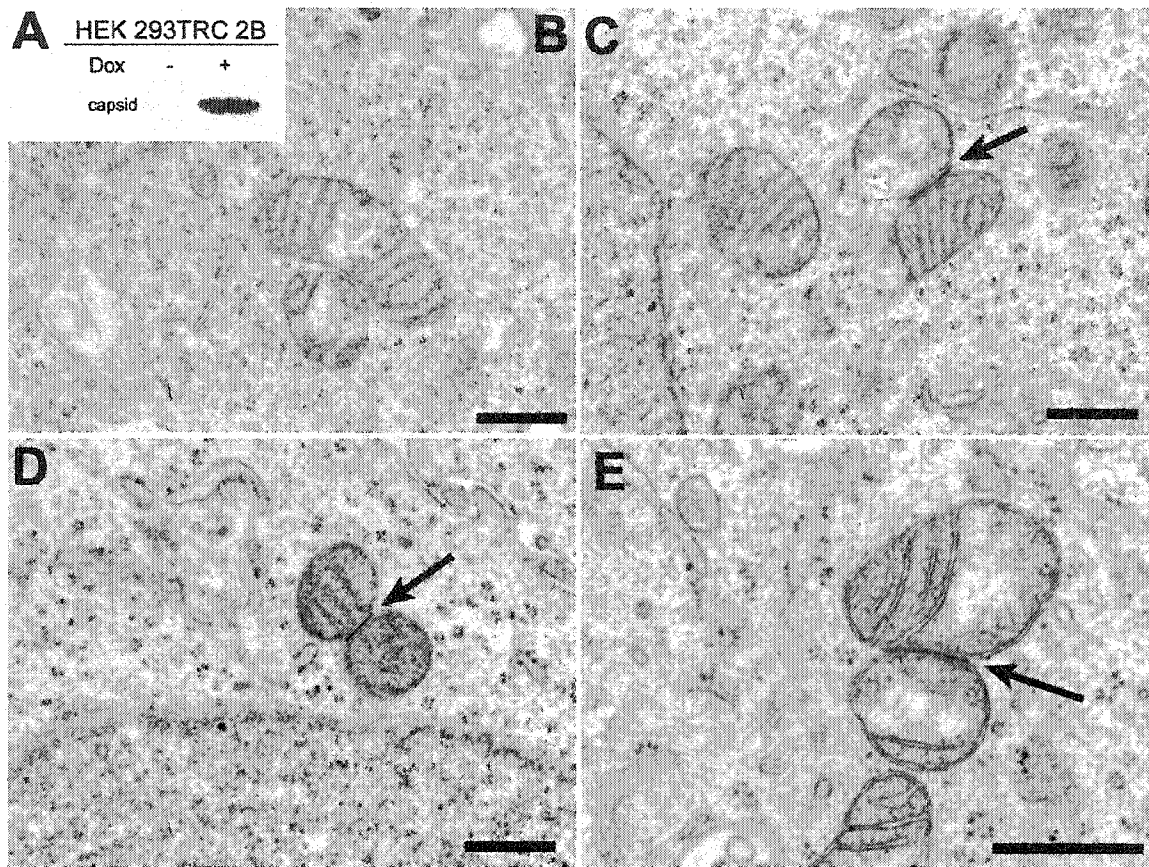


**Figure 4.7. Expression of capsid induces the formation of electron dense zones between mitochondria.** A) Stably transfected HEK 293T cells which inducibly express the RV capsid (HEK 293TRC 2B) were grown in the presence or absence of doxycycline (Dox) for 24 hours. Dox treatment induces capsid expression. Cells were then lysed in 1% NP-40 lysis buffer and capsid expression was detected by immunoblotting with 7W7. HEK 293TRC 2B cells were grown in the presence or absence of doxycycline for 48 hours before being fixed and processed for transmission electron microscopy (B-E). B) In uninduced cells, mitochondria display typical morphology and plaques are absent. C-E) Induction of capsid results in the formation of electron dense plaques between adjacent mitochondria (arrows). Bar = 500 nm.

to capsid expression. HEK 293TRC 2B cells were cultured in normal growth medium or in normal growth medium containing doxycycline to induce capsid expression and then cells were stained with the mitochondrial membrane potential sensitive dye TMRE prior to analysis by flow cytometry. TMRE fluorescence was used to determine the effects of capsid expression on transmembrane potential. An increased number of counts in the pool of cells displaying low TMRE staining (M1) is indicative of a loss of transmembrane potential. No significant shift in TMRE fluorescence was detected in HEK 293TRC 2B cells at either two or five days post-induction of capsid when compared to uninduced cells (Figure 4.8 A). In contrast, the addition 2  $\mu$ M staurosporine, a potent inducer of apoptosis, to the culture medium for 4 h prior to flow cytometry resulted in an increase in the number of counts in M1, as expected. These results suggest that, in these cells, capsid does not decrease mitochondrial membrane potential.

Another possibility is that capsid has anti-apoptotic properties and that targeting of this protein to mitochondria is able to confer protection from the loss of mitochondrial transmembrane potential. Accordingly, we examined the ability of capsid to protect mitochondria from the effects of pro-apoptotic drugs. Capsid expression was induced in the HEK 293TRC 2B cell line. Forty-eight hours post-induction 2  $\mu$ M staurosporine was added to capsid expressing and control cells for five hours to induce loss of membrane potential. Cells were stained with the membrane potential sensitive dye TMRE prior to analysis by flow cytometry. Staurosporine had a dramatic effect on membrane potential, increasing the number of counts in M1 over two fold over untreated cells or untreated cells expressing capsid (Figure 4.8B). Expression of capsid, however, neither protected nor sensitized mitochondrial membranes to loss of TMRE fluorescence induced by staurosporine. These results suggest that capsid does not act on mitochondrial membranes in either a pro- or anti-apoptotic manner in HEK 293T cells.

#### **4.6. Effects of the capsid-p32 interaction on virus replication**

To determine the importance of the capsid-p32 interaction during viral replication, the arginine to alanine mutations in the p32-binding region of capsid were subcloned into a RV infectious clone (Yao and Gillam, 1999). Genomic RNA was

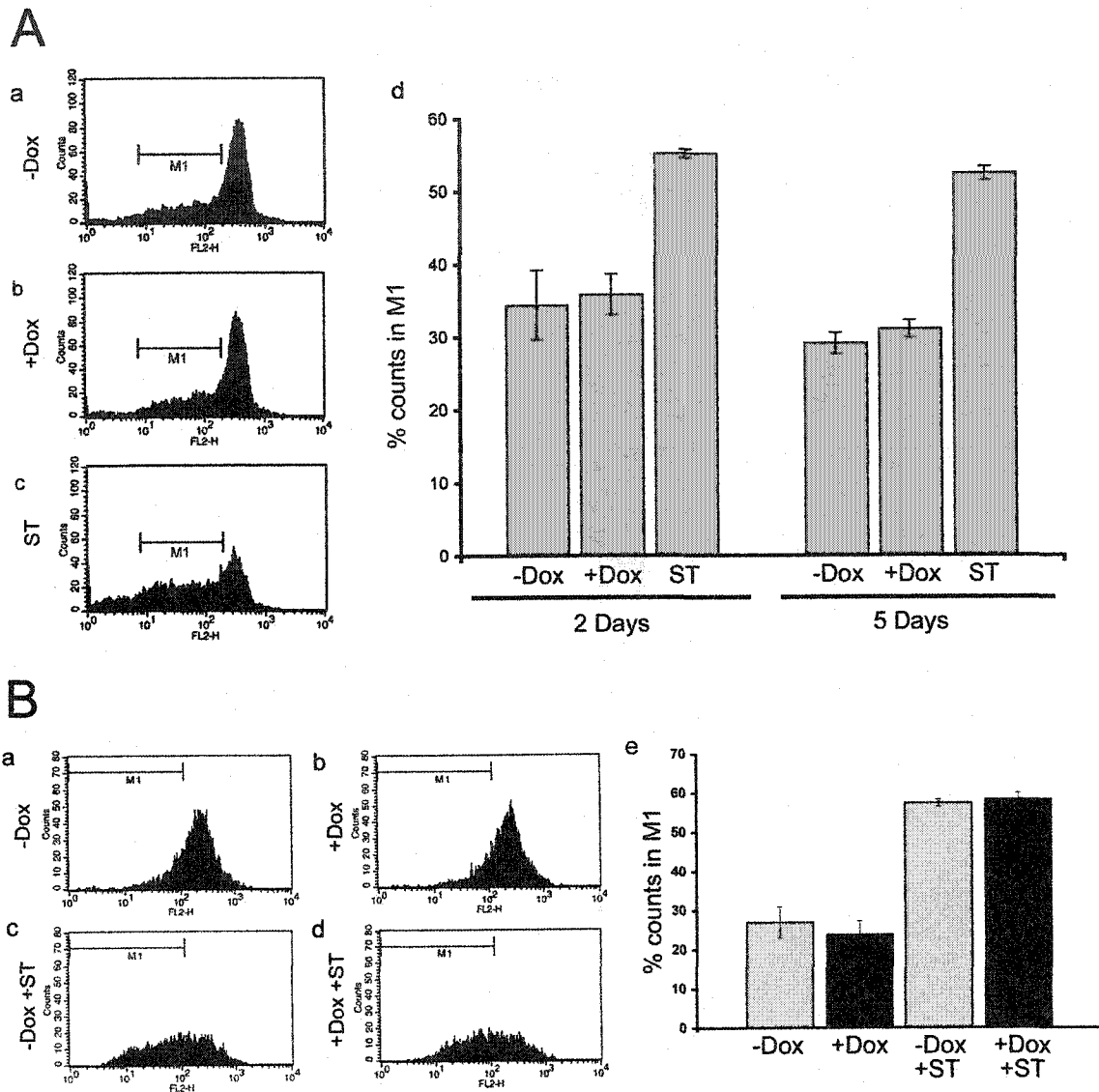


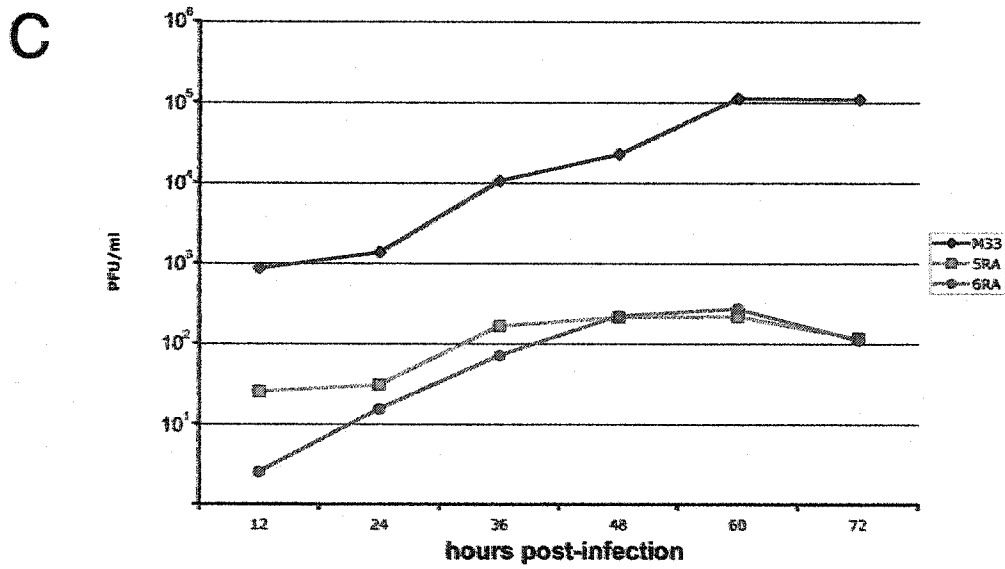
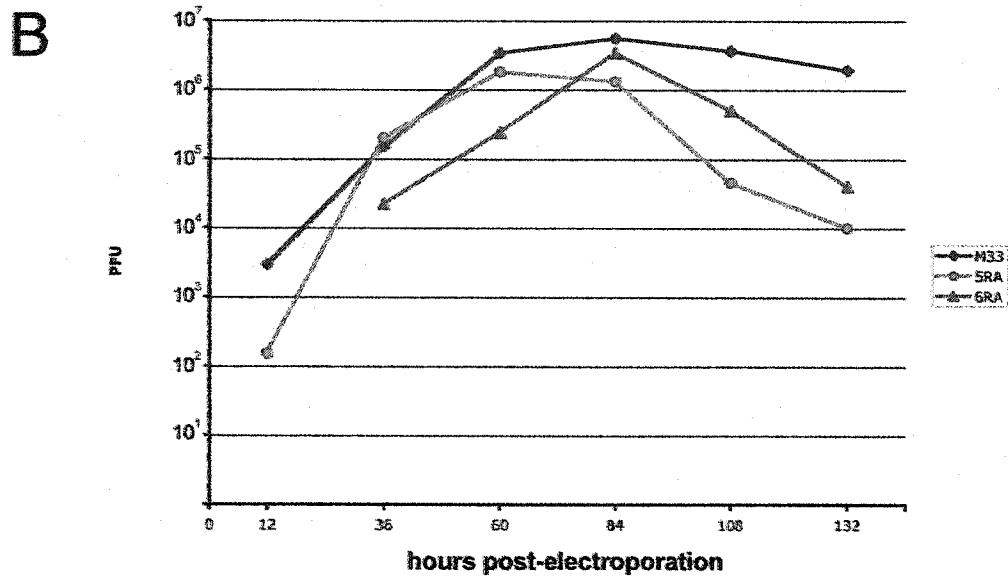
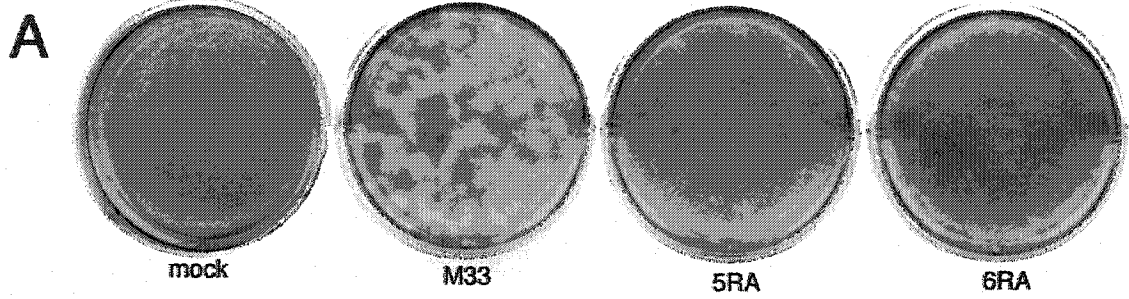
**Figure 4.8. Effects of capsid on mitochondrial membrane potential.** A) Capsid does not result in a decrease of mitochondrial membrane potential. Mitochondrial membrane potential was measured in HEK 293TRC 2B cells by staining mitochondria with the membrane potential sensitive dye TMRE and quantitation by flow cytometry. Prior to staining, cells were cultured in medium lacking doxycycline (-Dox) (i), medium containing doxycycline to induce capsid (+Dox)(ii), or treated with 2  $\mu$ M staurosporine (ST) for 4 hours (iii). The percentage of counts in M1 for each treatment at either 2 or 5 days is shown in iv. B) Capsid does not prevent loss of membrane potential. HEK 293TRC 2B cells were cultured in the absence (i and ii) or presence (iii and iv) of doxycycline for 2 days. Cells were then treated with 2  $\mu$ M staurosporine (ST) for 5 hours (ii and iv). The percentage of counts in M1 for each treatment is shown in v.

transcribed *in vitro* and equal amounts of RNA (10  $\mu$ g) were electroporated into BHK-21 cells. Media were collected at 12 h post-electroporation and then every 24 h afterwards. The amount of infectious virus produced was determined by plaque assay. Wild type M33 RV produced, large, clear plaques, which were easily visualized by neutral red staining and closely resembled the plaques previously described for this infectious clone (Yao and Gillam, 1999) (Figure 4.9 A). The 5RA strain produced plaques that were similar in size to M33, but the plaques were more opaque. In contrast, the 6RA strain produced very small and opaque plaques (Figure 4.9 A).

Titers of all viruses peaked between 60 and 84 h post-electroporation, however, both RA mutants exhibited reduced virus titers (Figure 4.9 B). At 60 h post-electroporation, the titers of the 5RA and 6RA viruses were approximately 53% and 7% of wild type respectively. Furthermore, the peak viral titers for each of the mutants were only 33% and 62% respectively of wild type indicating that formation or secretion of virus was less efficient than wild type. Subsequent to the achievement of peak virus titers, the titers of the 5RA and 6RA viruses decreased rapidly whereas the titer of wild type virus remained relatively high. Not surprisingly, the 11RA mutant did not produce infectious virus as no plaques were observed when medium from cells electroporated with this mutant was titered. These results indicate that viruses containing the arginine to alanine mutations, which result in decreased binding of capsid to p32, display a decreased ability to produce and/or secrete infectious virus.

To confirm that viral proteins are expressed in electroporated cells and to confirm that decreased virus titers were not a result of inefficient electroporation, BHK cells, electroporated with equivalent amounts of infectious RNA (10  $\mu$ g), were processed for double labeling immunofluorescence three days post-electroporation. Cells were stained with antibodies to the RV envelope protein E1 to label cells expressing viral proteins and to p32 to label all cells (Figure 4.10). The percentage of cells expressing E1 was determined in three randomly selected fields from each of two independent experiments (Table 4-1). RNAs encoding the wild type RV or RNAs encoding the 5RA or the 6RA mutations in capsid all expressed E1 in approximately the same percentage of cells (88 to 97%). However, RNA encoding the 11RA mutation in capsid expressed E1 in a much

**Figure 4.9. Viruses encoding arginine to alanine mutations in capsid exhibit replication defects.** A) Morphology of plaques. Virus was collected from the media of BHK cells three days after electroporation with infectious RNA for wild type rubella virus (M33), or viruses containing the 5RA and 6RA mutations in capsid. Virus containing media were added to RK-13 cells and cells were overlaid with agar. Six days later, plaques were stained with neutral red solution. B) BHK cells were electroporated with 10  $\mu\text{g}$  of *in vitro* synthesized RNA for the wild type rubella virus (M33) and the arginine to alanine mutants (5RA, 6 RA, or 11RA). Media from electroporated cells were collected every 24 hours starting at 12 hours post electroporation and virus titers were quantitated by plaque assay in RK-13 cells. No virus was detected at 12 hours for 6RA or for 11RA at any timepoint. A representative experiment is shown. C) One step growth curve. Vero cells were infected with wild type rubella virus (M33) or virus containing the arginine to alanine mutations (5RA and 6RA) at an MOI of 5 PFU/cell and medium was collected every 12 hours post-infection. Virus titers were determined by plaque assay in RK-13 cells. The average of two independent experiments is shown.



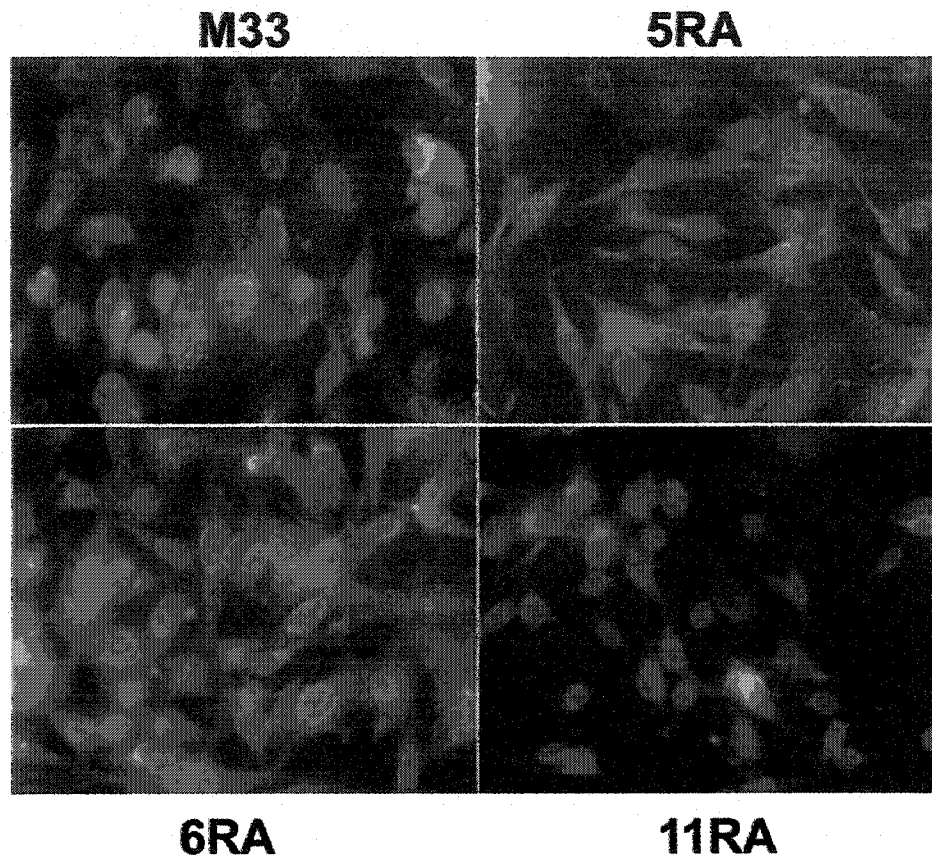


**Figure 4.10. Rubella virus mutant genomic RNAs support synthesis of RV structural proteins.** BHK cells were electroporated with equivalent amounts of *in vitro* synthesized RNA (10  $\mu$ g) for the wild type rubella virus (M33), or viruses containing the 5RA, 6RA or 11RA mutations in capsid. Three days post-electroporation, cells were processed for indirect immunofluorescence microscopy and were double labeled with mouse monoclonal antibodies to E1 (B2) and a rabbit polyclonal antibody to p32. Primary antibodies were detected with Texas Red-conjugated goat anti-mouse IgG and FITC-conjugated donkey anti-rabbit IgG.

**Table 4-1. Percentage of Electroporated Cells Expressing E1**

<b>RNA</b>	<b>E1 expressing cells/total cells</b>	<b>% expressing E1(std dev)</b>
None	0/30	0
WT	233/240	97.1 ( $\pm$ 3.0)
5RA	210/218	96.3 ( $\pm$ 3.3)
6RA	226/257	87.9 ( $\pm$ 9.0)
11RA	63/239	26.4 ( $\pm$ 9.0)

smaller proportion of cells (26%). These results confirm that RNAs for each of the RA mutant strains are able to support production of virus structural proteins. The lower percentage of cells expressing E1 in the 11RA mutant is likely a result of the inability of the mutant capsids to form infectious virus particles (see Figure 4.2C and Figure 4.9B) and thus, the percentage of E1 expressing cells electroporated with the 11RA mutant likely represents the electroporation efficiency. These results also indicate that the 5RA and the 6RA mutant viruses are able to replicate and assemble virus particles which, in turn, are able to spread to, and infect, neighbouring cells. Therefore, these results also indicate that both the 5RA and 6RA capsids are able to incorporate genomic RNA into virions. This result is significant since we were unable to confirm binding of the 6RA mutant capsid to RNA in an *in vitro* RNA binding experiment (see Figure 4.2 D). However, despite the ability of the 5RA and 6RA viruses to produce infectious virus, virus titers were decreased compared to wild type suggesting that the RA mutants display an inability to replicate as efficiently as wild type.

To confirm that the replication defects of the 5RA and 6RA strains were due to inefficient replication, as opposed to lower production of virus from electroporated RNA, one-step growth curves for these viruses were determined. Virus obtained from electroporated BHK cells was used to infect Vero cells at an MOI of 5 PFU/cell and media was collected every 12 h post-infection. Wild type virus displayed exponential growth and achieved a maximum virus titer of  $1.1 \times 10^5$ /ml at 60 h post-infection (Figure 4.9 C). In contrast, viruses encoding either of the arginine to alanine mutants displayed peak virus titers which were three orders of magnitude lower than the wild type virus (Figure 4.9 C). These results suggest that the region of capsid which is important for binding to p32 is also important for virus replication since viruses encoding arginine to alanine mutations in capsid replicate less efficiently. One possibility is that the capsid-p32 interaction is directly involved in regulating virus replication. However, we cannot rule out that other factors such as altered binding to genomic RNA could be responsible for the decreased replication of the arginine to alanine mutants.

#### **4.7. Capsid arginine to alanine mutants do not display altered cytopathic effect**

One possible explanation for the inability of the arginine to alanine mutants to replicate efficiently is that these viruses display increased cytopathic effect. Increased cell death would decrease virus titers by reducing the number of cells producing virus. Furthermore, both capsid (Duncan et al., 2000) and p32 (Jiang et al., 1999; Sunayama et al., 2004) have been hypothesized to play a role in the regulation of apoptosis. To determine if this was the case, RK-13 cells, which are highly sensitive to RV cytopathic effect, were infected with wild type virus or viruses encoding the arginine to alanine mutations in capsid. Metabolic activity of infected cells, 48 h post-infection, was determined using a MTT based assay. MTT is cleaved to formazan by the respiratory chain of the mitochondria in metabolically intact cells. Thus, this assay can be used as a method to determine cell numbers spectrophoretically as a function of mitochondrial activity in living cells. Wild type RV efficiently reduced the metabolic activity of infected cultures to approximately 50% of the uninfected controls (Figure 4.11). No significant differences in metabolic activity were observed between cultures infected with wild type, 5RA or 6RA strains indicating that the RA mutants do not differ from wild type virus in their ability to induce cytopathic effect. Thus, these results suggest that the decreased ability of the RA mutants to replicate efficiently are not due to increased cytopathic effect.

#### **4.8. Summary**

The interaction of the RV capsid with the host cell protein p32 was examined in detail. Capsid was shown to play an important role in the reorganization of mitochondria during virus infection, a process which is well documented in RV infected cells. For instance, capsid expression was shown to be sufficient to induce mitochondrial clustering in Vero cells in the absence of other viral proteins and for the formation of electron dense, confronting membranes between adjacent mitochondria. This work also confirmed that capsid interacts with p32 on the cytoplasmic face of the mitochondria. Interaction between capsid and p32 was shown to be important for aggregation of mitochondria in

the juxtannuclear region. Furthermore, these results suggest that this interaction may be biologically relevant since it was demonstrated that mutant viruses encoding capsids that bind p32 weakly, replicate poorly.

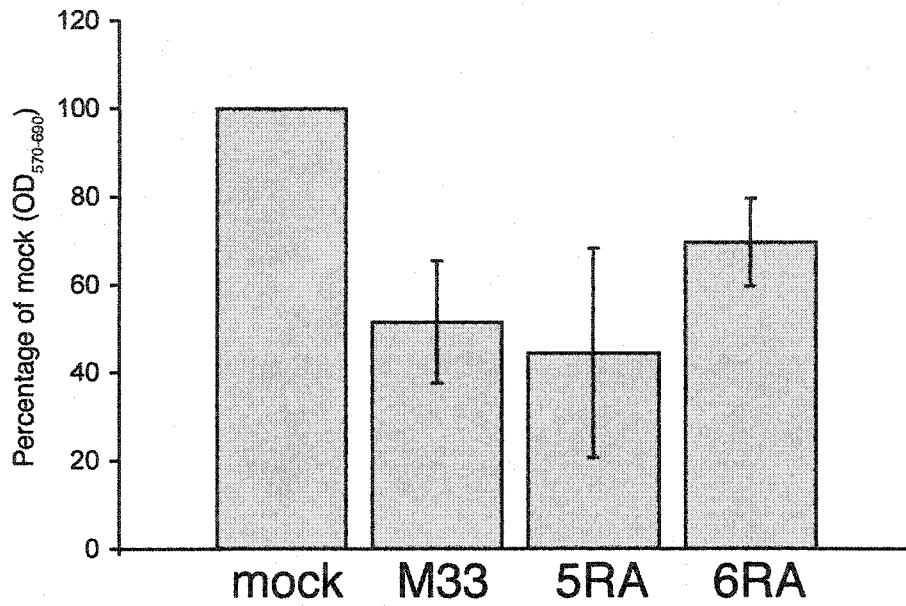


**Figure 4.11. Capsid arginine to alanine mutations do not alter cell viability.** RK-13 cells were infected with wild type rubella virus (M33) or virus containing the arginine to alanine mutations (5RA and 6 RA). 48 hours post-infection, cell viability was determined using an MTT based assay. Readings were normalized to mock infected cells. Results are an average of 4 independent experiments.

## **CHAPTER 5. DISCUSSION**

## 5.1. Overview

Studies by our lab and others have shown that RV replication and assembly differs significantly from that of other togaviruses. One of the most exciting aspects of recent work on RV regards the capsid protein. The main function of this protein is to oligomerize with itself and genomic RNA to form the nucleocapsid. However, it is becoming increasingly clear that, in addition to forming the nucleocapsid, capsid may play an integral role in several other important processes including the replication of genomic RNA (Chen and Icenogle, 2004; Tzeng and Frey, 2003) and induction of apoptosis (Duncan et al., 2000). For this thesis, we examined the interaction of capsid with cellular proteins as a means of elucidating the mechanisms by which capsid carries out its various functions and to identify novel functions of capsid.

We identified four host cell proteins that interact with the RV capsid. These proteins are: p32, Par-4, PKC $\zeta$  and the poly(A) binding protein. For this thesis, two of these interactions were investigated in further detail. Capsid was shown to interact with p32 at the cytoplasmic face of mitochondria and with Par-4 on intracellular membranes. Overlapping, but distinct regions in the amino terminal portion of capsid were shown to interact with these host cell proteins. We also showed that capsid expression causes aggregation of mitochondria to the perinuclear region and the formation of confronting membranes between adjacent mitochondria. The role of p32 in this phenomenon was further examined. Our studies suggest that capsid is able to interact with p32 at the cytoplasmic face of mitochondria and that this interaction is important for mitochondrial clustering. The importance of this interaction during RV replication was confirmed using mutant viruses in which capsids were unable to bind p32. These viruses replicated to lower titers indicating that the interaction of capsid with p32 may be important for efficient virus replication.

## **5.2. The amino terminus of the RV capsid is multifunctional and interacts with host cell proteins p32 and Par-4**

The regions of capsid that bind p32 and Par-4 were mapped to overlapping, but distinct, regions in the amino terminus of capsid (amino acid residues 30 to 69 and 30 to 79 respectively) (Figures 3.8 and 3.12). Interestingly, this region of capsid is also highly immunogenic (Wolinsky et al., 1991), which may explain why capsid antibodies inefficiently co-immunoprecipitated p32 and Par-4.

In addition to binding of cellular factors, this region of capsid is notable for several other reasons. For one, it contains the RNA binding domain. Amino acid residues 28 to 56 have been shown to be sufficient for binding genomic RNA (Liu et al., 1996). Serine 46, the major phosphorylated residue within capsid also resides within this region (Law et al., 2003). Phosphorylation of serine 46 has been shown to negatively regulate binding of capsid to genomic RNA. In addition to binding genomic RNA, the amino terminus of capsid may play a role in replication of genomic RNA. In a recent study, capsid expression was found to complement a 507 nucleotide deletion in the nonstructural ORF of a RV replicon (Tzeng and Frey, 2003). Interestingly, expression of amino acid residues 1 to 88 of capsid was found to be sufficient for complementation. Thus, the amino terminal portion of capsid appears to be important for multiple aspects of capsid function since, in addition to RNA binding and phosphorylation, this region is also involved in interactions with host cell proteins. This finding is not particularly surprising since this region of capsid is predicted to be more exposed and flexible than other regions of capsid. For instance, the carboxy terminus is membrane associated and therefore inaccessible to the aqueous cellular environment. The structure of RV capsid has not been determined, but by analogy with the capsid protein of Sindbis virus, the central portion of RV capsid is expected to be highly structured (Choi et al., 1991; Lee et al., 1996c; Zhang et al., 2002). In the Sindbis virus capsid, the analogous region interacts with other capsid molecules and forms the structural component of the nucleocapsid. Therefore, the amino terminus of the RV capsid is likely the region that is most accessible and functions as the “business” end of capsid.

Our results regarding the p32 binding domain of capsid conflict with those of another study published during the time that this work was carried out. Mohan *et al.* (2002) reported that amino acid residues 1 to 28 of capsid interact with p32 in the yeast two-hybrid system whereas we had previously determined that amino acid residues 30 to 69 of capsid are sufficient for full strength binding to p32. Furthermore, in our hands, a construct encoding amino acid residues 1 to 45 of capsid did not interact with p32 using the two-hybrid system. While we are unable reconcile the differences between these two sets of data, we have produced evidence that specific arginine residues within amino acid residues 30 to 69 of capsid are important for binding to p32. Specifically, mutation of these arginine residues to alanine resulted in the decreased association of capsid with p32 by immunoprecipitation (Figure 4.2). Furthermore, our findings are consistent with several other studies indicating that the p32-binding regions of other proteins contain multiple clusters of arginine residues (Bryant *et al.*, 2000; Hall *et al.*, 2002; Wang *et al.*, 1997). For instance, p32-binding domain of the Epstein-Barr virus EBNA-1 protein contains two arginine rich clusters, both of which are necessary for stable interaction with p32 in cultured cells (Van Scoy *et al.*, 2000; Wang *et al.*, 1997). We observed nearly identical results for the RV capsid since mutation of either of the arginine rich regions (5RA or 6RA) within amino acid residues 30 to 69 of capsid resulted in the loss of stable capsid-p32 interactions (Figure 4.2). Therefore, we are confident that the region of capsid involved in binding p32 resides within amino acid residues 30 to 69 and that arginine residues within this region are important for binding.

Together, our results have shown that two host cell proteins interact with the multifunctional amino terminal portion of capsid and that two arginine rich clusters within the p32 binding domain were shown to be important for the interaction of capsid with p32.

### **5.3. Localization of capsid to mitochondria**

The majority of capsid in infected cells is presumably associated with organelles of the secretory pathway (ER and Golgi). Capsid is cotranslationally inserted into ER membranes and remains membrane associated following processing by host cell signal

peptidase, which separates capsid from the envelope glycoproteins. Capsid is then targeted to the Golgi, where virus budding occurs. Targeting of capsid to the Golgi and the importance of the E2 signal peptide in this process are reasonably well studied (Baron et al., 1992; Hobman et al., 1990; Law et al., 2001).

Recent work by us, and others, has shown that pools of capsid exist at specific subcellular locations other than the ER or Golgi. For instance, capsid has been shown to be associated with viral replication complexes by immunogold electron microscopy and to colocalize with the RV nonstructural protein p150 at replication complexes (Kujala et al., 1999; Lee et al., 1999). Furthermore, it was previously demonstrated by immunogold electron microscopy that capsid is also present at the cytoplasmic surface of mitochondria (Lee et al., 1999). The work presented in this thesis, also demonstrates that a pool capsid is present at the cytoplasmic surface of mitochondria (Figures 3.6 and 3.7).

Interestingly, unlike transport of capsid to the Golgi, targeting of capsid to sites outside of the secretory pathway appears to be independent of interactions with E2 and E1 since capsid does not colocalize with the envelope proteins at these locations. For example, p150 colocalizes with capsid but not E2 in RV infected cells (Kujala et al., 1999). We have also shown that in Vero cells transfected with a plasmid encoding the RV structural proteins, E1 does not colocalize with mitochondria (Figure 3.6). Furthermore, we demonstrated that capsid is able to associate with mitochondria even in the absence of E2 and E1 indicating that capsid contains the required information for transport to mitochondrial membranes (Figure 4.3).

We originally hypothesized that interaction of capsid with p32 was necessary for targeting of capsid to mitochondria. This hypothesis was attractive to us since our data from the yeast two-hybrid system indicated that capsid binds the carboxy terminus of p32 (Figure 3.8B). We assumed that binding of capsid to the carboxy terminus would leave the amino terminal mitochondrial targeting sequence of p32 exposed. Thus, we reasoned that capsid might bind to nascent p32 in the cytosol and then be ferried to mitochondria together with p32. We attempted to prevent association of capsid with mitochondria by over expressing a truncated p32 mutant (GFPp32m) that is unable to be imported into mitochondria and remains cytosolic. To our surprise, capsid was found to colocalize with

mitochondria even in cells expressing GFPp32m (Figure 4.4). Thus, capsid appears to be targeted to mitochondria independently of p32, although we cannot completely rule out that endogenous p32 is still able to target capsid to mitochondria in GFPp32m expressing cells. Recently, a short motif was identified in the core protein of the hepatitis C virus that targets core to the outer mitochondrial membrane (Schwer et al., 2004). A similar motif (termed R2 (RXXHXXR)) was identified near the carboxy terminus of the RV capsid by our lab and we have begun to investigate the importance of this domain in targeting of capsid to mitochondria. R2, but not the E2 signal peptide, was found to be necessary for the association of capsid with mitochondria (Personal communication. Jason Everitt, University of Alberta). How this motif targets capsid to mitochondria remains unknown but these results confirm that a specific signal within capsid is important for the association of this protein with mitochondria. The role of this motif in targeting of capsid to mitochondria is currently under investigation by others in our lab.

While the localization of capsid at sites of virus replication suggests that capsid may play a role in regulating replication of genomic RNA, a finding which is corroborated by several recent studies (Chen and Icenogle, 2004; Tzeng and Frey, 2003), the significance of capsid at mitochondria is less clear. However, there is prior evidence that mitochondria play an important role in RV replication. For example, analysis of the lipid composition of RV virions identified cardiolipin, a phospholipid which is found nearly exclusively in mitochondrial membranes, as a component of the RV virion (Bardeletti and Gautheron, 1976). While this result is somewhat surprising, morphological examination of RV infected cells has shown that mitochondria aggregate at sites of virus replication (Lee et al., 1996a) and that Golgi membranes are also closely associated with these regions in infected cells (Risco et al., 2003). The close association of mitochondria with sites of virus replication and assembly suggests that mitochondria may be more directly involved in virus replication and/or assembly than previously assumed. The presence of a pool of capsid at the cytoplasmic surface of mitochondria suggests that capsid may play a direct role in the regulation of mitochondrial function or localization during RV infection.

#### 5.4. Effects of capsid on mitochondrial distribution

We have demonstrated that capsid expression greatly affects the distribution of mitochondria in cultured cells. In contrast to untransfected cells, which display a lacey mitochondrial staining distributed throughout the cytoplasm, the mitochondria in capsid expressing cells aggregate at the juxtannuclear region (Figures 3.6 and 4.3). Furthermore, we found that capsid expression resulted in the formation of electron dense zones or confronting membranes between adjacent mitochondria (Figure 4.7). Both of these alterations to mitochondria in capsid expressing cells correlate with previous work by Lee *et al.* (1996a) showing that mitochondria cluster to replication sites and form confronting membranes in RV infected cells (Lee et al., 1996a). Significantly, these results demonstrate that capsid expression alone is able to induce these mitochondrial changes in the absence of other viral proteins or virus replication. Thus, capsid likely plays an important role in these aspects of RV cytopathic effect.

The function of mitochondrial aggregation in RV infected cells is not clear, however, a number of other viruses are known to cause a similar redistribution of mitochondria. For example, mitochondria cluster in proximity to replication complexes in Vero cells infected with the alphavirus Semliki Forest virus (although confronting membranes are not observed) (Lee et al., 1996a). Mitochondrial aggregation has also been observed in *Drosophila melanogaster* cells infected with the alphavirus flock house virus (Miller et al., 2001). Interestingly, this virus also forms replication complexes at mitochondrial membranes. African swine fever virus causes a redistribution of mitochondria in Vero cells (Rojo et al., 1998). In a manner similar to that of RV infected cells, mitochondria cluster to viral factories, the sites of virus assembly, near the nucleus. Clustering of mitochondria was inhibited by the drug nocodazole indicating that mitochondrial aggregation is dependent upon transport along microtubules. Expression of the hepatitis B virus X protein, like the RV capsid, is sufficient to induce clustering of mitochondria to a juxtannuclear region (Takada et al., 1999). While X protein expression leads to apoptotic cell death, clustering of mitochondria in itself is not likely to be the cause of death since Vero cells expressing the RV capsid display aggregated mitochondria but do not show visible signs of apoptosis (Figure 4.3.). Moreover, we were

unable to detect either pro- or anti-apoptotic effects of capsid expression in HEK 293TRC 2B cells (Figure 4.8.). Similarly, clustered mitochondria in African swine fever virus infected cells appeared normal in morphology (Rojo et al., 1998). Rather, it is thought that aggregation of mitochondria to sites in close proximity to virus replication factories serves to provide a source of cellular energy to assist virus replication (Garzon et al., 1990; Lee et al., 1996a; Miller et al., 2001; Rojo et al., 1998).

Our data are consistent with aggregation of mitochondria being beneficial for virus replication since recombinant viruses encoding capsid mutants that were unable to induce efficient clustering of mitochondria do not replicate as efficiently as wild type virus (Figure 4.9). Thus, one purpose of the association of capsid with mitochondria could be to induce changes in mitochondrial localization which are beneficial for virus replication.

## **5.5. The capsid-p32 interaction**

### **5.5.1. Model of the capsid-p32 interaction**

Interaction of capsid with a mitochondrial protein was intriguing in light of studies by others documenting links between mitochondria and RV replication (Bardeletti and Gautheron, 1976; Lee et al., 1996a) and studies by us demonstrating that capsid expression alters mitochondria localization (Figures 4.3). Further analysis revealed that capsid and p32 colocalize at the cytoplasmic surface of mitochondria (Figure 4.4). Thus, it follows that capsid-p32 interactions may play a role in the migration of mitochondria to RV replication sites and/or the formation of confronting membranes in infected cells. Indeed, our work has shown that capsid mutants which lack p32 binding sites do not induce clustering of mitochondria to the perinuclear region as efficiently as wild type capsid (Figure 4.3) suggesting that the interaction of capsid with p32 is directly involved in this process. In further support of this possibility, capsid lacking the amino terminal p32-binding domain was found to target to mitochondria but not induce mitochondrial aggregation (Personal communication. Jason Everitt, University of Alberta).

We have developed a model to explain the process by which capsid interacts with p32 to cause mitochondrial aggregation (Figure 5.1). In this model, capsid is targeted to mitochondria independently of p32, perhaps via a recently identified putative mitochondrial targeting sequence in capsid. Once associated with the cytoplasmic surface of the mitochondria, capsid is then able to bind to and complex with p32.

Interestingly, our data suggest that capsid associates with the mature form of p32 but is not imported into mitochondria. The precise mechanism by which this occurs is not known. One possibility is that capsid binds to a pool of p32 as it leaves the mitochondria. However, this scenario seems unlikely since there is no obvious mechanism for export of p32 from the mitochondria. Rather, we propose that binding of capsid to the carboxy-terminal portion of newly synthesized p32 in the cytosol leaves the amino terminal mitochondrial targeting sequence of p32 exposed. This would allow partial translocation of p32 into the mitochondrial matrix and cleavage of the leader peptide. We then propose that complete import of p32 is prevented by its association with capsid in the cytosol. A similar mechanism prevents import of the cellular enzyme fumarase into the mitochondria of *Saccharomyces cerevisiae*. In yeast, a single translation product leads to both cytosolic and mitochondrial distribution of fumarase (Stein et al., 1994). This translation product contains an amino terminal mitochondrial targeting sequence which results in the targeting of fumarase to the mitochondria, cleavage of the leader sequence by mitochondrial matrix peptidase and the import of a pool of fumarase to the mitochondrial matrix. However, approximately 70-80% of fumarase exists in the cytosol. Interestingly, this pool of fumarase lacks the leader peptide indicating that cytosolic fumarase has been processed in the mitochondrial matrix. This occurs as a result of the association of fumarase with ribosomes in the cytosol (Knox et al., 1998). Following membrane potential driven import of the fumarase mitochondrial targeting sequence, the leader sequence is cleaved. However, the protein remains bound to ribosomes in the cytosol which prevents complete import into the mitochondrial matrix. This results in the release of fumarase into the cytosol. Indeed, other studies have shown that if Hsp70 in the mitochondrial matrix is unable to bind to imported proteins, the protein in the import channel can reverse direction following cleavage of the leader peptide and exit out of the

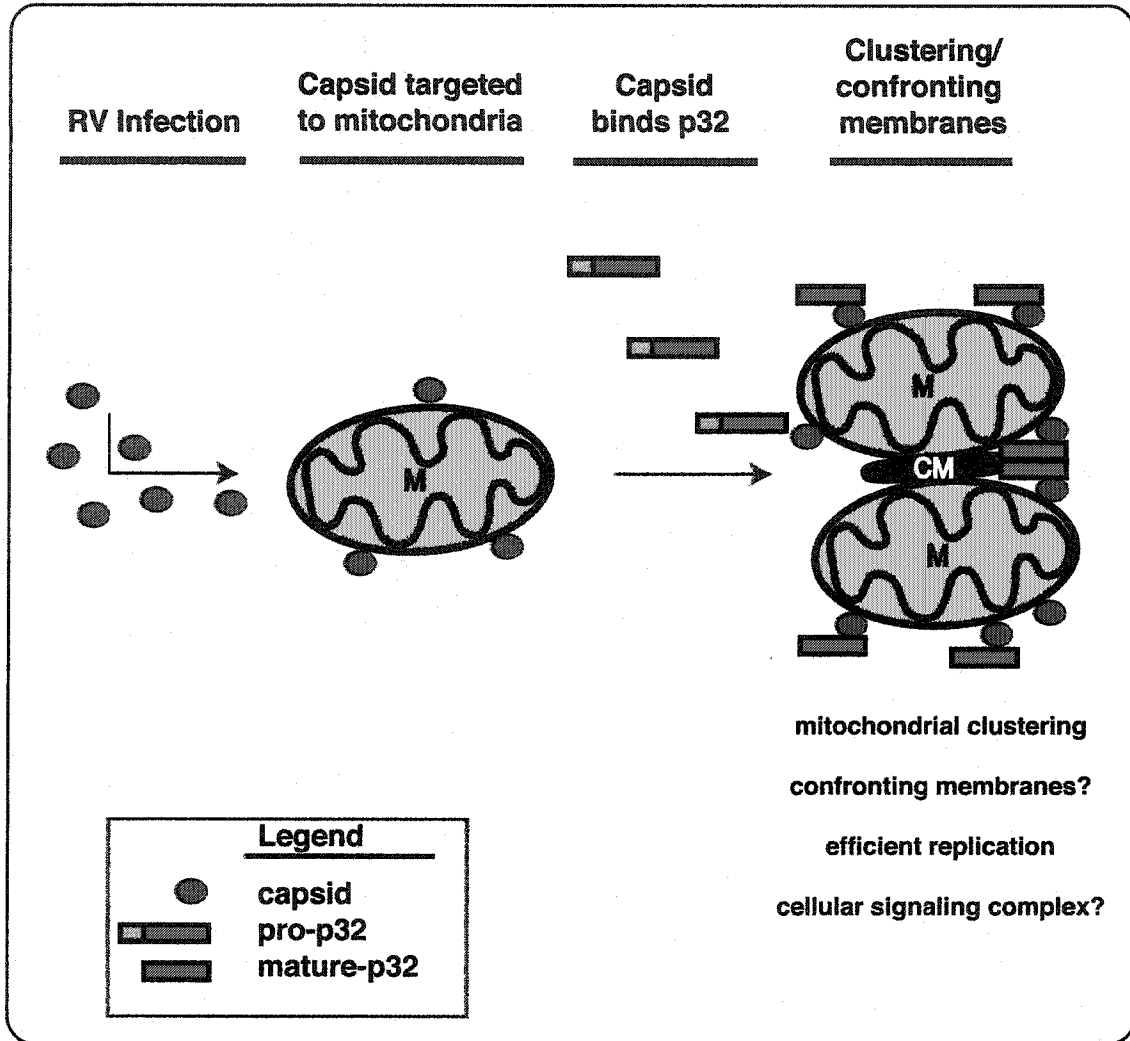


**Figure 5.1. Model of the interaction between rubella virus capsid and p32.** During RV infection, the structural proteins are translated and capsid is cleaved from the RV structural polypeptide at the ER. A pool of capsid is then targeted to mitochondria (M) by a mechanism which is independent of p32. Capsid accumulates at the cytoplasmic surface of the mitochondria where it is able to bind to nascent p32. We propose that the mitochondrial targeting sequence of p32 is imported into the mitochondrial matrix and cleaved. Association of p32 with capsid prevents further import of p32 allowing for capsid-p32 complexes to form on the cytoplasmic surface of mitochondria. These complexes could have adhesive properties resulting in mitochondrial aggregation and may also play a role in the formation of confronting membranes (CM) and cellular signaling complexes.

mitochondria (Ungermann et al., 1994). Thus, capsid could function in a similar manner as ribosomes do in fumarase import by retaining p32 in the cytosol.

In our model, capsid and p32 form a complex on the cytoplasmic face of mitochondria. In support of this, our data suggest that capsid is not translocated into the mitochondria (Figure 3.7), a finding that is consistent with Lee *et al.* (1999) who showed that capsid antibodies stain the cytoplasmic face of mitochondrial membranes in RV infected cells. One particularly challenging obstacle to this part of our model is that we were unable to detect p32 staining at the surface of mitochondria in Vero cells expressing capsid. One possible explanation for this observation is that the capsid-p32 interaction is transient and that p32 is imported into mitochondria following binding to capsid. Alternatively, it is possible that p32 antibodies do not recognize p32 which is complexed with capsid at the cytoplasmic surface of mitochondria. This could occur if binding to capsid alters the structure of p32. Following processing of the mitochondrial targeting sequence, p32 forms a donut shaped, trimeric complex (Jiang et al., 1999). Capsid interacts with the carboxy terminus of p32, a region involved in intermolecular homotypic interactions necessary for formation of the trimer (Mohan et al., 2002 and Figure 3.8). Thus it is possible that interaction with capsid disrupts the trimeric structure of p32. A more likely possibility is that p32 is inaccessible to antibodies in paraformaldehyde fixed cells when it is part of a protein complex bound to capsid. In support of the association of capsid and p32 at the cytoplasmic face of mitochondria, capsid efficiently recruited a dominant negative GFP tagged p32 lacking the mitochondrial targeting sequence, to mitochondria (Figures 4.4 and 4.5). This construct is unable to be imported into mitochondria and thereby confirms that capsid and p32 can interact at the cytoplasmic surface of mitochondria. Thus, our GFP studies are consistent with the existence of a stable capsid-p32 interaction at the cytoplasmic surface of mitochondria.

Finally, retention of p32 in the cytosol results in the formation of capsid-p32 complexes at the cytoplasmic surface of mitochondria. Both capsid and p32 are known to form homoligomers (Baron and Forsell, 1991; Jiang et al., 1999), thus, it is interesting to speculate that capsid-p32 complexes may function as a scaffold. In this manner, capsid

and p32 could act as a molecular adhesive to drive aggregation of mitochondria. In addition, this complex could have additional functions such as mediating host cell signaling.

A particularly interesting question arising from our studies regards the composition of the electron dense zones found between opposing mitochondria in RV infected cells (Lee et al., 1996a) and in capsid-expressing cells (Figure 4.7). The composition of these structures is unknown but the colocalization of capsid and p32 at the cytoplasmic surface of mitochondria is consistent with these two proteins having a role in the formation of these structures. For example, the electron dense structures may be composed of multimeric complexes of capsid and p32. Formation of confronting cisternae in infected cells occurs late in infection (Lee et al., 1996a), which would allow for accumulation of capsid-p32 complexes. We have attempted to determine if capsid and/or p32 were localized to these structures by immunogold electron microscopy but we were unable to confidently identify either of these proteins at electron dense zones. However, it is likely that our failure to do so was due to technical problems. It would be worthwhile to further examine the localization of these proteins to electron dense zones in a subsequent study. Furthermore, this method could be used to confirm the presence of p32 at the cytoplasmic face of mitochondria.

### **5.5.2. Function of the capsid-p32 interaction**

One approach we employed to further investigate the significance of the capsid-p32 interaction was to interfere with binding of capsid to p32 by introducing specific arginine to alanine mutations within the p32-binding region of capsid. Using this approach, we have demonstrated that interaction of capsid with p32 is important for efficient RV replication since infectious clones encoding mutant capsids which do not bind p32 replicate to much lower titers than wild type virus (Figure 4.9).

The fact that the amino terminus of capsid is multifunctional makes analysis of this region complicated since mutations designed to interfere with p32-binding may also interfere with phosphorylation or binding to genomic RNA. Furthermore, such mutations could potentially alter capsid stability or structure. However, careful analysis of these

mutations showed that capsid stability, phosphorylation, and RLP assembly were not significantly affected when only one of the arginine clusters (5RA or 6RA) within the amino terminus of capsid was mutated (Figure 4.2). Indirect evidence showed that these mutants are also able to bind genomic RNA to form infectious virus (Figure 4.10). However, alterations in binding efficiency were observed using an *in vitro* binding assay. This is an important factor to consider when interpreting the results obtained using the arginine to alanine mutants. Mutations to arginine residues within the amino terminus could also conceivably interfere with the function of capsid in regulating genomic RNA replication (Chen and Icenogle, 2004; Tzeng and Frey, 2003). While we cannot rule out the possibility that 5RA or 6RA mutations affect this function independently of the capsid-p32 interaction, this is unlikely since even an infectious clone containing the 11RA mutation, which renders capsid non-functional, was able to express the virus structural proteins indicating that replication of infectious RNA had occurred (Figure 4.10). Thus, the major defect we observed is that the capsid mutants do not stably associate with p32.

Our finding that the capsid-p32 interaction is important during virus replication is in agreement with another study showing that enhanced replication occurs in cells overexpressing p32 (Mohan et al., 2002). However, we have not yet determined the mechanisms by which the capsid-p32 interaction affects virus replication. It is interesting to speculate that the decreased replication of the RA mutant virus is related to the inability of these viruses to support mitochondrial aggregation since this is the only aspect of RV biology we have so far identified that is affected by the capsid-p32 interaction. Presumably mitochondrial aggregation would benefit virus replication by supplying a source of energy for virus replication. At this time, however, we cannot rule out that the capsid-p32 interaction may also play some other role in replication.

In addition to mitochondrial aggregation, the capsid-p32 interaction may have additional functions. Elucidating additional functions of p32 in RV replication has proven difficult though since the precise physiological function of p32 remains to be clearly defined. Numerous studies have determined that p32 is normally localized to the mitochondrial matrix (Dedio et al., 1998; Muta et al., 1997; Seytter et al., 1998). The

yeast homolog of p32 may be important for oxidative phosphorylation since a knockout strain grew poorly on a non-fermentable carbon source in one study (Muta et al., 1997). However, only one study to date has reported a function for p32 in the mitochondria of higher eukaryotes. In this study, p32 was reported to modulate apoptosis by interacting with Hrk, a pro-apoptotic BH3-only protein of the Bcl-2 subfamily. Binding of p32 to other cellular proteins at extramitochondrial sites has also been demonstrated to regulate several cellular processes. For instance, p32 has been shown to bind nuclear splicing factors and to regulate RNA splicing activity (Krainer et al., 1991; Petersen-Mahrt et al., 1999). It has also been demonstrated that p32 binds a number of PKC isoforms and regulates their kinase activity (Robles-Flores et al., 2002; Storz et al., 2000). The significance of these studies remains unclear since p32 is not normally localized in compartments where it would interact with these proteins. In addition to binding the RV capsid, binding of p32 to a number of viral proteins has been reported (See Table 3-1). The majority of these virus proteins are arginine rich, nucleic acid binding proteins. The functional significance of these interactions vary but a common feature of these interactions is that they typically involve the relocalization of p32 from mitochondria to alternate subcellular localizations such as the cytoplasm or nucleus. Thus, it is likely that several viruses have independently developed mechanisms to hijack p32 from its normal mitochondrial location.

It is possible that p32 may function differently depending on its subcellular localization. Such a multifunctional nature for mitochondrial proteins is not unusual. For example, cytochrome c functions in electron transport in the mitochondrial intra-membrane space but as an activator of caspase-9 in the cytosol (van Gurp et al., 2003). Thus, p32 may possess one function in the mitochondrial matrix but still play a role in RV replication. Binding of capsid to p32 would serve to retain p32 in the cytosol where it could then mediate these effects. In addition to mitochondrial clustering, p32 could have other functions when bound to capsid. However, we have not been able to demonstrate any additional functions of p32.

One particularly intriguing possibility is that this interaction may play a role in modulating apoptosis. This is an attractive hypothesis since both capsid and p32 have

been implicated in regulating apoptosis (Duncan et al., 2000; Jiang et al., 1999; Meenakshi et al., 2003; Sunayama et al., 2004). Determination of the crystal structure of p32 showed that the protein exists as a homotrimeric doughnut structure with an asymmetric charge distribution (Jiang et al., 1999). In this regard, it was proposed that p32 may act as a calcium buffer that modulates the concentration of divalent metal ions and consequently regulates opening of the permeability transition pore of the mitochondrial inner membrane, a process which is known to have a critical role in apoptosis (Heiden and Thompson, 1999). Accordingly, binding to capsid may affect the ability of p32 to act as a calcium buffer. A more recent study has shown that p32 is necessary for apoptosis induction by Hrk, a pro-apoptotic BH3-only protein (Sunayama et al., 2004). Our data suggest that capsid-p32 interactions are unlikely to be involved in regulating apoptosis since we were unable to demonstrate that capsid expression was either pro- or anti-apoptotic (Figure 4.8). In addition, viruses expressing mutant capsids did not significantly differ in their ability to cause cytopathology compared to wild type virus (Figure 4.11). Finally, capsid expression was not found to affect mitochondrial transmembrane potential in RK-13 cells which are highly sensitive to RV induced apoptosis (Personal communication. Jason Everitt, University of Alberta). However, Hrk expression is largely restricted to brain and lymphoid tissue and therefore is most likely not expressed in HEK 293T or RK-13 cells. Thus, the role of the capsid-p32 interaction in mediating apoptosis may need to be better studied in other cell types.

We have also examined the role of the capsid-p32 interaction in modulating host cell signaling events since p32 has been shown to interact with various PKC isoforms (Robles-Flores et al., 2002; Storz et al., 2000). While we observed that capsid was able to downregulate AP-1 activity, this activity did not appear to be modulated by p32 expression (Figure A2.B). Similarly, the ability of capsid mutants, which do not bind p32, to undergo phosphorylation or assemble into RLPs was not affected suggesting that p32 does not regulate bulk phosphorylation of capsid or assembly of virions.

One possibility that we have not tested is that the capsid-p32 interaction is involved in regulating replication of the genomic RNA. This is an interesting possibility for several reasons. First of all, a region of capsid containing the p32 binding site has

been found to be necessary for complementation of a RV replicon containing a mutation in the nonstructural ORF (Tzeng and Frey, 2003). In addition, human p32 was shown to overcome a post-transcriptional block to HIV replication in murine cells (Zheng et al., 2003). In both cases, the authors proposed that these effects were achieved by increasing RNA stability. Thus, it is possible that capsid interacts with p32 to increase the stability of RV genomic RNA during virus replication. Although p32 has yet to be identified at RV replication complexes, our studies do not rule out the possibility that capsid-p32 complexes exist at this location. An interesting experiment would be to test the ability of the RA mutant capsids (5RA and 6RA), which do not bind p32, to complement replication of these replicons.

The replication of mutant viruses expressing capsids that are unable to bind p32 deserves further investigation to determine how this interaction benefits RV replication. In this respect, a crucial experiment to verify that the interaction of capsid with p32 is important for RV replication would be to test the ability of RV to replicate in cells which do not express p32. These experiments are necessary to confirm that the defects observed using the arginine to alanine capsid mutants are due to decreased p32 binding and not other effects of these mutations such as altered binding to genomic RNA. According to our model, interaction of capsid with p32 is necessary for mitochondrial aggregation which, in turn, is important for efficient replication of viral genomic RNA. We would expect that mitochondrial aggregation would not occur in RV infected cells lacking p32. Furthermore, we expect that RV replication would be inhibited in the absence of p32. This experiment would prove that the effects we report in this thesis are not due to unknown defects in the capsid mutants or the loss of binding of capsid to other cellular proteins which are important for replication. Testing this hypothesis has been a complicated matter since cell lines which do not express p32 are not available to our knowledge. We also attempted to knockdown p32 in RK-13 and Vero cells by RNA interference. Unfortunately, we were unable to achieve reproducible knockdown of p32 despite using several different systems (Silencer siRNA construction kit, Ambion and the vector based GeneSuppressor System, IMGENEX) and targeting several different regions of p32. Our failure to knockdown p32 is likely a result of choosing a region of the p32

mRNA incompatible with knockdown. We also attempted to interfere with capsid-p32 interactions using dominant negative constructs but these experiments were unsuccessful since various truncated forms of p32 were targeted to the nucleus. Interestingly, a study published during the preparation of this thesis reported the knockdown of p32 by RNA interference (Sunayama et al., 2004) so knockdown studies may now be possible.

While further studies are needed to clarify the exact mechanisms by which the capsid-p32 interaction is involved in mitochondrial aggregation and RV replication, these studies have the potential to shed new light on the role of the RV capsid during virus infection.

## **5.6. Interaction of capsid with other host cell proteins**

In addition to p32, we identified several other novel capsid-interacting host cell proteins. While the interactions between capsid and these proteins were not studied in great detail, the identification of these proteins may lead to the elucidation of the mechanisms by which capsid performs additional functions in infected cells. The possible implications for the interaction of capsid with these proteins are discussed below.

### **5.6.1. Par-4**

The finding that capsid interacts with Par-4, a protein which sensitizes cells to apoptotic stimuli (Sells et al., 1997) was particularly interesting to us since it suggested that capsid may play a direct role in modulating cytopathic effect in the host cell. Par-4 was originally identified in a screen for proteins that are upregulated during apoptosis in prostate cells and has been shown to be upregulated in numerous other cell types undergoing apoptosis (Sells et al., 1994). Par-4 expression in itself does not normally induce apoptosis but, rather, Par-4 acts to sensitize cells to apoptotic stimuli (Sells et al., 1997). The carboxy terminus of Par-4 contains a leucine zipper domain that binds to the zinc finger domain of PKC $\zeta$  inhibiting the kinase activity of this protein (Diaz-Meco et al., 1999; Diaz-Meco et al., 1996). PKC $\zeta$  plays an important role in mediating pro-survival NF- $\kappa$ B pathway by activating the I $\kappa$ B kinase (Lallena et al., 1999). Thus, the

ability of Par-4 to sensitize cells to apoptotic stimuli depends on its ability to block the protective effects of NF- $\kappa$ B (Camandola and Mattson, 2000; Chakraborty et al., 2001; Chang et al., 2002; Chendil et al., 2002; Diaz-Meco et al., 1999; Nalca et al., 1999).

Originally, we hypothesized that interactions between capsid and Par-4 would function to protect cells from induction of apoptosis. In support of this, we found that capsid binds the carboxy terminal portion of Par-4 containing a leucine zipper domain (Figure 3.12) (Sells et al., 1997). The leucine zipper domain is necessary for Par-4 function (Guo et al., 1998) and has been shown to interact with a number of other proteins, including PKC $\zeta$  (Diaz-Meco et al., 1996). Capsid may compete with PKC $\zeta$  such that it would be unable to inhibit PKC $\zeta$  and NF- $\kappa$ B signaling in infected cells. Another option is that capsid is able to bind both Par-4 and PKC $\zeta$  simultaneously. This could very well be the case since we detected PKC $\zeta$  in GST-pulldowns. The interaction of capsid to PKC $\zeta$  could be indirect and mediated through Par-4. This complex could also block Par-4 mediated inhibition of PKC $\zeta$ . In fact, Par-4 exists in a ternary complex with PKC $\zeta$  and p62 (Chang et al., 2002). Binding of p62 to this complex allows PKC $\zeta$  activation. Conceivably, capsid could function in a similar manner to p62 in preserving PKC $\zeta$  activity. However, we have not done competitive binding studies to determine if capsid can compete with PKC $\zeta$  for binding to Par-4.

Despite the amount of work dedicated to elucidating the function of Par-4, the intracellular localization of this protein is not well characterized. We found that capsid and Par-4 colocalize at intracellular membranes that were probably ER. These results are consistent with previous studies showing that Par-4 is localized in the cytoplasm (Boghaert et al., 1997; Guo et al., 1998) and suggest that capsid and Par-4 can interact *in vivo*.

Interestingly, capsid expression did not block the ability of Par-4 to downregulate NF- $\kappa$ B activity in luciferase assays conducted in HEK 293T cells (Appendix A2). While these results may appear to contradict our model, it is important to appreciate the complexities of NF- $\kappa$ B signaling. It is well known that NF- $\kappa$ B activity is regulated by many factors including the subunit composition of the transcription factor, stimulus type and cell type. It is possible that binding of capsid to Par-4 plays a more important role in

the regulation of NF- $\kappa$ B activation in other cell types or during virus infection. We experienced some difficulty in coimmunoprecipitating capsid and Par-4 from transfected cells. While we have hypothesized that these interactions may be disrupted by the antibodies we used for immunoprecipitation, it is also possible that the capsid-Par-4 interaction is transient or unstable in the cell types we have used. It would be very interesting to examine this interaction in other cell types, specifically neurons. Par-4 has been shown to play an important role in neuronal apoptosis and degeneration (Guo et al., 1998; Mattson et al., 1999). Furthermore, neurological lesions are a common feature of CRS (Frey, 1997) and RV has been shown to induce apoptotic cell death in rat glial cell cultures (Domegan and Atkins, 2002). Thus, the capsid-Par-4 interaction may play a more significant role in neuronal cells or other cell types, perhaps due to expression of cofactors that stabilize the capsid-Par- interaction.

While we have not been able to demonstrate a functional role for the capsid-Par-4 interaction in RV biology, this interaction is particularly interesting in light of studies which have shown that RV induces apoptosis in a cell type dependent manner (Duncan et al., 1999). This interaction deserves further investigation to elucidate the mechanisms by which capsid may modulate Par-4 function during RV infection.

### **5.6.2. PKC $\zeta$**

As discussed above, the atypical protein kinase C isoform PKC $\zeta$  plays a crucial role in regulating the pro-survival NF- $\kappa$ B and AP-1 signaling pathways (Huang et al., 2000; Lallena et al., 1999). Our original hypothesis was that capsid acts to preserve PKC $\zeta$  activity by interacting with Par-4 (see Figure A.1). In addition, PKC $\zeta$  has also been demonstrated to bind another capsid-interacting protein, p32 (Robles-Flores et al., 2002). However, the effects of p32 binding on the kinase activity of PKC $\zeta$  are not known. It has been reported that p32 is able to negatively regulate PKC $\mu$  activity (Storz et al., 2000) while it appears to activate PKC $\delta$  activity (Robles-Flores et al., 2002). The interaction of capsid with three host cell proteins involved in regulating survival pathways raises the possibility that these proteins exist in a complex which regulates PKC $\zeta$  activity, perhaps to influence cellular signaling.

Our hypothesis is largely speculative since it remains unclear how capsid is binding to PKC $\zeta$ . While this interaction may be direct, it is equally possible that capsid binds PKC $\zeta$  indirectly through p32 and/or Par-4 since both of these proteins have been shown to bind PKC $\zeta$  (Diaz-Meco et al., 1996). In addition, we did not detect PKC $\zeta$  as a capsid-interacting protein in our yeast two-hybrid screen. It is possible that these four proteins exist as a single complex with all four proteins interacting to regulate PKC $\zeta$  activity. However, this seems unlikely since capsid was found to interact with p32 and Par-4 at distinct intracellular locations. This raises the interesting possibility that capsid might interact with PKC $\zeta$  through p32 or Par-4 at two different locations. In this case, capsid could act as a scaffold to regulate PKC $\zeta$  activity. For instance, binding of capsid to p32 would be expected to retain p32 in the cytosol. This interaction would be necessary to prevent mitochondrial import of p32 leaving it able to bind PKC $\zeta$ . To confirm the importance of these interactions, the precise intracellular localization of PKC $\zeta$  must be determined in cells expressing capsid. The functional relevance of PKC $\zeta$  activity in RV infected cells should also be investigated. This can be done using constitutively active and kinase dead PKC $\zeta$  mutants.

Together, our results indicate that capsid interacts with several cellular proteins which have been implicated in regulating NF- $\kappa$ B and AP-1 activation and suggest that interactions between capsid and PKC $\zeta$ , whether direct or indirect, may mediate cellular signaling events. However, future work must be done to confirm the importance of PKC $\zeta$  in NF- $\kappa$ B and AP-1 activation in RV infected cells. The results from these experiments will shed light on the functions of capsid in modulating the host cell survival.

### **5.6.3. The Poly(A) binding protein**

The fourth capsid-interacting protein identified in this thesis is the cytoplasmic poly(A) binding protein (Yanagida et al., 2004) which was found to associate with capsid in GST-pulldown experiments. Although no further characterization of this interaction was performed, this interaction has the potential to be relevant to our understanding of regulation of genomic RNA replication by capsid. Poly(A) binding protein

simultaneously binds both the poly(A) tract at the 3' end of eukaryotic mRNAs and a protein complex bound to the 5' end of the mRNA (Gallie, 1998). These interactions function to stimulate translation and to stabilize mRNA. Poly(A) binding protein almost certainly binds to RV genomic RNA to aid translation of the nonstructural proteins. However, binding of poly(A) binding protein to genomic RNA at a later stages of replication could pose serious problems since attachment of ribosomes to the genomic RNA could prevent packaging of the genome into nucleocapsids. Thus, capsid may act to regulate formation of poly(A) binding protein-RNA interactions. For instance, capsid accumulation late in infection could bind to the poly(A) binding protein and inhibit formation of these ribonucleoprotein complexes. This could lead to more efficient packaging of viral RNA into nucleocapsids.

While this model is purely speculative, capsid has been shown to play a role in modulating replication of RV genomic RNA in a recent study (Chen and Icenogle, 2004). Interestingly, it was found that expression of high levels of capsid, prior to RV infection, significantly reduced virus infectivity. Unfortunately, levels of viral protein and RNA were not determined in these cells so the precise step at which replication is blocked is not known. These results could be explained if capsid expression is preventing translation of viral mRNAs. However, RV does not significantly inhibit translation of host cell mRNAs so a mechanism would have to exist to specifically block translation of viral RNA. Further investigation of the capsid-poly(A) binding protein interaction may elucidate specific mechanisms by which capsid regulates viral replication.

### **5.7. Concluding remarks**

RV remains one of the leading causes of congenital defects in the world. Recent work has led to a basic understanding of the molecular biology of this virus, but many aspects of virus replication and cytopathogenesis remain unknown. The work presented here has identified several cellular proteins which interact with the capsid protein. This work further suggests that capsid is multifunctional in nature and indicates the importance of virus-host interactions during RV infection. The challenge now remains to

characterize how RV proteins regulate virus replication and cytopathogenesis through interactions with cellular proteins.

## **REFERENCES**

- Ausubel, F.M. 1992. Current protocols in molecular biology. Published by Greene Pub. Associates and Wiley-Interscience : J. Wiley, New York. v. (loose leaf) pp.
- Avila, L., W.E. Rawls, and P.B. Dent. 1972. Experimental infection with rubella virus. I. Acquired and congenital infection in rats. *J Infect Dis.* 126:585-92.
- Barba, G., F. Harper, T. Harada, M. Kohara, S. Goulinet, Y. Matsuura, G. Eder, Z. Schaff, M.J. Chapman, T. Miyamura, and C. Brechot. 1997. Hepatitis C virus core protein shows a cytoplasmic localization and associates to cellular lipid storage droplets. *Proc Natl Acad Sci U S A.* 94:1200-5.
- Bardeletti, G., and D.C. Gautheron. 1976. Phospholipid and cholesterol composition of rubella virus and its host cell BHK 21 grown in suspension cultures. *Arch Virol.* 52:19-27.
- Bardeletti, G., M. Henry, R. Sohler, and D. Gautheron. 1972. Primary effects of the rubella virus on the metabolism of BHK-21 cells grown in suspension cultures. *Arch Gesamte Virusforsch.* 39:26-34.
- Bardeletti, G., J. Tektoff, and D. Gautheron. 1979. Rubella virus maturation and production in two host cell systems. *Intervirology.* 11:97-103.
- Baric, R.S., G.W. Nelson, J.O. Fleming, R.J. Deans, J.G. Keck, N. Casteel, and S.A. Stohlman. 1988. Interactions between coronavirus nucleocapsid protein and viral RNAs: implications for viral transcription. *J Virol.* 62:4280-7.
- Baron, M.D., T. Ebel, and M. Suomalainen. 1992. Intracellular transport of rubella virus structural proteins expressed from cloned cDNA. *J Gen Virol.* 73 ( Pt 5):1073-86.
- Baron, M.D., and K. Forsell. 1991. Oligomerization of the structural proteins of rubella virus. *Virology.* 185:811-9.
- Beatch, M.D., and T.C. Hobman. 2000. Rubella virus capsid associates with host cell protein p32 and localizes to mitochondria. *J Virol.* 74:5569-76.
- Berra, E., M.T. Diaz-Meco, I. Dominguez, M.M. Municio, L. Sanz, J. Lozano, R.S. Chapkin, and J. Moscat. 1993. Protein kinase C zeta isoform is critical for mitogenic signal transduction. *Cell.* 74:555-63.
- Bienz, K., D. Egger, Y. Rasser, and W. Bossart. 1983. Intracellular distribution of poliovirus proteins and the induction of virus-specific cytoplasmic structures. *Virology.* 131:39-48.
- Boghaert, E.R., S.F. Sells, A.J. Walid, P. Malone, N.M. Williams, M.H. Weinstein, R. Strange, and V.M. Rangnekar. 1997. Immunohistochemical analysis of the proapoptotic protein Par-4 in normal rat tissues. *Cell Growth Differ.* 8:881-90.
- Bowden, D.S., J.S. Pedersen, B.H. Toh, and E.G. Westaway. 1987. Distribution by immunofluorescence of viral products and actin containing cyto skeletal filaments in Rubella virus infected cells. *Arch. Virol.* 92:211-219.
- Brown, A.S., P. Cohen, J. Harkavy-Friedman, V. Babulas, D. Malaspina, J.M. Gorman, and E.S. Susser. 2001. A.E. Bennett Research Award. Prenatal rubella, premorbid abnormalities, and adult schizophrenia. *Biol Psychiatry.* 49:473-86.
- Bruni, R., and B. Roizman. 1996. Open reading frame P--a herpes simplex virus gene repressed during productive infection encodes a protein that binds a splicing factor and reduces synthesis of viral proteins made from spliced mRNA. *Proc Natl Acad Sci U S A.* 93:10423-7.

- Bryant, H.E., D.A. Matthews, S. Wadd, J.E. Scott, J. Kean, S. Graham, W.C. Russell, and J.B. Clements. 2000. Interaction between herpes simplex virus type 1 IE63 protein and cellular protein p32. *J Virol.* 74:11322-8.
- Camandola, S., and M.P. Mattson. 2000. Pro-apoptotic action of PAR-4 involves inhibition of NF-kappaB activity and suppression of BCL-2 expression. *J Neurosci Res.* 61:134-9.
- Carette, J.E., K. Guhl, J. Wellink, and A. Van Kammen. 2002a. Coalescence of the sites of cowpea mosaic virus RNA replication into a cytopathic structure. *J Virol.* 76:6235-43.
- Carette, J.E., J. van Lent, S.A. MacFarlane, J. Wellink, and A. van Kammen. 2002b. Cowpea mosaic virus 32- and 60-kilodalton replication proteins target and change the morphology of endoplasmic reticulum membranes. *J Virol.* 76:6293-301.
- Chakraborty, M., S.G. Qiu, K.M. Vasudevan, and V.M. Rangnekar. 2001. Par-4 drives trafficking and activation of Fas and FasL to induce prostate cancer cell apoptosis and tumor regression. *Cancer Res.* 61:7255-63.
- Chang, S., J.H. Kim, and J. Shin. 2002. p62 forms a ternary complex with PKCzeta and PAR-4 and antagonizes PAR-4-induced PKCzeta inhibition. *FEBS Lett.* 510:57-61.
- Chantler, J.K., J.S. Wolinsky, and A.J. Tingle. 2001. Rubella Virus. In *Fields' Virology*. B.N. Fields, D.M. Knipe, P.M. Howley, and D.E. Griffin, editors. Lippincott Williams & Wilkins, Philadelphia. 963-990.
- Chen, J.P., J.H. Strauss, E.G. Strauss, and T.K. Frey. 1996. Characterization of the rubella virus nonstructural protease domain and its cleavage site. *J Virol.* 70:4707-13.
- Chen, M.H., and J.P. Icenogle. 2004. Rubella virus capsid protein modulates viral genome replication and virus infectivity. *J Virol.* 78:4314-22.
- Chen, M.R., J.F. Yang, C.W. Wu, J.M. Middeldorp, and J.Y. Chen. 1998. Physical association between the EBV protein EBNA-1 and P32/TAP/hyaluronectin. *J Biomed Sci.* 5:173-9.
- Chendil, D., A. Das, S. Dey, M. Mohiuddin, and M.M. Ahmed. 2002. Par-4, a pro-apoptotic gene, inhibits radiation-induced NF kappa B activity and Bcl-2 expression leading to induction of radiosensitivity in human prostate cancer cells PC-3. *Cancer Biol Ther.* 1:152-60.
- Cho, J., W. Baek, S. Yang, J. Chang, Y.C. Sung, and M. Suh. 2001. HCV core protein modulates Rb pathway through pRb down-regulation and E2F-1 up-regulation. *Biochim Biophys Acta.* 1538:59-66.
- Choi, H.K., L. Tong, W. Minor, P. Dumas, U. Boege, M.G. Rossmann, and G. Wengler. 1991. Structure of Sindbis virus core protein reveals a chymotrypsin-like serine proteinase and the organization of the virion. *Nature.* 354:37-43.
- Clarke, D.M., T.W. Loo, I. Hui, P. Chong, and S. Gillam. 1987. Nucleotide sequence and in vitro expression of rubella virus 24S subgenomic messenger RNA encoding the structural proteins E1, E2 and C. *Nucleic Acids Res.* 15:3041-57.
- Clarke, D.M., T.W. Loo, H. McDonald, and S. Gillam. 1988. Expression of rubella virus cDNA coding for the structural proteins. *Gene.* 65:23-30.
- Compton, S.R., D.B. Rogers, K.V. Holmes, D. Fertsch, J. Remenick, and J.J. McGowan. 1987. In vitro replication of mouse hepatitis virus strain A59. *J Virol.* 61:1814-20.

- Cooper, L.Z., P.R. Ziring, A.B. Ockerse, B.A. Fedun, B. Kiely, and S. Krugman. 1969. Rubella. Clinical manifestations and management. *Am J Dis Child*. 118:18-29.
- Dales, L., S.J. Hammer, and N.J. Smith. 2001. Time trends in autism and in MMR immunization coverage in California. *Jama*. 285:1183-5.
- Dedio, J., W. Jahnen-Dechent, M. Bachmann, and W. Muller-Esterl. 1998. The multiligand-binding protein gC1qR, putative C1q receptor, is a mitochondrial protein. *J Immunol*. 160:3534-42.
- Diaz-Meco, M.T., E. Berra, M.M. Municio, L. Sanz, J. Lozano, I. Dominguez, V. Diaz-Golpe, M.T. Lain de Lera, J. Alcami, C.V. Paya, and et al. 1993. A dominant negative protein kinase C zeta subspecies blocks NF-kappa B activation. *Mol Cell Biol*. 13:4770-5.
- Diaz-Meco, M.T., M.J. Lallena, A. Monjas, S. Frutos, and J. Moscat. 1999. Inactivation of the Inhibitory kappaB Protein Kinase/Nuclear Factor kappaB Pathway by Par-4 Expression Potentiates Tumor Necrosis Factor alpha-induced Apoptosis. *J Biol Chem*. 274:19606-19612.
- Diaz-Meco, M.T., M.M. Municio, S. Frutos, P. Sanchez, J. Lozano, L. Sanz, and J. Moscat. 1996. The product of par-4, a gene induced during apoptosis, interacts selectively with the atypical isoforms of protein kinase C. *Cell*. 86:777-86.
- Domegan, L.M., and G.J. Atkins. 2002. Apoptosis induction by the Therien and vaccine RA27/3 strains of rubella virus causes depletion of oligodendrocytes from rat neural cell cultures. *J Gen Virol*. 83:2135-43.
- Dominguez, G., C.Y. Wang, and T.K. Frey. 1990. Sequence of the genome RNA of Rubella virus: evidence for genetic rearrangement during Togavirus evolution. *Virology*. 177:225-238.
- Duncan, R., A. Esmaili, L.M. Law, S. Bertholet, C. Hough, T.C. Hobman, and H.L. Nakhasi. 2000. Rubella virus capsid protein induces apoptosis in transfected RK13 cells. *Virology*. 275:20-9.
- Duncan, R., J. Muller, N. Lee, A. Esmaili, and H.L. Nakhasi. 1999. Rubella virus-induced apoptosis varies among cell lines and is modulated by Bcl-XL and caspase inhibitors. *Virology*. 255:117-28.
- Egger, D., B. Wolk, R. Gosert, L. Bianchi, H.E. Blum, D. Moradpour, and K. Bienz. 2002. Expression of hepatitis C virus proteins induces distinct membrane alterations including a candidate viral replication complex. *J Virol*. 76:5974-84.
- Frangioni, J.V., and B.G. Neel. 1993. Solubilization and purification of enzymatically active glutathione S-transferase (pGEX) fusion proteins. *Anal Biochem*. 210:179-87.
- Frey, T.K. 1994. Molecular biology of rubella virus. *Adv Virus Res*. 44:69-160.
- Frey, T.K. 1997. Neurological aspects of rubella virus infection. *Intervirology*. 40:167-75.
- Frey, T.K., and I.D. Marr. 1988. Sequence of the region coding for virion proteins C and E2 and the carboxy terminus of the non-structural proteins of rubella virus: Comparison to alphaviruses. *Gene*. 62:85-99.
- Froshauer, S., J. Kartenbeck, and A. Helenius. 1988. Alphavirus RNA replicase is located on the cytoplasmic surface of endosomes and lysosomes. *J Cell Biol*. 107:2075-86.
- Gallie, D.R. 1998. A tale of two termini: a functional interaction between the termini of an mRNA is a prerequisite for efficient translation initiation. *Gene*. 216:1-11.

- Garbutt, M., H. Chan, and T.C. Hobman. 1999a. Secretion of rubella virions and virus-like particles in cultured epithelial cells. *Virology*. 261:340-6.
- Garbutt, M., L.M. Law, H. Chan, and T.C. Hobman. 1999b. Role of rubella virus glycoprotein domains in assembly of virus-like particles. *J Virol*. 73:3524-33.
- Garzon, S., H. Strykowski, and G. Charpentier. 1990. Implication of mitochondria in the replication of Nodamura virus in larvae of the Lepidoptera, *Galleria mellonella* (L.) and in suckling mice. *Arch Virol*. 113:165-76.
- Ghebrehiwet, B., B.L. Lim, E.I. Peerschke, A.C. Willis, and K.B. Reid. 1994. Isolation, cDNA cloning, and overexpression of a 33-kD cell surface glycoprotein that binds to the globular "heads" of C1q. *J Exp Med*. 179:1809-21.
- Ginsberg-Fellner, F., M.E. Witt, B. Fedun, F. Taub, M.J. Dobersen, R.C. McEvoy, L.Z. Cooper, A.L. Notkins, and P. Rubinstein. 1985. Diabetes mellitus and autoimmunity in patients with the congenital rubella syndrome. *Rev Infect Dis*. 7 Suppl 1:S170-6.
- Gorbalenya, A.E., E.V. Koonin, and M.M. Lai. 1991. Putative papain-related thiol proteases of positive-strand RNA viruses. Identification of rubi- and aphthovirus proteases and delineation of a novel conserved domain associated with proteases of rubi-, alpha- and coronaviruses. *FEBS Lett*. 288:201-5.
- Gregg, N.M. 1941. Congenital cataract following German measles in the mother. *Trans. Ophthalmol. Soc. Aust.* 3:35-46.
- Gros, C., and G. Wengler. 1996. Identification of an RNA-stimulated NTPase in the predicted helicase sequence of the Rubella virus nonstructural polyprotein. *Virology*. 217:367-72.
- Guarente, L. 1993. Strategies for the identification of interacting proteins. *Proc Natl Acad Sci U S A*. 90:1639-41.
- Guo, Q., W. Fu, J. Xie, H. Luo, S.F. Sells, J.W. Geddes, V. Bondada, V.M. Rangnekar, and M.P. Mattson. 1998. Par-4 is a mediator of neuronal degeneration associated with the pathogenesis of Alzheimer disease. *Nat Med*. 4:957-62.
- Hahn, Y.S., A. Grakoui, C.M. Rice, E.G. Strauss, and J.H. Strauss. 1989. Mapping of RNA- temperature-sensitive mutants of Sindbis virus: complementation group F mutants have lesions in nsP4. *J Virol*. 63:1194-202.
- Hall, K.T., M.S. Giles, M.A. Calderwood, D.J. Goodwin, D.A. Matthews, and A. Whitehouse. 2002. The Herpesvirus Saimiri open reading frame 73 gene product interacts with the cellular protein p32. *J Virol*. 76:11612-22.
- Hayman, M.L., M.M. Miller, D.M. Chandler, C.C. Goulah, and L.K. Read. 2001. The trypanosome homolog of human p32 interacts with RBP16 and stimulates its gRNA binding activity. *Nucleic Acids Res*. 29:5216-25.
- Heiden, M.G.V., and C.B. Thompson. 1999. Bcl-2 proteins: regulators of apoptosis or of mitochondrial homeostasis? *Nat Cell Biolog*. 1:E209-E216.
- Hemphill, M.L., R.Y. Forng, E.S. Abernathy, and T.K. Frey. 1988. Time course of virus-specific macromolecular synthesis during rubella virus infection in Vero cells. *Virology*. 162:65-75.

- Herrmann, K.L. 1991. Rubella in the United States: toward a strategy for disease control and elimination. *Epidemiol Infect.* 107:55-61.
- Herwald, H., J. Dedio, R. Kellner, M. Loos, and W. Muller-Esterl. 1996. Isolation and characterization of the kininogen-binding protein p33 from endothelial cells. Identity with the gC1q receptor. *J Biol Chem.* 271:13040-7.
- Hobman, T.C. 1993. Targeting of viral glycoproteins to the Golgi complex. *Trends Microbiol.* 1:124-30.
- Hobman, T.C., and S. Gillam. 1989. In vitro and in vivo expression of rubella virus glycoprotein E2: the signal peptide is contained in the C-terminal region of capsid protein. *Virology.* 173:241-50.
- Hobman, T.C., H.F. Lemon, and K. Jewell. 1997. Characterization of an endoplasmic reticulum retention signal in the rubella virus E1 glycoprotein. *J Virol.* 71:7670-80.
- Hobman, T.C., M.L. Lundstrom, and S. Gillam. 1990. Processing and intracellular transport of rubella virus structural proteins in COS cells. *Virology.* 178:122-33.
- Hobman, T.C., M.L. Lundstrom, C.A. Mauracher, L. Woodward, S. Gillam, and M.G. Farquhar. 1994. Assembly of rubella virus structural proteins into virus-like particles in transfected cells. *Virology.* 202:574-85.
- Hobman, T.C., Z.Y. Qiu, H. Chaye, and S. Gillam. 1991. Analysis of rubella virus E1 glycosylation mutants expressed in COS cells. *Virology.* 181:768-72.
- Hobman, T.C., R. Shukin, and S. Gillam. 1988. Translocation of rubella virus glycoprotein E1 into the endoplasmic reticulum. *J Virol.* 62:4259-64.
- Hobman, T.C., L. Woodward, and M.G. Farquhar. 1992. The rubella virus E1 glycoprotein is arrested in a novel post-ER, pre-Golgi compartment. *J Cell Biol.* 118:795-811.
- Hobman, T.C., L. Woodward, and M.G. Farquhar. 1993. The rubella virus E2 and E1 spike glycoproteins are targeted to the Golgi complex. *J Cell Biol.* 121:269-81.
- Hobman, T.C., L. Woodward, and M.G. Farquhar. 1995. Targeting of a heterodimeric membrane protein complex to the Golgi: rubella virus E2 glycoprotein contains a transmembrane Golgi retention signal. *Mol Biol Cell.* 6:7-20.
- Hofmann, J., M.W. Pletz, and U.G. Liebert. 1999. Rubella virus-induced cytopathic effect in vitro is caused by apoptosis. *J Gen Virol.* 80 ( Pt 7):1657-64.
- Honore, B., P. Madsen, H.H. Rasmussen, J. Vandekerckhove, J.E. Celis, and H. Leffers. 1993. Cloning and expression of a cDNA covering the complete coding region of the P32 subunit of human pre-mRNA splicing factor SF2. *Gene.* 134:283-7.
- Hovi, T., and A. Vaheri. 1970. Rubella virus-specific ribonucleic acids in infected BHK21 cells. *J Gen Virol.* 6:77-83.
- Huang, C., J. Li, N. Chen, W. Ma, G.T. Bowden, and Z. Dong. 2000. Inhibition of atypical PKC blocks ultraviolet-induced AP-1 activation by specifically inhibiting ERKs activation. *Mol Carcinog.* 27:65-75.

- Jansen, V.A., N. Stollenwerk, H.J. Jensen, M.E. Ramsay, W.J. Edmunds, and C.J. Rhodes. 2003. Measles outbreaks in a population with declining vaccine uptake. *Science*. 301:804.
- Jiang, J., Y. Zhang, A.R. Krainer, and R.M. Xu. 1999. Crystal structure of human p32, a doughnut-shaped acidic mitochondrial matrix protein. *Proc Natl Acad Sci U S A*. 96:3572-7.
- Jin, D.Y., H.L. Wang, Y. Zhou, A.C. Chun, K.V. Kibler, Y.D. Hou, H. Kung, and K.T. Jeang. 2000. Hepatitis C virus core protein-induced loss of LZIP function correlates with cellular transformation. *Embo J*. 19:729-40.
- Johnstone, R.W., R.H. See, S.F. Sells, J. Wang, S. Muthukkumar, C. Englert, D.A. Haber, J.D. Licht, S.P. Sugrue, T. Roberts, V.M. Rangnekar, and Y. Shi. 1996. A novel repressor, par-4, modulates transcription and growth suppression functions of the Wilms' tumor suppressor WT1. *Mol Cell Biol*. 16:6945-56.
- Kaariainen, L., and H. Soderlund. 1978. Structure and replication of alphaviruses. *Curr Top Microbiol Immunol*. 82:15-69.
- Kamer, G., and P. Argos. 1984. Primary structural comparison of RNA-dependent polymerases from plant, animal and bacterial viruses. *Nucleic Acids Res*. 12:7269-82.
- Katow, S., and A. Sugiura. 1988. Low pH-induced conformational change of rubella virus envelope proteins. *J Gen Virol*. 69 ( Pt 11):2797-807.
- Kaye, J.A., M. del Mar Melero-Montes, and H. Jick. 2001. Mumps, measles, and rubella vaccine and the incidence of autism recorded by general practitioners: a time trend analysis. *Bmj*. 322:460-3.
- Kieser, A., T. Seitz, H.S. Adler, P. Coffey, E. Kremmer, P. Crespo, J.S. Gutkind, D.W. Henderson, J.F. Mushinski, W. Kolch, and H. Mischak. 1996. Protein kinase C-zeta reverts v-raf transformation of NIH-3T3 cells. *Genes Dev*. 10:1455-66.
- Kittlesen, D.J., K.A. Chianese-Bullock, Z.Q. Yao, T.J. Braciale, and Y.S. Hahn. 2000. Interaction between complement receptor gC1qR and hepatitis C virus core protein inhibits T-lymphocyte proliferation. *J Clin Invest*. 106:1239-49.
- Knox, C., E. Sass, W. Neupert, and O. Pines. 1998. Import into mitochondria, folding and retrograde movement of fumarase in yeast. *J Biol Chem*. 273:25587-93.
- Kono, R., Y. Hayakawa, M. Hibi, and K. Ishii. 1969. Experimental vertical transmission of rubella virus in rabbits. *Lancet*. 1:343-7.
- Kozak, M. 1987. An analysis of 5'-noncoding sequences from 699 vertebrate messenger RNAs. *Nucleic Acids Res*. 15:8125-48.
- Krainer, A.R., A. Mayeda, D. Kozak, and G. Binns. 1991. Functional expression of cloned human splicing factor SF2: homology to RNA-binding proteins, U1 70K, and Drosophila splicing regulators. *Cell*. 66:383-94.
- Kujala, P., T. Ahola, N. Ehsani, P. Auvinen, H. Vihinen, and L. Kaariainen. 1999. Intracellular distribution of rubella virus nonstructural protein P150. *J Virol*. 73:7805-11.

- Kujala, P., A. Ikaheimonen, N. Ehsani, H. Vihinen, P. Auvinen, and L. Kaariainen. 2001. Biogenesis of the Semliki Forest virus RNA replication complex. *J Virol.* 75:3873-84.
- Laine, S., A. Thouard, J. Derancourt, M. Kress, D. Sitterlin, and J.M. Rossignol. 2003. In vitro and in vivo interactions between the hepatitis B virus protein P22 and the cellular protein gC1qR. *J Virol.* 77:12875-80.
- Lallena, M.J., M.T. Diaz-Meco, G. Bren, C.V. Paya, and J. Moscat. 1999. Activation of IkappaB kinase beta by protein kinase C isoforms. *Mol Cell Biol.* 19:2180-8.
- Law, L.M., R. Duncan, A. Esmaili, H.L. Nakhasi, and T.C. Hobman. 2001. Rubella virus E2 signal peptide is required for perinuclear localization of capsid protein and virus assembly. *J Virol.* 75:1978-83.
- Law, L.M., J.C. Everitt, M.D. Beatch, C.F. Holmes, and T.C. Hobman. 2003. Phosphorylation of rubella virus capsid regulates its RNA binding activity and virus replication. *J Virol.* 77:1764-71.
- Lee, J.Y., D.S. Bowden, and J.A. Marshall. 1996a. Membrane junctions associated with rubella virus infected cells. *J Submicrosc Cytol Pathol.* 28:101-8.
- Lee, J.Y., D. Hwang, and S. Gillam. 1996b. Dimerization of rubella virus capsid protein is not required for virus particle formation. *Virology.* 216:223-7.
- Lee, J.Y., J.A. Marshall, and D.S. Bowden. 1992. Replication complexes associated with the morphogenesis of rubella virus. *Arch Virol.* 122:95-106.
- Lee, J.Y., J.A. Marshall, and D.S. Bowden. 1994. Characterization of rubella virus replication complexes using antibodies to double-stranded RNA. *Virology.* 200:307-12.
- Lee, J.Y., J.A. Marshall, and D.S. Bowden. 1999. Localization of rubella virus core particles in vero cells. *Virology.* 265:110-9.
- Lee, S., K.E. Owen, H.K. Choi, H. Lee, G. Lu, G. Wengler, D.T. Brown, M.G. Rossmann, and R.J. Kuhn. 1996c. Identification of a protein binding site on the surface of the alphavirus nucleocapsid and its implication in virus assembly. *Structure.* 4:531-41.
- Lee, W.M., and P. Ahlquist. 2003. Membrane synthesis, specific lipid requirements, and localized lipid composition changes associated with a positive-strand RNA virus RNA replication protein. *J Virol.* 77:12819-28.
- Liang, Y., and S. Gillam. 2000. Mutational analysis of the rubella virus nonstructural polyprotein and its cleavage products in virus replication and RNA synthesis. *J Virol.* 74:5133-41.
- Liang, Y., J. Yao, and S. Gillam. 2000. Rubella virus nonstructural protein protease domains involved in trans- and cis-cleavage activities. *J Virol.* 74:5412-23.
- Lim, B.L., K.B. Reid, B. Ghebrehiwet, E.I. Peerschke, L.A. Leigh, and K.T. Preissner. 1996. The binding protein for globular heads of complement C1q, gC1qR. Functional expression and characterization as a novel vitronectin binding factor. *J Biol Chem.* 271:26739-44.
- Liu, Z., D. Yang, Z. Qiu, K.T. Lim, P. Chong, and S. Gillam. 1996. Identification of domains in rubella virus genomic RNA and capsid protein necessary for specific interaction. *J Virol.* 70:2184-90.
- Lopez, S., J.S. Yao, R.J. Kuhn, E.G. Strauss, and J.H. Strauss. 1994. Nucleocapsid-glycoprotein interactions required for assembly of alphaviruses. *J Virol.* 68:1316-23.

- Lu, W., S.Y. Lo, M. Chen, K. Wu, Y.K. Fung, and J.H. Ou. 1999. Activation of p53 tumor suppressor by hepatitis C virus core protein. *Virology*. 264:134-41.
- Lundstrom, M.L., C.A. Mauracher, and A.J. Tingle. 1991. Characterization of carbohydrates linked to rubella virus glycoprotein E2. *J Gen Virol*. 72 ( Pt 4):843-50.
- Luo, Y., H. Yu, and B.M. Peterlin. 1994. Cellular protein modulates effects of human immunodeficiency virus type 1 Rev. *J Virol*. 68:3850-6.
- Madsen, K.M., A. Hviid, M. Vestergaard, D. Schendel, J. Wohlfahrt, P. Thorsen, J. Olsen, and M. Melbye. 2002. A population-based study of measles, mumps, and rubella vaccination and autism. *N Engl J Med*. 347:1477-82.
- Maes, R., A. Vaheri, D. Sedwick, and S. Plotkin. 1966. Synthesis of virus and macromolecules by rubella-infected cells. *Nature*. 210:384-5.
- Magliano, D., J.A. Marshall, D.S. Bowden, N. Vardaxis, J. Meanger, and J.Y. Lee. 1998. Rubella virus replication complexes are virus-modified lysosomes. *Virology*. 240:57-63.
- Marr, L.D., A. Sanchez, and T.K. Frey. 1991. Efficient in vitro translation and processing of the rubella virus structural proteins in the presence of microsomes. *Virology*. 180:400-405.
- Marr, L.D., C.Y. Wang, and T.K. Frey. 1994. Expression of the rubella virus nonstructural protein ORF and demonstration of proteolytic processing. *Virology*. 198:586-92.
- Mastromarino, P., L. Cioe, S. Rieti, and N. Orsi. 1990. Role of membrane phospholipids and glycolipids in the Vero cell surface receptor for rubella virus. *Med Microbiol Immunol (Berl)*. 179:105-14.
- Matthews, D.A., and W.C. Russell. 1998. Adenovirus core protein V interacts with p32--a protein which is associated with both the mitochondria and the nucleus. *J Gen Virol*. 79 ( Pt 7):1677-85.
- Mattson, M.P., W. Duan, S.L. Chan, and S. Camandola. 1999. Par-4: an emerging pivotal player in neuronal apoptosis and neurodegenerative disorders. *J Mol Neurosci*. 13:17-30.
- Mauracher, C.A., S. Gillam, R. Shukin, and A.J. Tingle. 1991. pH-dependent solubility shift of rubella virus capsid protein. *Virology*. 181:773-7.
- McDonald, H., T.C. Hobman, and S. Gillam. 1991. The influence of capsid protein cleavage on the processing of E2 and E1 glycoproteins of rubella virus. *Virology*. 183:52-60.
- Meenakshi, J., Anupama, S.K. Goswami, and K. Datta. 2003. Constitutive expression of hyaluronan binding protein 1 (HABP1/p32/gC1qR) in normal fibroblast cells perturbs its growth characteristics and induces apoptosis. *Biochem Biophys Res Commun*. 300:686-93.
- Megyeri, K., K. Berencsi, T.D. Halazonetis, G.C. Prendergast, G. Gri, S.A. Plotkin, G. Rovera, and E. Gonczol. 1999. Involvement of a p53-dependent pathway in rubella virus-induced apoptosis. *Virology*. 259:74-84.
- Melancon, P., and H. Garoff. 1987. Processing of the Semliki Forest virus structural polyprotein: role of the capsid protease. *J Virol*. 61:1301-9.
- Miller, D.J., M.D. Schwartz, and P. Ahlquist. 2001. Flock house virus RNA replicates on outer mitochondrial membranes in *Drosophila* cells. *J Virol*. 75:11664-76.

- Mizushima, S., and S. Nagata. 1990. pEF-BOS, a powerful mammalian expression vector. *Nucleic Acids Res.* 18:5322.
- Mohan, K.V., B. Ghebrehiwet, and C.D. Atreya. 2002. The N-terminal conserved domain of rubella virus capsid interacts with the C-terminal region of cellular p32 and overexpression of p32 enhances the viral infectivity. *Virus Res.* 85:151-61.
- Murch, S.H., A. Anthony, D.H. Casson, M. Malik, M. Berelowitz, A.P. Dhillon, M.A. Thomson, A. Valentine, S.E. Davies, and J.A. Walker-Smith. 2004. Retraction of an interpretation. *Lancet.* 363:750.
- Muta, T., D. Kang, S. Kitajima, T. Fujiwara, and N. Hamasaki. 1997. p32 protein, a splicing factor 2-associated protein, is localized in mitochondrial matrix and is functionally important in maintaining oxidative phosphorylation. *J Biol Chem.* 272:24363-70.
- Mylonis, I., V. Drosou, S. Brancorsini, E. Nikolakaki, P. Sassone-Corsi, and T. Giannakouros. 2003. Temporal association of protamine 1 with the inner nuclear membrane protein LBR during spermiogenesis. *J Biol Chem.*
- Naeye, R.L., and W. Blanc. 1965. Pathogenesis of congenital rubella. *Jama.* 194:1277-83.
- Nakhasi, H.L., D. Thomas, D.X. Zheng, and T.Y. Liu. 1989. Nucleotide sequence of capsid, E2 and E1 protein genes of Rubella virus vaccine strain RA27/3. *Nucleic Acids Res.* 17:4393-4.
- Nalca, A., S.G. Qiu, N. El-Guendy, S. Krishnan, and V.M. Rangnekar. 1999. Oncogenic Ras sensitizes cells to apoptosis by Par-4. *J Biol Chem.* 274:29976-83.
- Nikolakaki, E., G. Simos, S.D. Georgatos, and T. Giannakouros. 1996. A nuclear envelope-associated kinase phosphorylates arginine-serine motifs and modulates interactions between the lamin B receptor and other nuclear proteins. *J Biol Chem.* 271:8365-72.
- Nusbacher, J., K. Hirschhorn, and L.Z. Cooper. 1967. Chromosomal abnormalities in congenital rubella. *N Engl J Med.* 276:1409-13.
- Oker-Blom, C. 1984. The gene order for rubella virus structural proteins is NH<sub>2</sub>-C-E2-E1-COOH. *J. Virol.* 51:354-358.
- Oker-Blom, C., N. Kalkkinen, L. Kaariainen, and R.F. Pettersson. 1983. Rubella virus contains one capsid protein and three envelope glycoproteins, E1, E2a, and E2b. *J Virol.* 46:964-73.
- Oker-Blom, C., I. Ulmanen, L. Kaariainen, and R.F. Pettersson. 1984. Rubella virus 40S genome RNA specifies a 24S subgenomic mRNA that codes for a precursor to structural proteins. *J Virol.* 49:403-8.
- Orenstein, W.A., K.J. Bart, A.R. Hinman, S.R. Preblud, W.L. Greaves, S.W. Doster, H.C. Stetler, and B. Sirotkin. 1984. The opportunity and obligation to eliminate rubella from the United States. *Jama.* 251:1988-94.
- Oshiro, L.S., N.J. Schmidt, and E.H. Lennette. 1969. Electron microscopic studies of Rubella virus. *J Gen Virol.* 5:205-10.
- Otsuka, M., N. Kato, H. Taniguchi, H. Yoshida, T. Goto, Y. Shiratori, and M. Omata. 2002. Hepatitis C virus core protein inhibits apoptosis via enhanced Bcl-xL expression. *Virology.* 296:84-93.

- Patterson, R.L., A. Koren, and R.L. Northrop. 1973. Experimental rubella virus infection of marmosets (*Saguinus species*). *Lab Anim Sci.* 23:68-71.
- Patwardhan, S., A. Gashler, M.G. Siegel, L.C. Chang, L.J. Joseph, T.B. Shows, M.M. Le Beau, and V.P. Sukhatme. 1991. EGR3, a novel member of the Egr family of genes encoding immediate-early transcription factors. *Oncogene.* 6:917-28.
- Peranen, J., and L. Kaariainen. 1991. Biogenesis of type I cytopathic vacuoles in Semliki Forest virus-infected BHK cells. *J Virol.* 65:1623-7.
- Petersen-Mahrt, S.K., C. Estmer, C. Ohrmalm, D.A. Matthews, W.C. Russell, and G. Akusjarvi. 1999. The splicing factor-associated protein, p32, regulates RNA splicing by inhibiting ASF/SF2 RNA binding and phosphorylation. *Embo J.* 18:1014-24.
- Petruzzello, R., N. Orsi, S. Macchia, S. Rieti, T.K. Frey, and P. Mastromarino. 1996. Pathway of rubella virus infectious entry into Vero cells. *J Gen Virol.* 77 ( Pt 2 ):303-8.
- Plotkin, S.A., A. Bou'E, and J.G. Bou'E. 1965. The in Vitro Growth of Rubella Virus in Human Embryo Cells. *Am J Epidemiol.* 81:71-85.
- Plotkin, S.A., and A. Vaheri. 1967. Human fibroblasts infected with rubella virus produce a growth inhibitor. *Science.* 156:659-61.
- Pugachev, K.V., E.S. Abernathy, and T.K. Frey. 1997. Improvement of the specific infectivity of the rubella virus (RUB) infectious clone: determinants of cytopathogenicity induced by RUB map to the nonstructural proteins. *J Virol.* 71:562-8.
- Pugachev, K.V., and T.K. Frey. 1998. Rubella virus induces apoptosis in culture cells. *Virology.* 250:359-70.
- Qiu, Z., T.C. Hobman, H.L. McDonald, N.O. Seto, and S. Gillam. 1992. Role of N-linked oligosaccharides in processing and intracellular transport of E2 glycoprotein of rubella virus. *J Virol.* 66:3514-21.
- Qiu, Z., D. Ou, T.C. Hobman, and S. Gillam. 1994. Expression and characterization of virus-like particles containing rubella virus structural proteins. *J Virol.* 68:4086-91.
- Qiu, Z., J. Yao, H. Cao, and S. Gillam. 2000. Mutations in the E1 hydrophobic domain of rubella virus impair virus infectivity but not virus assembly. *J Virol.* 74:6637-42.
- Randall, G., M. Lagunoff, and B. Roizman. 1997. The product of ORF O located within the domain of herpes simplex virus 1 genome transcribed during latent infection binds to and inhibits in vitro binding of infected cell protein 4 to its cognate DNA site. *Proc Natl Acad Sci U S A.* 94:10379-84.
- Ray, R.B., R. Steele, K. Meyer, and R. Ray. 1997. Transcriptional repression of p53 promoter by hepatitis C virus core protein. *J Biol Chem.* 272:10983-6.
- Ray, R.B., R. Steele, K. Meyer, and R. Ray. 1998. Hepatitis C virus core protein represses p21WAF1/Cip1/Sid1 promoter activity. *Gene.* 208:331-6.
- Reef, S.E., T.K. Frey, K. Theall, E. Abernathy, C.L. Burnett, J. Icenogle, M.M. McCauley, and M. Wharton. 2002. The changing epidemiology of rubella in the 1990s: on the verge of elimination and new challenges for control and prevention. *Jama.* 287:464-72.

- Risco, C., J.L. Carrascosa, and T.K. Frey. 2003. Structural maturation of rubella virus in the Golgi complex. *Virology*. 312:261-9.
- Robertson, S.E., D.A. Featherstone, M. Gacic-Dobo, and B.S. Hersh. 2003. Rubella and congenital rubella syndrome: global update. *Rev Panam Salud Publica*. 14:306-15.
- Robles-Flores, M., E. Rendon-Huerta, H. Gonzalez-Aguilar, G. Mendoza-Hernandez, S. Islas, V. Mendoza, M.V. Ponce-Castaneda, L. Gonzalez-Mariscal, and F. Lopez-Casillas. 2002. p32 (gC1qBP) is a general protein kinase C (PKC)-binding protein; interaction and cellular localization of P32-PKC complexes in rat hepatocytes. *J Biol Chem*. 277:5247-55.
- Rojo, G., M. Chamorro, M.L. Salas, E. Vinuela, J.M. Cuezva, and J. Salas. 1998. Migration of mitochondria to viral assembly sites in African swine fever virus-infected cells. *J Virol*. 72:7583-8.
- Rorke, L.B., A. Fabiyi, T.S. Elizan, and J.L. Sever. 1968. Experimental cerebrovascular lesions in congenital and neonatal rubella-virus infections of ferrets. *Lancet*. 2:153-4.
- Rozanov, D.V., B. Ghebrehiwet, B. Ratnikov, E.Z. Monosov, E.I. Deryugina, and A.Y. Strongin. 2002. The cytoplasmic tail peptide sequence of membrane type-1 matrix metalloproteinase (MT1-MMP) directly binds to gC1qR, a compartment-specific chaperone-like regulatory protein. *FEBS Lett*. 527:51-7.
- Rozanov, M.N., E.V. Koonin, and A.E. Gorbalenya. 1992. Conservation of the putative methyltransferase domain: a hallmark of the 'Sindbis-like' supergroup of positive-strand RNA viruses. *J Gen Virol*. 73 ( Pt 8):2129-34.
- Ruggieri, A., T. Harada, Y. Matsuura, and T. Miyamura. 1997. Sensitization to Fas-mediated apoptosis by hepatitis C virus core protein. *Virology*. 229:68-76.
- Sacco, R., T. Tsutsumi, R. Suzuki, M. Otsuka, H. Aizaki, S. Sakamoto, M. Matsuda, N. Seki, Y. Matsuura, T. Miyamura, and T. Suzuki. 2003. Antiapoptotic regulation by hepatitis C virus core protein through up-regulation of inhibitor of caspase-activated DNase. *Virology*. 317:24-35.
- Sambrook, J., E.F. Fritsch, and T. Maniatis. 1989. Molecular cloning : a laboratory manual. Cold Spring Harbor Laboratory, Cold Spring Harbor, N.Y.
- Sato, H., M. Hishiyama, and A. Shishido. 1976. Growth of rubella, measles and mumps viruses in rat fetus. *Jpn J Med Sci Biol*. 29:39-44.
- Schlesinger, S., and M.J. Schlesinger. 2001. Togaviridae: The Viruses and Their Replication. *In* Fields' Virology. B.N. Fields, D.M. Knipe, P.M. Howley, and D.E. Griffin, editors. Lippincott Williams & Wilkins, Philadelphia. 895-916.
- Schmidt, M., N. Tuominen, T. Johansson, S.A. Weiss, K. Keinanen, and C. Oker-Blom. 1998. Baculovirus-mediated large-scale expression and purification of a polyhistidine-tagged rubella virus capsid protein. *Protein Expr Purif*. 12:323-30.
- Schwer, B., S. Ren, T. Pietschmann, J. Kartenbeck, K. Kaehlcke, R. Bartenschlager, T.S.B. Yen, and M. Ott. 2004. Targeting of Hepatitis C Virus Core Protein to Mitochondria through a Novel C-Terminal Localization Motif. *J. Virol*. 78:7958-7968.

- Sedwick, W.D., and F. Sokol. 1970. Nucleic acid of rubella virus and its replication in hamster kidney cells. *J Virol.* 5:478-89.
- Sells, S.F., S.S. Han, S. Muthukumar, N. Maddiwar, R. Johnstone, E. Boghaert, D. Gillis, G. Liu, P. Nair, S. Monnig, P. Collini, M.P. Mattson, V.P. Sukhatme, S.G. Zimmer, D.P. Wood, Jr., J.W. McRoberts, Y. Shi, and V.M. Rangnekar. 1997. Expression and function of the leucine zipper protein Par-4 in apoptosis. *Mol Cell Biol.* 17:3823-32.
- Sells, S.F., D.P. Wood, Jr., S.S. Joshi-Barve, S. Muthukumar, R.J. Jacob, S.A. Crist, S. Humphreys, and V.M. Rangnekar. 1994. Commonality of the gene programs induced by effectors of apoptosis in androgen-dependent and -independent prostate cells. *Cell Growth Differ.* 5:457-66.
- Seytter, T., F. Lottspeich, W. Neupert, and E. Schwarz. 1998. Mam33p, an oligomeric, acidic protein in the mitochondrial matrix of *Saccharomyces cerevisiae* is related to the human complement receptor gC1q-R. *Yeast.* 14:303-10.
- Sheridan, E., C. Aitken, D. Jeffries, M. Hird, and P. Thayalasekaran. 2002. Congenital rubella syndrome: a risk in immigrant populations. *Lancet.* 359:674-5.
- Shrivastava, A., S.K. Manna, R. Ray, and B.B. Aggarwal. 1998. Ectopic expression of hepatitis C virus core protein differentially regulates nuclear transcription factors. *J Virol.* 72:9722-8.
- Simos, G., and S.D. Georgatos. 1994. The lamin B receptor-associated protein p34 shares sequence homology and antigenic determinants with the splicing factor 2-associated protein p32. *FEBS Lett.* 346:225-8.
- Smith, C.A., R.E. Petty, and A.J. Tingle. 1987. Rubella virus and arthritis. *Rheum Dis Clin North Am.* 13:265-74.
- Stanwick, T.L., and J.V. Hallum. 1974. Role of interferon in six cell lines persistently infected with rubella virus. *Infect Immun.* 10:810-5.
- Stein, I., Y. Peleg, S. Even-Ram, and O. Pines. 1994. The single translation product of the FUM1 gene (fumarase) is processed in mitochondria before being distributed between the cytosol and mitochondria in *Saccharomyces cerevisiae*. *Mol Cell Biol.* 14:4770-8.
- Storz, P., A. Hausser, G. Link, J. Dedio, B. Ghebrehiwet, K. Pfizenmaier, and F.J. Johannes. 2000. Protein kinase C [micro] is regulated by the multifunctional chaperon protein p32. *J Biol Chem.* 275:24601-7.
- Strauss, J.H., and E.G. Strauss. 1994. The Alphaviruses: Gene expression, replication and evolution. *Microbiological Reviews.* 58:491-562.
- Strauss, J.H., E.G. Strauss, and R.J. Kuhn. 1995. Budding of alphaviruses. *Trends Microbiol.* 3:346-50.
- Sunayama, J., Y. Ando, N. Itoh, A. Tomiyama, K. Sakurada, A. Sugiyama, D. Kang, F. Tashiro, Y. Gotoh, Y. Kuchino, and C. Kitanaka. 2004. Physical and functional interaction between BH3-only protein Hrk and mitochondrial pore-forming protein p32. *Cell Death Differ.*
- Suomalainen, M., H. Garoff, and M.D. Baron. 1990. The E2 signal sequence of rubella virus remains part of the capsid protein and confers membrane association in vitro. *J Virol.* 64:5500-9.

- Szabo, J., L. Cervenak, F.D. Toth, Z. Prohaszka, L. Horvath, K. Kerekes, Z. Beck, A. Bacsi, A. Erdei, E.I. Peerschke, G. Fust, and B. Ghebrehiwet. 2001. Soluble gC1q-R/p33, a cell protein that binds to the globular "heads" of C1q, effectively inhibits the growth of HIV-1 strains in cell cultures. *Clin Immunol.* 99:222-31.
- Takada, S., Y. Shirakata, N. Kaneniwa, and K. Koike. 1999. Association of hepatitis B virus X protein with mitochondria causes mitochondrial aggregation at the nuclear periphery, leading to cell death. *Oncogene.* 18:6965-73.
- Takkinen, K., G. Vidgren, J. Ekstrand, U. Hellman, N. Kalkkinen, C. Wernstedt, and R.F. Pettersson. 1988. Nucleotide sequence of the rubella virus capsid protein gene reveals an unusually high G/C content. *J Gen Virol.* 69 ( Pt 3):603-12.
- Tange, T.O., T.H. Jensen, and J. Kjems. 1996. In vitro interaction between human immunodeficiency virus type 1 Rev protein and splicing factor ASF/SF2-associated protein, p32. *J Biol Chem.* 271:10066-72.
- Taylor, B., E. Miller, R. Lingam, N. Andrews, A. Simmons, and J. Stowe. 2002. Measles, mumps, and rubella vaccination and bowel problems or developmental regression in children with autism: population study. *Bmj.* 324:393-6.
- Tzeng, W.P., M.H. Chen, C.A. Derdeyn, and T.K. Frey. 2001. Rubella virus DI RNAs and replicons: requirement for nonstructural proteins acting in cis for amplification by helper virus. *Virology.* 289:63-73.
- Tzeng, W.P., and T.K. Frey. 2003. Complementation of a deletion in the rubella virus p150 nonstructural protein by the viral capsid protein. *J Virol.* 77:9502-10.
- Ungermann, C., W. Neupert, and D.M. Cyr. 1994. The role of Hsp70 in conferring unidirectionality on protein translocation into mitochondria. *Science.* 266:1250-3.
- Vaheri, A., and V.J. Cristofalo. 1967. Metabolism of rubella virus-infected BHK 21 cells. Enhanced glycolysis and late cellular inhibition. *Arch Gesamte Virusforsch.* 21:425-36.
- van der Meer, Y., E.J. Snijder, J.C. Dobbe, S. Schleich, M.R. Denison, W.J. Spaan, and J.K. Locker. 1999. Localization of mouse hepatitis virus nonstructural proteins and RNA synthesis indicates a role for late endosomes in viral replication. *J Virol.* 73:7641-57.
- van Gurp, M., N. Festjens, G. van Loo, X. Saelens, and P. Vandenabeele. 2003. Mitochondrial intermembrane proteins in cell death. *Biochem Biophys Res Commun.* 304:487-97.
- van Regenmortel, M.H.V., C.M. Fauquet, D.H.L. Bishop, E.B. Carstens, M.K. Estes, S.M. Lemon, J. Maniloff, M.A. Mayo, D.J. McGeoch, C.R. Pringle, and R.B. Wickner. 2000. Virus taxonomy : classification and nomenclature of viruses : seventh report of the International Committee on Taxonomy of Viruses. Academic Press, San Diego. 1167 pp.
- Van Scoy, S., I. Watakabe, A.R. Krainer, and J. Hearing. 2000. Human p32: a coactivator for Epstein-Barr virus nuclear antigen-1-mediated transcriptional activation and possible role in viral latent cycle DNA replication. *Virology.* 275:145-57.
- von Bonsdorff, C.H., and A. Vaheri. 1969. Growth of rubella virus in BHK21 cells: electron microscopy of morphogenesis. *J Gen Virol.* 5:47-51.

- Wakefield, A.J., S.H. Murch, A. Anthony, J. Linnell, D.M. Casson, M. Malik, M. Berelowitz, A.P. Dhillon, M.A. Thomson, P. Harvey, A. Valentine, S.E. Davies, and J.A. Walker-Smith. 1998. Ileal-lymphoid-nodular hyperplasia, non-specific colitis, and pervasive developmental disorder in children. *Lancet*. 351:637-41.
- Wang, C.Y., G. Dominguez, and T.K. Frey. 1994. Construction of rubella virus genome-length cDNA clones and synthesis of infectious RNA transcripts. *J Virol*. 68:3550-7.
- Wang, Y., J.E. Finan, J.M. Middeldorp, and S.D. Hayward. 1997. P32/TAP, a cellular protein that interacts with EBNA-1 of Epstein-Barr virus. *Virology*. 236:18-29.
- Waxham, M.N., and J.S. Wolinsky. 1985. Detailed immunologic analysis of the structural polypeptides of rubella virus using monoclonal antibodies. *Virology*. 143:153-65.
- Wengler, G. 1984. Identification of a transfer of viral core protein to cellular ribosomes during the early stages of alphavirus infection. *Virology*. 134:435-42.
- Wolinsky, J.S., M. McCarthy, O. Allen-Cannady, W.T. Moore, R. Jin, S.N. Cao, A. Lovett, and D. Simmons. 1991. Monoclonal antibody-defined epitope map of expressed rubella virus protein domains. *J Virol*. 65:3986-94.
- Xu, Z., A. Hirasawa, H. Shinoura, and G. Tsujimoto. 1999. Interaction of the alpha(1B)-adrenergic receptor with gC1q-R, a multifunctional protein. *J Biol Chem*. 274:21149-54.
- Yanagida, M., T. Hayano, Y. Yamauchi, T. Shinkawa, T. Natsume, T. Isobe, and N. Takahashi. 2004. Human fibrillarin forms a sub-complex with splicing factor 2-associated p32, protein arginine methyltransferases, and tubulins alpha 3 and beta 1 that is independent of its association with preribosomal ribonucleoprotein complexes. *J Biol Chem*. 279:1607-14.
- Yao, J., and S. Gillam. 1999. Mutational analysis, using a full-length rubella virus cDNA clone, of rubella virus E1 transmembrane and cytoplasmic domains required for virus release. *J Virol*. 73:4622-30.
- Yao, J., and S. Gillam. 2000. A single-amino-acid substitution of a tyrosine residue in the rubella virus E1 cytoplasmic domain blocks virus release. *J Virol*. 74:3029-36.
- Yao, J., D. Yang, P. Chong, D. Hwang, Y. Liang, and S. Gillam. 1998. Proteolytic processing of rubella virus nonstructural proteins. *Virology*. 246:74-82.
- Yoneda, T., M. Urade, M. Sakuda, and T. Miyazaki. 1986. Altered growth, differentiation, and responsiveness to epidermal growth factor of human embryonic mesenchymal cells of palate by persistent rubella virus infection. *J Clin Invest*. 77:1613-21.
- Yu, L., P.M. Loewenstein, Z. Zhang, and M. Green. 1995a. In vitro interaction of the human immunodeficiency virus type 1 Tat transactivator and the general transcription factor TFIIB with the cellular protein TAP. *J Virol*. 69:3017-23.
- Yu, L., Z. Zhang, P.M. Loewenstein, K. Desai, Q. Tang, D. Mao, J.S. Symington, and M. Green. 1995b. Molecular cloning and characterization of a cellular protein that interacts with the human immunodeficiency virus type 1 Tat transactivator and encodes a strong transcriptional activation domain. *J Virol*. 69:3007-16.

Zhang, W., S. Mukhopadhyay, S.V. Pletnev, T.S. Baker, R.J. Kuhn, and M.G. Rossmann. 2002. Placement of the structural proteins in Sindbis virus. *J Virol.* 76:11645-58.

Zhao, H., B. Lindqvist, H. Garoff, C.H. von Bonsdorff, and P. Liljestrom. 1994. A tyrosine-based motif in the cytoplasmic domain of the alphavirus envelope protein is essential for budding. *Embo J.* 13:4204-11.

Zheng, D.X., L. Dickens, T.Y. Liu, and H.L. Nakhasi. 1989. Nucleotide sequence of the 24S subgenomic messenger RNA of a vaccine strain (HPV77) of rubella virus: comparison with a wild-type strain (M33). *Gene.* 82:343-9.

Zheng, Y.H., H.F. Yu, and B.M. Peterlin. 2003. Human p32 protein relieves a post-transcriptional block to HIV replication in murine cells. *Nat Cell Biol.* 5:611-8.

Zhu, N., A. Khoshnan, R. Schneider, M. Matsumoto, G. Dennert, C. Ware, and M.M. Lai. 1998. Hepatitis C virus core protein binds to the cytoplasmic domain of tumor necrosis factor (TNF) receptor 1 and enhances TNF-induced apoptosis. *J Virol.* 72:3691-7.

## **APPENDIX I. Effect of capsid expression on host cell signaling pathways**

## **Involvement of capsid in regulating host cell signaling pathways**

The identification of Par-4, p32 and the atypical protein kinase C isoform PKC $\zeta$  as capsid-interacting proteins was a particularly interesting finding since both Par-4 and p32 have been demonstrated to bind PKC $\zeta$  (Diaz-Meco et al., 1996; Robles-Flores et al., 2002). This kinase is involved in the regulation of cellular survival pathways by activating both NF- $\kappa$ B and AP-1 signaling (Berra et al., 1993; Diaz-Meco et al., 1993; Huang et al., 2000; Kieser et al., 1996). Thus, the identification of interactions between capsid and these host cell proteins raised the possibility that capsid may play a direct role in modulating specific cellular survival pathways (Figure A.1).

To determine if capsid is able to regulate NF- $\kappa$ B activity through interactions with either p32 or Par-4 we conducted luciferase reporter assays. HEK 293T cells were transiently cotransfected with a plasmid containing a luciferase reporter downstream of an NF- $\kappa$ B enhancer element and plasmids encoding capsid, p32 or Par-4 (either alone or in combination). Forty-four hours post-transfection, NF- $\kappa$ B activity was induced by the addition of 50 ng/ml TNF- $\alpha$  to the growth medium for 6 hours. As expected, over-expression of Par-4 efficiently decreased NF- $\kappa$ B activity (Figure A.2A). In contrast, expression of capsid did not affect NF- $\kappa$ B signaling. Furthermore, expression of capsid did not reproducibly affect the inhibition of NF- $\kappa$ B by Par-4. These results suggest that capsid is not able to prevent the ability of Par-4 to downregulate NF- $\kappa$ B activity in HEK 293T cells in response to TNF- $\alpha$ . Interestingly, over-expression of p32 increased NF- $\kappa$ B activity by approximately 50% and this increase was not affected by capsid expression. However, the significance of this finding is not clear since p32 is expected to be imported into mitochondria where it is unlikely that it can directly affect NF- $\kappa$ B activity.

To determine if these proteins regulate AP-1 activation, luciferase assays were conducted as described above except HEK 293T cells were transfected with an AP-1 luciferase reporter plasmid and AP-1 signaling was activated by serum stimulation. Interestingly, exogenous expression of capsid, Par-4 and p32 all decreased AP-1 signaling (Figure A2.B). Whereas capsid expression decreased AP-1 activity to approximately 25% of the reporter plasmid alone, over-expression of Par-4 or p32 only decreased AP-1 activity to approximately 45%. These results indicate that capsid

expression is sufficient to downregulate the activity of the AP-1 signaling pathway. The mechanism by which capsid is having this effect is not clear since the ability of capsid to downregulate AP-1 was not dramatically affected by coexpression of either Par-4 or p32. However, a small synergistic effect of Par-4 was observed when capsid was coexpressed with this protein.

These results may appear to contradict our model that interactions between capsid and host cell proteins act to maintain the activity of protective signaling pathways. However, we were unable to determine the mechanism by which capsid downregulates AP-1 activity. We attempted to examine the role of PKC $\zeta$  in AP-1 signaling by expressing constitutively active and kinase dead PKC $\zeta$  constructs but we were unable to detect protein expression from these plasmids. One possibility is that capsid may downregulate AP-1 activity through a PKC $\zeta$  independent mechanism. While these results are inconclusive as to the mechanisms by which capsid decreases AP-1 signaling, the fact that capsid is able to influence cellular signaling remains a significant finding. Further investigation will serve to elucidate the roles of both capsid and host cell proteins in regulating host cell signaling during RV infection.

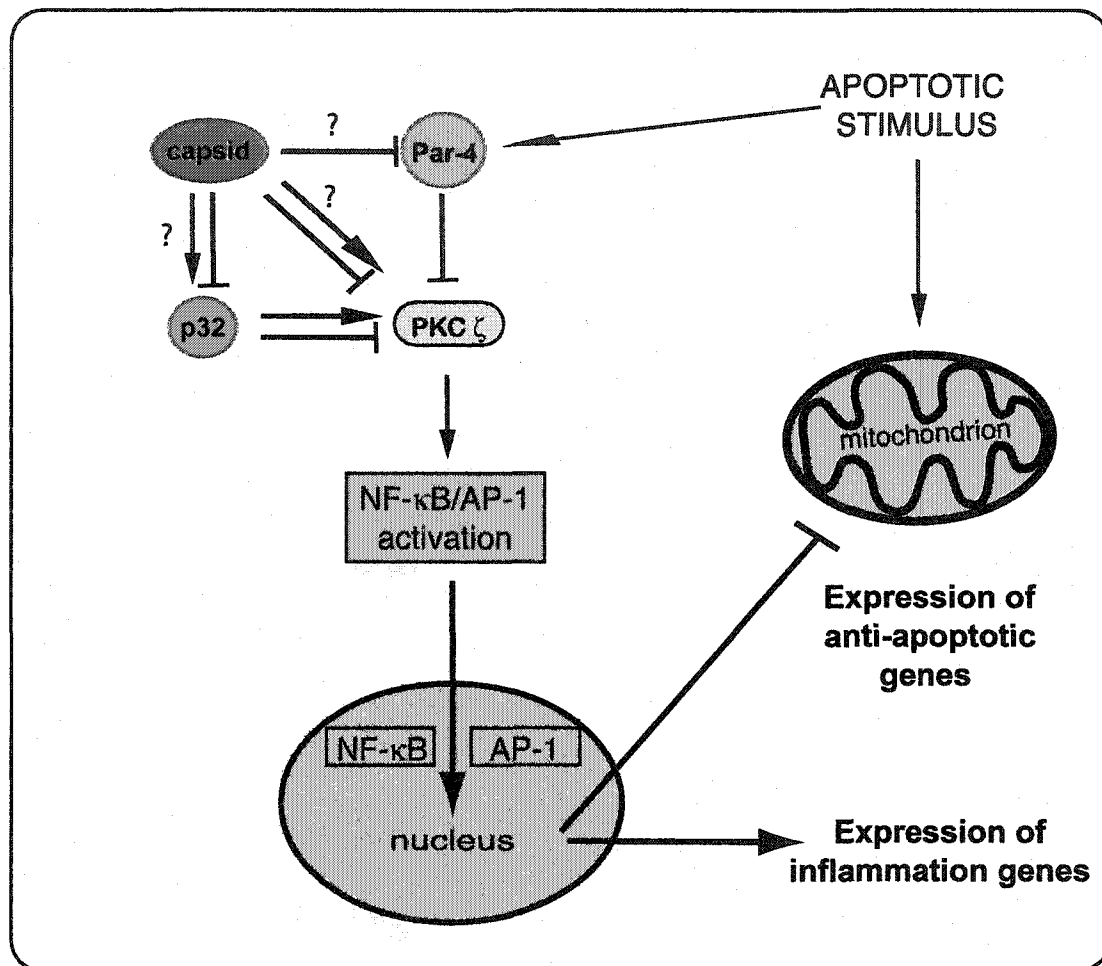


**Figure A.1. Mechanism by which capsid may alter cell signaling pathways via its interaction with cellular proteins.** Rubella virus infection leads to apoptotic signals in the infected cell. In addition to affecting mitochondrial integrity, these signals may result in upregulation of Par-4 expression. Par-4 binds to and inhibits the kinase activity of PKC $\zeta$  resulting in a loss of pro-survival signaling through NF- $\kappa$ B and/or AP-1. In this manner, Par-4 sensitizes cells to apoptotic stimuli. Capsid may function to maintain prosurvival signaling by preventing inhibition of PKC $\zeta$ . For instance, capsid may sequester Par-4 or block the ability of Par-4 to inhibit the kinase activity of PKC $\zeta$ . In addition capsid may regulate PKC $\zeta$  activity through p32. However, it is difficult to predict the effect of interactions between capsid and p32 since reports on the regulatory effects of p32 on PKC $\zeta$  are not known. Alternatively, capsid may form complexes directly with PKC $\zeta$ . The effects of specific interactions between capsid and cellular proteins are speculative and indicated with question marks.

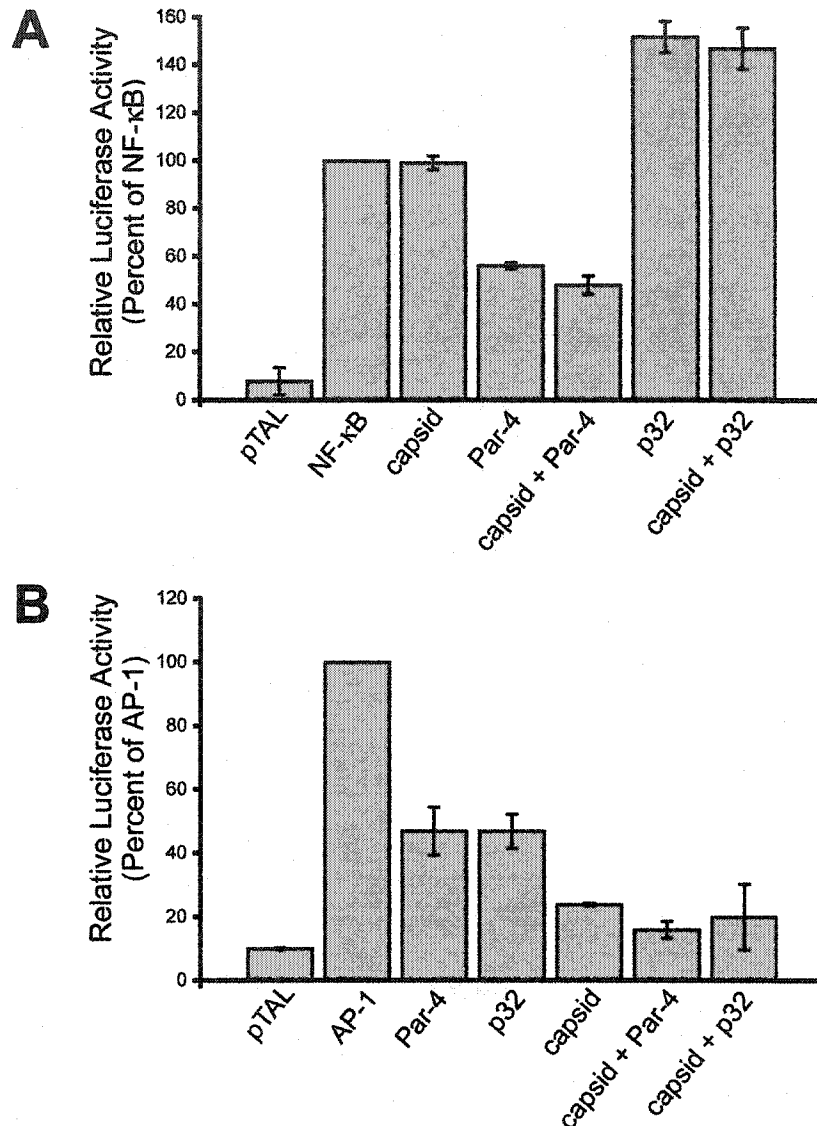


**Figure A.2. Effects of capsid expression on NF- $\kappa$ B and AP-1 activity.** HEK 293T cells were cotransfected with luciferase reporter plasmids (containing NF- $\kappa$ B or AP-1 enhancer elements or lacking an enhancer element (pTAL)), a plasmid encoding  $\beta$ -galactosidase and plasmids encoding capsid, p32 and Par-4 as indicated. Cells were transfected with equal amounts of plasmid DNA (3  $\mu$ g) in each case and transfection efficiencies were normalized to  $\beta$ -galactosidase activity. Twenty-four hours post-transfection, cells were serum starved for 20 hours. Activation of the NF- $\kappa$ B signaling pathway was induced by the addition of TNF- $\alpha$  (50 ng/ml) to the growth medium for 6 hours (A). Activation of the AP-1 signaling pathway was induced by the addition of normal growth medium containing 10% serum for 6 hours (B). Following activation, cells were lysed and luciferase activities were determined. Values shown are the mean of three independent transfections. All values were normalized to the luciferase activity of cells transfected with the NF- $\kappa$ B (A) or the AP-1 (B) reporter plasmid in the absence of exogenous capsid, p32 or Par-4.

## **CURRICULUM VITAE**

**Name:** Martin Denis Beatch

**Address:** Department of Cell Biology  
University of Alberta  
Edmonton, AB  
T6G 2H7  
CANADA

Phone: (780) 492-6595

Fax: (780) 492-0450

**Education:**

1991-1996 B.Sc. with Honors in Zoology with first class Honors,  
University of Alberta, AB, Canada  
Undergraduate thesis supervisor: Dr. Bruce R. Stevenson

1997-2004 Ph.D. Dept. of Cell Biology,  
University of Alberta, AB, Canada  
Supervisor: Dr. Tom C. Hobman

**Scholastic Awards:**

*Undergraduate*

1994 Scholarship, Bamfield Marine Biology Station, Bamfield, BC  
1994-95, 1995-96 Deans List, University of Alberta  
1995 A William Rowan Memorial Prize  
For students of outstanding merit entering fourth year of  
Honours Zoology, University of Alberta

*Graduate*

1997 Graduate Studies and Research Scholarship, University of Alberta  
1998-2002 Full-Time Studentship, Alberta Heritage Foundation for Medical  
Research  
1999 Travel grant, American Society for Virology – 18<sup>th</sup> annual meeting  
2000 Travel grant, American Society for Virology – 19<sup>th</sup> annual meeting  
2000-2003 Doctoral Research Award, Medical Research Council of Canada  
2000-2003 Walter H. Johns Graduate Fellowship, University of Alberta

**Memberships:**

1999-2003 American Society for Virology

## **Invited Presentations**

Characterization of interactions between rubella virus capsid and host cell proteins. 18<sup>th</sup> annual meeting of the American Society for Virology. Amherst, Massachusetts. July 1999.

Characterization of the interaction between rubella virus capsid and host-cell proteins and their effects on signaling. 22<sup>nd</sup> annual meeting of the American Society for Virology. Davis, California. July 2003.

## **Bibliography:**

### *Publications in reviewed journals*

**Beatch, M.**, L.A. Jesaitis, W.G. Gallin, D.A. Goodenough, and B.R. Stevenson. 1996. The tight junction protein ZO-2 contains three PDZ (PSD-95/Discs-Large/ZO-1) domains and an alternatively spliced region. *J. Biol. Chem.* 271:25723-25726.

**Beatch, M.** and T. Hobman. 2000. Rubella virus capsid associates with host cell protein p32 and localizes to mitochondria. *J. Virology.* 74(12):5569-5576.

Law, L.M.J., Everitt, J.C., **Beatch, M.D.**, Holmes, C.F.B. and Hobman, T.C. 2003. Phosphorylation of Rubella virus capsid regulates its RNA binding activity and virus replication. *J. Virology.* 77(3):1820-1829.

### *Published abstracts*

Stevenson, B.R., **M. Beatch**, L.A. Jesaitis, W. Gallin, D.A. Goodenough. 1996. The tight junction protein ZO-2 contains three PDZ domains and an alternatively spliced region. *Mol. Biol. Cell* 7:606a.

**Beatch, M.** and T.C. Hobman. 1998. Association of rubella virus capsid protein with host cell proteins. Fifth International Symposium on Positive Strand RNA Viruses. St. Petersburg, Florida.

**Beatch, M.** and T.C. Hobman. 2000. The amino-terminus of rubella virus capsid interacts with two host cell proteins. 19<sup>th</sup> annual meeting of the American Society for Virology. Fort Collins, Colorado.

**Beatch, M.** and T.C. Hobman. 2001. Rubella virus capsid interacts with host-cell protein Par-4. Sixth International Symposium on Positive Strand RNA Viruses. Paris, France.

**Beatch, M.** and T.C. Hobman. 2002. Interaction of Rubella virus capsid with Host-cell proteins. IUBMB Symposium on Genome Replication of RNA Viruses. Helsinki, Finland.

***Book Chapters***

Everitt J.C., M.D. Beatch, LM.J. Law, and T.C. Hobman. 2004. Replication and Assembly of Rubella Virus. *In* Structure and Assembly of Togaviruses and Flaviviruses. J.H. Strauss and R.J. Kuhn editors. Springer-Verlag. In Press.